

Automation of Manual Assembly: Integrating Design Methods to Enhance Sub-Assembly Production Rate and Operator Ergonomics

*A Major Qualifying Project Submitted to the Faculty of
Worcester Polytechnic Institute
In partial fulfillment of the requirements for the BS in ME*

[4/28/2016]

Submitted By

Cameron DeWallace

James West

Justin Hence

Sponsor

MilliporeSigma

Advisor

Pradeep Radhakrishnan

I. ABSTRACT

MilliporeSigma produces single-use manufacturing plastic assemblies for biological therapeutics. Due to the very high degree of customization present in these assemblies, the associated assembly process is manual and is not necessarily scalable. Manual assembly also results in challenges such as operator fatigue and incorrect assemblies. In order to improve and overcome these challenges, the team conducted detailed research into various aspects of the Danvers Mobius Production Unit. By integrating a structured design methodology ranging from studying the current operational model, interviews with key stakeholders, observations on the shop floor to developing activity maps for the various processes, different avenues for automation were identified. After brainstorming and generating different automation concepts for various stages of the assembly operation, the team decided to focus on further enhancing concepts for tube-insertion. In particular, the focus was on inserting small tubes, which is not only a challenging and repetitive process but also causes operator fatigue. The report will detail different design and analyses carried out as well as the results from testing the fabricated proof of concept.

II. Acknowledgements

We would like to thank the entire team at MilliporeSigma for their support and guidance throughout this project. We specifically would like to acknowledge the following people at their Danvers Manufacturing Plant:

- Ataa El-Roby, Engineering Manager, Process Automation
- Kevin L. Roy, Head of Engineering
- Tom Maloney, Process Engineering Manager
- Steve Corum, Engineering Systems Development Administrator

We also would like to thank the faculty and staff in ME Department especially Barbara Furhman, Administrative Assistant VI, ME department, Peter Hefti, Manager-Experimentation Lab and the staff at the office of Corporate Engagement especially Sharon Deffely and Shiela Bailey for their help at various stages of this project.

Finally, we would like to thank our advisor, Professor Pradeep Radhakrishnan, for his guidance and input throughout this project.

This work is dedicated to my family and friends.

- Cameron

I would like to dedicate this paper to my friends and family who have been there for me throughout my time in this program. A special thanks to my grandmother, Ma, you may not be here physically but you will always be in my heart.

- James West

I dedicate this work to my family and friends who have offered their support while I was in school.

- Justin Hence

III. Executive Summary

The Danvers manufacturing plant of MilliporeSigma manufactures disposable pharmaceutical grade mixing assemblies. These assemblies produced in their facilities production room ‘Mobius’, can consist of as few as a couple components to several hundred components. Due to these variations in their product assemblies, the assembly process employed at their facility is still largely manual. This has impacts on their production and scalability. The manual assembly activities also have an indirect cost on the organization because of the ergonomic effects these processes have on the concerned operators. Therefore, the team was tasked to identify assembly activities that are suitable for automation and suggest suitable and scalable designs for the same.

A. Approach

The project team initiated activities in the project based on techniques in new product development that involves understanding and assessing customer requirements, brainstorming and developing design concepts, analyzing, testing and prototyping of possible solutions. The first step in the process was to gain significant understanding of the activities at the Danvers plant. Observational visits to the plant and Mobius clean room facility as well as interactions with site management were organized. Various aspects of manufacturing such as bag manufacturing, port sealing, and assembly activities such as tube insertions, clamping, packaging and testing were witnessed by the team. During visits to the assembly room, the team observed that the assembly process begins with the operator collecting different components unique to a

specific product to their workstation. The components include tubes, connectors, clamps, filters and bags and can be of varying dimensions. The assembly task was divided into sub-assemblies. The team observed that the operator's general operational process for each sub-assembly was to pick up tubes and clamps, insert the clamp onto the tube and then proceed to insert the connector into the tube and finalizing the process by aligning the clamp and clamping with a pneumatic crimper, or for specific cases a simple crimper. Similar activities were witnessed for other assemblies. Such visual observations enabled the team to develop detailed activity diagrams using which the team arrived at theoretical values for process times and also identified critical ergonomic aspects in the work flow.

The activity diagrams, timing data and operator ergonomics were key factors while brainstorming conceptual designs for automating different sections of the assembly process. The most time consuming and ergonomically challenging activity that the team found through visual observations and theoretical studies was the tube insertion process. The site management concurred with the observations and the team proceeded to develop design concepts for automating the process of tube insertion to various connectors. The team decided to focus on developing a machine concept that could be used on a majority of assemblies specifically ones where the tube diameter sizes range from 0.125 in to 0.25in; the reason for this choice is that repetitive activity is a real concern for the operator ergonomics.

B. Design Results and Analysis

Following a highly iterative process along with taking the constraints related to cleanroom operations into account, the team arrived at a semi-automated design for the tube insertion process as shown in Figure 1. As shown in the figure, our team chose to employ the use of a mandrel based tube support system with a ball screw propulsion system and linear rail & cart system along with a generalized clamping mechanism. In this design a mandrel is introduced to support a tube being inserted onto a connector piece; the mandrel is a long thin rod that has a tube inserted onto it before operation. This member is an integral part of this mechanism, and various diameter mandrels can be used for varying tube diameters.

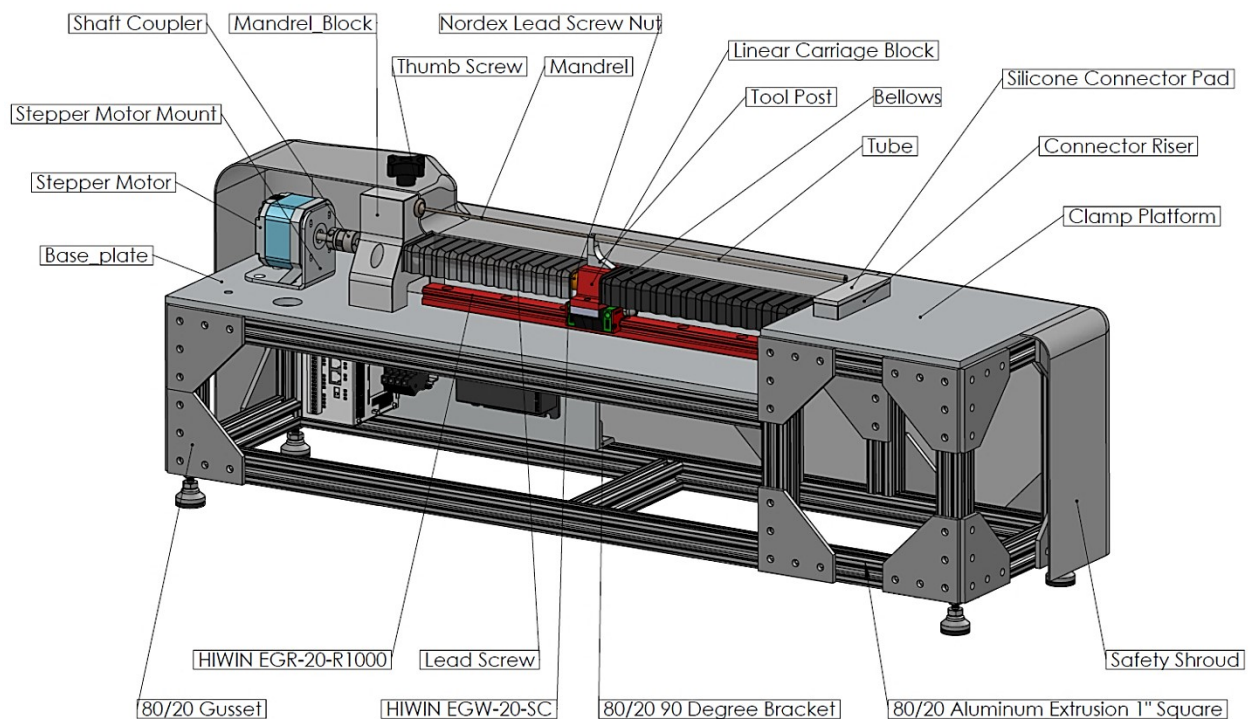


Figure 1: Isometric view of the machine proposed for automation

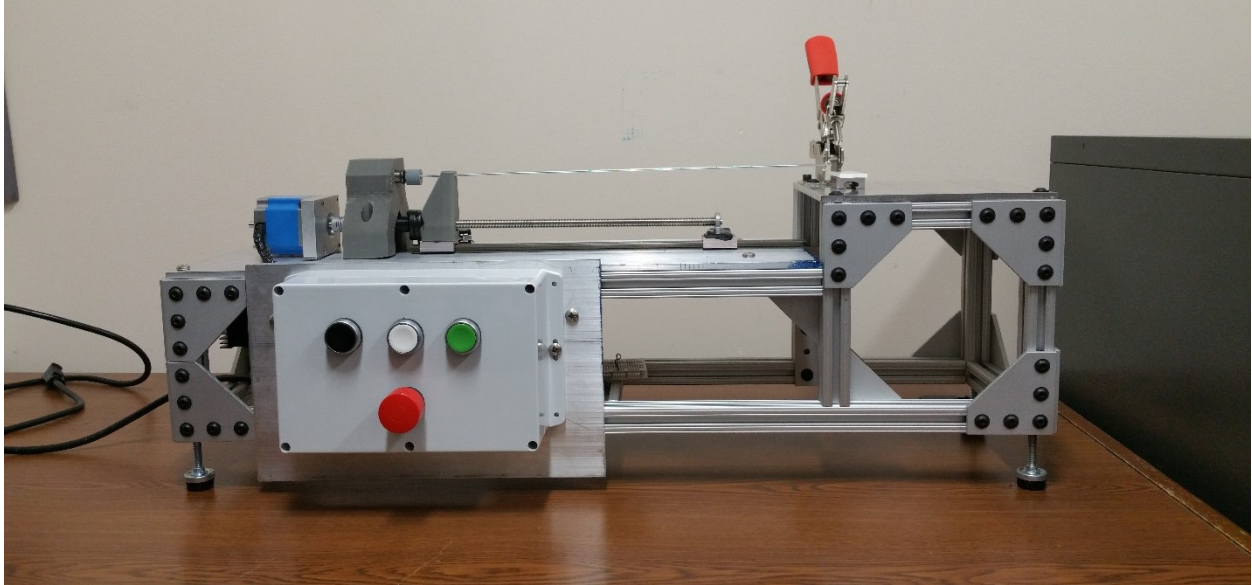


Figure 2: Proof of Concept Mechanism

The process of tube insertion for this machine begins with the operator loading a tube onto the mandrel and placing the desired connector under the clamp. After the operator is clear of the clamping zone they proceed to use the toggle clamp to secure the connector in place. With the tube inserted and the connector clamped the operator proceeds to use the control panel to activate the mechanism.

The team also conducted a fatigue analysis of the mandrel, as it is the critical component in the system due to its susceptibility to bending and deflections, and predicted a standard life of 10 million cycles under standard operating conditions with a relatively high safety factors for stress (7.6) and buckling (6) using material characteristics of an ASTM CF 8M stainless steel mandrel. The team also performed a dynamic analysis of the system using the bond graph approach and in the process estimated damping characteristics of the tube being inserted.

The team also conducted detailed FMEA that helped identify improvement aspects and a few have already been incorporated into the system shown in Figure 1. In addition, we have developed a hypothetical standard operating procedure in the event of this design being used in a production environment.

C. Recommendations for Future Work

Incorporating techniques to mitigate the friction between the mandrel and the tube would be important in order to make this concept production ready. Similarly, other issues identified in the FMEA that are yet to be tackled have to be completed. Besides, custom-made adjustable toggle clamps can be incorporated that can deliver forces suited to individual assemblies. Automating insertion of tubes on to the mandrel through a storage container and clamping of connectors are other avenues for future work in addition to testing with multiple tubes and connectors.

In realizing the proof of concept machine our team found that much of the translational energy was being converted into buckling of the tube. To fix this we propose the use of our initial outer diameter friction gripping method to prevent this buckling from happening. Figure 12 will highlight the design of such a gripper. This mechanism would be integrated onto the ball screw of the machine to move in series with the pushing mechanism.

IV. Table of Contents

1. Introduction	1
A. Project Goals:	4
2. Methodology.....	5
A. Process Understanding and Data Collection	6
B. Methods Understanding	9
C. Ergonomics.....	9
D. Timing.....	10
E. Safety and Clean Room Constraints	10
3. Machine Design.....	13
A. Gripping	15
B. 6-3-5 Designs	19
C. Integration of Individual Automation Concepts.....	21
D. Material Selection	25
E. Proof of Concept.....	26
F. Design Finalization and Analysis	28
i. Machine Sizing.....	28
ii. Materials Selection	30

iii. Static and Fatigue Stress Analysis	32
iv. Dynamic Modeling of the system.....	38
v. Failure Mode Effects Analysis (FMEA)	45
4. Conclusions	49
5. Recommendations and Future Work	51
6. References	54
7. Appendix A: Theoretical Timing Data	55
8. Appendix B: Mandrel Stress Analysis.....	58
A. Mandrel Static Stress Analysis.....	58
i. Material Properties	58
ii. Piece Dimensions	58
iii. Silicone Tubing	59
iv. Stress Concentration Factors	59
B. Force Analysis and Singularity Functions	60
i. Step Function.....	60
ii. Weight Functions of the Mandrel.....	60
iii. Weight Functions of the Tube	60
iv. Static Stress Analysis for a Cantilevered Configuration	60

v. Reactionary Components.....	60
vi. Shear Function.....	61
vii. Moment Function	61
viii. Slope Function.....	61
ix. Deflection Function	61
x. Static Stress Analysis Under Mandrel and Tube Weight	61
xi. Principal Stresses.....	61
xii. Von-Mises Stress.....	62
xiii. Static Elastic Safety Factor	62
xiv. Modified Mohr Theory.....	62
xv. Buckling Analysis of the Mandrel.....	62
xvi. Assumptions	62
C. Fatigue Analysis.....	64
i. Assumptions	64
ii. Notch Sensitivity Factor	65
iii. Alternating and Mean Components of Stress.....	65
9. Appendix C: Design Concepts	67
10. Appendix D: Brain-Mapping Diagrams for Unused Projects.....	83

V. List of Figures

Figure 1: Isometric view of the machine proposed for automation.....	vi
Figure 2: Proof of Concept Mechanism.....	vii
Figure 3: Sample Assembly 1 (10 total components) from MilliporeSigma.....	2
Figure 4: Sample Assembly 2 (40 total components) from MilliporeSigma.....	3
Figure 5: Flow chart describing methodology used.....	5
Figure 6: Flow Chart Describing Timing Data.....	8
Figure 7: Diagram describing design methodology.....	12
Figure 8: Process Mind Mapping Diagram.....	14
Figure 9: Grasping Figures Techniques from [6].....	16
Figure 10: Jamming Grippers [6].....	16
Figure 11: Component Grasping Idea 1 “Roller grip”.....	18
Figure 12: Friction Gripper Concept.....	18
Figure 13: 6-3-5 Design Concept of General Clamping.....	20
Figure 14: Re-Done Initial Mandrel Tube Support System.....	21
Figure 15: General Mandrel Support Tube Translational Insertion Concept.....	22
Figure 16: Mandrel Block and Force Plate Concept.....	23
Figure 17: Design Iteration with ball screw, padded platform.....	24
Figure 18: Current Design Concept Render.....	25
Figure 19: Proof of Concept Mechanism.....	27

Figure 20: This chart is sample data generated by analysis of 96 assemblies from a list provided by <i>MilliporeSigma</i>	28
Figure 21: This chart shows the quantity of tube Inner Diameters found in our data acquisition	29
Figure 22: Material Strength Comparisons [10], [11]	31
Figure 23: Fracture Toughness of Materials	31
Figure 24: Strength to Weight Ratios	32
Figure 25: Mandrel Reference Diagram	33
Figure 26: Mandrel Finite Element Analysis: Von Mises Stresses	37
Figure 27: Mandrel Finite Element Analysis: Deflection.....	37
Figure 28: Stainless Steel Mandrel Fatigue Life Diagram.....	38
Figure 29: Empirical Test Configuration for K Coefficient	40
Figure 30: Empirical Test Method for Damping Coefficient	40
Figure 31: Cross Sectional View of the Core Mechanism.....	41
Figure 32: Casual Bond Graph of our System	42
Figure 33: Lumped Parameter Simplified Model	44
Figure 34: Normalized Amplitude of Oscillation at Tool Post During Insertion	44
Figure 35: Pneumatic Connector Clamping Device	67
Figure 36: Pneumatic Wide Range Clamping Device	68
Figure 37: Retracting Connector Clamping Mechanism	69
Figure 38: Pneumatic Connector Clamp.....	70
Figure 39: Pneumatic Connector Clamping Device	71

Figure 40: Connector Specific Clamp Tooling.....	72
Figure 41: Tube Gripper for a Large Range of Sizes.....	73
Figure 42: Soft Concave Connector Pads for Clamping.....	74
Figure 43: Part Dispensing Machine.....	75
Figure 44: Part Manipulation and Delivery	76
Figure 45: Pneumatic Part Delivery System.....	77
Figure 46: Part Organization as well as Part Delivery.....	78
Figure 47: Connector Dispenser for Quick Part Kitting.....	79
Figure 48: Part Delivery System.....	80
Figure 49: Automated Part Dispenser and Delivery System	81
Figure 50: Room Optimization and Part Delivery System	82
Figure 51: Zip Tie Process Diagram.....	83
Figure 52: Connector Assembly Process	84
Figure 53: Oetiker Clamping Process.....	85
Figure 54: Room Optimization and Material Presentation Process.....	86

VI. List of Tables

Table 1: Properties of Proposed Materials[10], [11]	30
Table 2: Mechanical Translation and Rotation Quantities [13].....	39
Table 3: Design failure mode effects analysis (DFMEA)	46
Table 4: Generalized Timing Data for Assemblies.....	55
Table 5: Theoretical Timing for Assembly X.1	56
Table 6: Theoretical Timing Data for Assembly X.2	57

VII. Nomenclature

Term	Meaning	Variable	Meaning
Mandrel	Long support rod	$q(x)$	Loading Function
O. D	Outer Diameter	$V(x)$	Shear Function
I.D	Inner Diameter	$M(x)$	Moment Function
ksi	Kilo-Pounds per square inch	$\Theta(x)$	Slope Function
S_y	Yield Strength of the Material	$\delta(x)$	Deflection Function
S_{UT}	Ultimate Tensile Strength of the Material	k_t	Stress Concentration Factor
S_{uc}	Ultimate Compressive Strength of the Material	σ_1	Principal Stress
S_{ft}	Material Fracture Toughness	σ_2	Principal Stress
S_e	Corrected Fatigue Strength	σ_3	Principal Stress
R	Material Density	σ_{von}	von Mises Stress
D	Large Diameter of Mandrel Base	N	Yield Stress Safety Factor
D	Mandrel Operational Diameter	N_{UTS}	Modified Mohr Safety Factor
R	Fillet Radius of mandrel	k_f	Notch Sensitivity Factor
$l_{mandrel}$	Length of the Mandrel	N_f	Fatigue Safety Factor
$J_{mandrel}$	Polar Moment of Inertia of the Mandrel	E	Modulus of Elasticity
w_m	Weight of the Mandrel per inch	C_1	Tensor Invariant
w_t	Weight of the Tube per inch	C_2	Tensor Invariant
σ_a'	Alternating Principal stress	C_3	Tensor Invariant
σ_m'	Mean Principal Stress		

1. Introduction

MilliporeSigma is an international leader in life sciences and pharmaceutical product production. The manufacturing of pharmaceutical filtration systems and pharmaceutical mixing products is one the company's largest endeavors. At their Danvers, MA plant, the biggest production is in their Mobius assembly facility, which manufactures disposable pharmaceutical grade mixing assemblies. The current process for product assembly is mostly done manually. This is due to extremely diverse customer requirements, making repeated manufacturing seldom done. These requirements for custom products has made it particularly difficult to implement any automation into the production line, leading to high cost, capacity constraints, and long lead times for product manufacturing.

These assemblies were observed to contain from only a few parts, less than 5, to over 50 components. Each of these assemblies also ranges in part geometry and function, which leads to different operational models for product assembly and the need for scalability.

An example assembly is shown in below. As seen in Figure 3, there are only a few components used. In Figure 4, however, there are many more components present which are unique in geometry and function. All the components such as bags, connectors, tubing, clamps, filters, etc. that are unique to a specific assembly are collected by the operator. The operator then manually connects different components as per the standard operating procedures laid out. Considerable manual force is then exerted from the person's wrist to ensure proper connection between components. Considering the fact that there are many assemblies completed by an operator during a shift and that the number of sub-assemblies can range, the operator's arms and wrists are under considerable strain due to the repetitive nature of the activity. This, in the long

term, affects productivity because of worker fatigue. Thus operator ergonomics is an important consideration in this project.

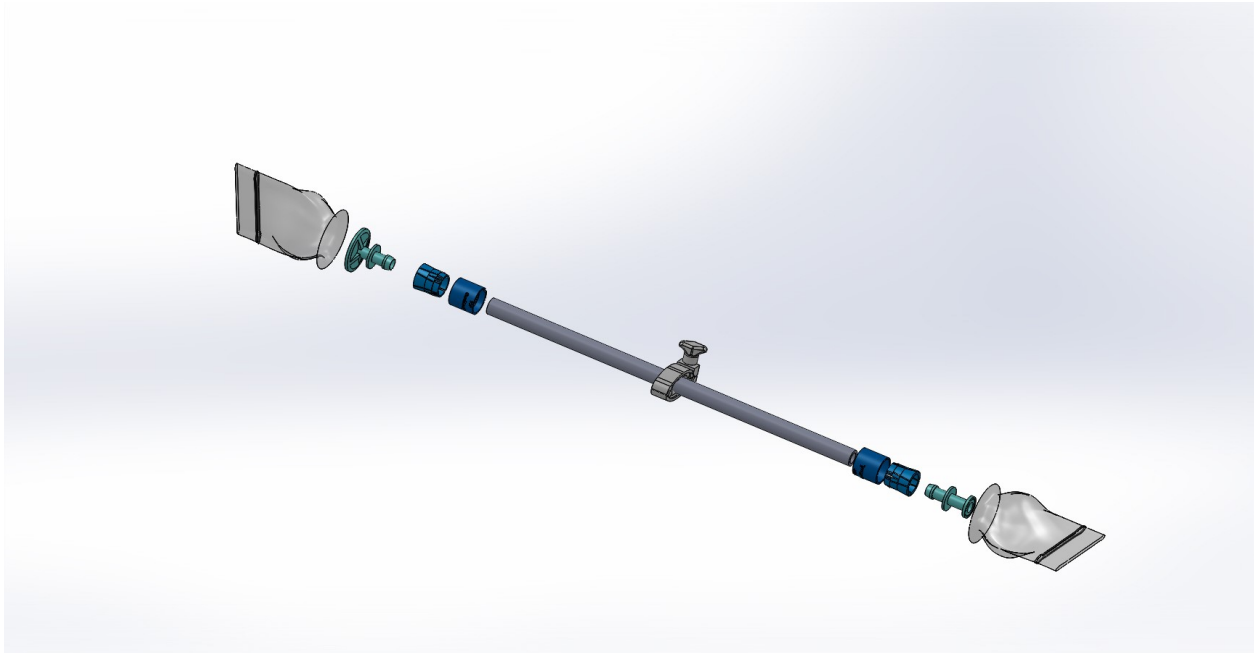


Figure 3: Sample Assembly 1 (10 total components) from MilliporeSigma

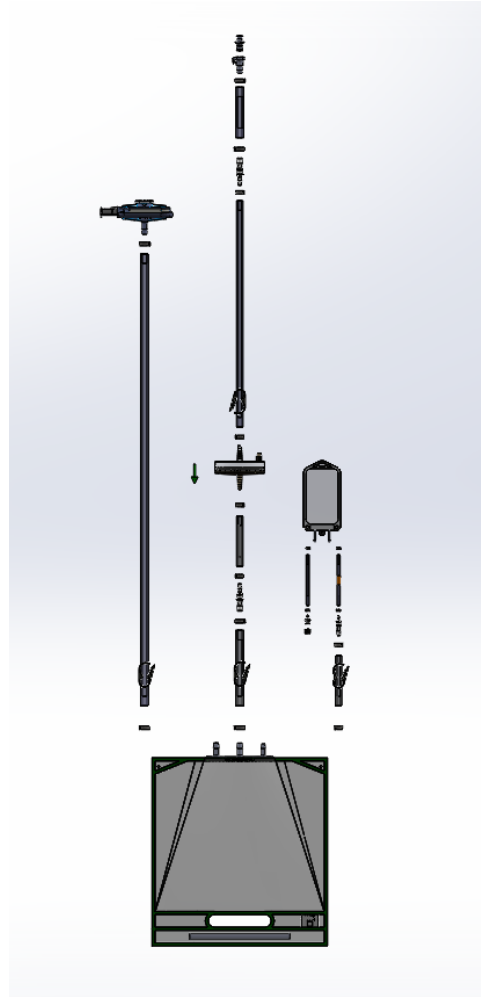


Figure 4: Sample Assembly 2 (40 total components) from MilliporeSigma

It can be noted that each assembly consists of different types of components but also a different amounts and positioning. Thus, due to this being highly manual there is a large impact on assembly time and throughput. Therefore, in order to tackle the twin aspects of improving productivity and enhancing operator ergonomics, the project aims to apply different methods in design theory and new product development to design a comprehensive and scalable automation solution.

A. Project Goals:

In order to present a comprehensive and scalable automation solution to tackle the twin issues of productivity and ergonomics enhancements, the project team set the following goals:

- i. Gain an in-depth understanding of the different assembly processes through process visualization, interaction with operators and site management
- ii. Develop activity maps of various operations and develop theoretical timing data so as to compare and narrow project focus area
- iii. Identify different segments and assembly aspects for automation and generate concepts through various techniques in new product development. Obtain feedback from site management to narrow project focus
- iv. Develop detailed designs for the focus area and carry out detailed static, dynamic and failure mode effects analysis (FMEA)
- v. Develop and test proof of concept and provide recommendations

2. Methodology

The methodology adopted to execute this project is illustrated using the flow chart shown in Figure 5 where the overall objective, which is to identify potential automation opportunities, is listed. As shown in the flow chart, automation could be partial or complete but in either case the team envisions a scalable solution applicable to various configurations.

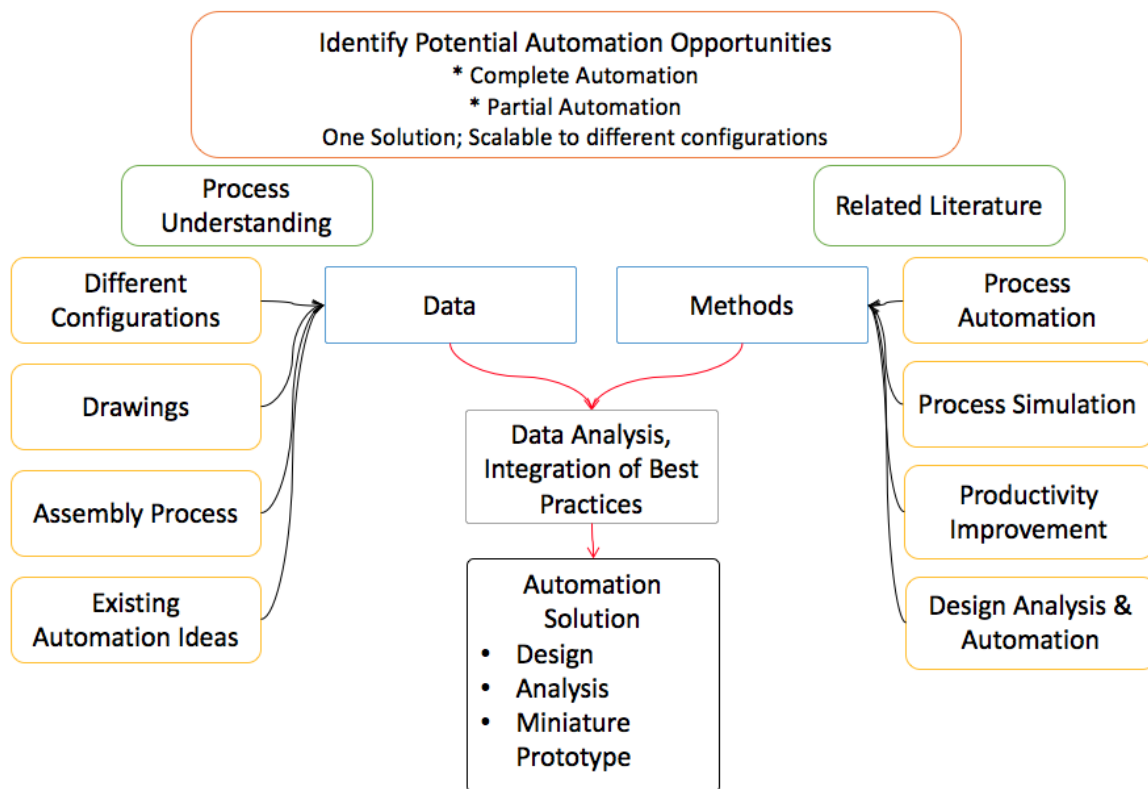


Figure 5: Flow chart describing methodology used

To identify these automation opportunities within the Danvers manufacturing plant, the team embarked on a twin strategy of developing an in-depth understanding of the process as well as reading related literature to keep up with technological updates in design and automation development. Process understanding process involved exploring and observing the assembly processes, understanding the different configurations, their drawings and also gaining a sense of

all the existing automation ideas that are in the pipeline. These activities (explained in detailed in the following sub-section) gave the team all the data required, which when combined with the methods in the literature helped the team arrive at a focus area for automation. Once the area for automation was identified, steps were initiated to generate concept designs, which were then finalized and analyzed following which a miniature prototype was developed.

A. Process Understanding and Data Collection

The project started with a general meeting with the engineering teams from Millipore Sigma where the broad spectrum desires for part of factory floor, spanning the entire clean room facility, were discussed. Our team proceeded to, during subsequent visits, tour the clean room facility and observe some of the processes happening in the 10,000 (particle count) clean room. Our team was guided through the facility by the engineering services manager, Ataa El-Roby, who explained the flow of the room and each process including bag manufacturing, tube-connector insertion, tube-clamp insertion, tube-clamp clamping and final goods assembly and packaging. Each activity posed a potential automation opportunity to be explored by the team.

As the team went through this process, it was important to understand the different assemblies produced in the plant. In order to do, MilliporeSigma provided the team with access to their repository of CAD models and drawings. Using appropriate macros, the team automatically generated bill of materials for a representative sample of close to 100 designs (out of several thousand) to identify the most common components across different assemblies. It was found that of all of the various components, including tubing, connectors, connection clamps, bags, tube clamps and filters, the most common denominator are tubes, connectors and Oetiker clamps. Besides, the assembly of these components was time intensive and posed a potential

automation opportunity. Our detailed findings from this study are presented in the Observation and Data Studies section.

During our shop floor visits, it was noted that the layout of the floor was dynamically changing based on the current operations. This evolving room layout was notably observed during three separate visits. The factory also had several mishaps where entire bags of components were dropped onto the floor rendering them unfit for use in pharmaceutical grade assemblies. In the transfer of parts, an operator spends considerable time transporting components to their workstation, a time which can be potentially reduced through automation. Therefore, orientation and delivery methods for the clean room was one of the potential focus for automation.

The last area of potential interest to our team was automation for the packaging of final goods. It was noted, during our observation sessions at the facility, that there were two tables with approximately eight operators in teams of two packaging final assemblies into various sized plastic packaging bags. These operators used various techniques, based on the assembly geometry and materials, to secure the assembly into its packaging. From our initial observations it was noted that automation of this process could alleviate the need for packaging efforts and re-allocate more work force into assembly production, as well as provide a large reduction in time spent on a single task and improve workplace ergonomics.

Though different automation opportunities were identified, they were based on the activity presented in the chart shown in Figure 6 below. As you may see from the figure, the assembly drawings of components can be used to generate manual assembly sequence and estimate theoretical times and that data can be used to compare with the time study of existing practices on the assembly lines. The differences encountered actually validated the different

opportunities for automation. Furthermore, during a meeting with the MilliporeSigma team, we had been made aware that their teams were already looking into the automation possibilities for the final goods packaging process. We were also advised to drop the component transfer and assembly line automation research for a similar reason. Our team then proceeded with the automation of tube-connector insertion process. Also, for optimal use, we were advised that the machine should have the ability of being process ready for varying component geometry at the discretion of the daily production load. By having a design that scales in use to larger or smaller components, production rates can be improved significantly.

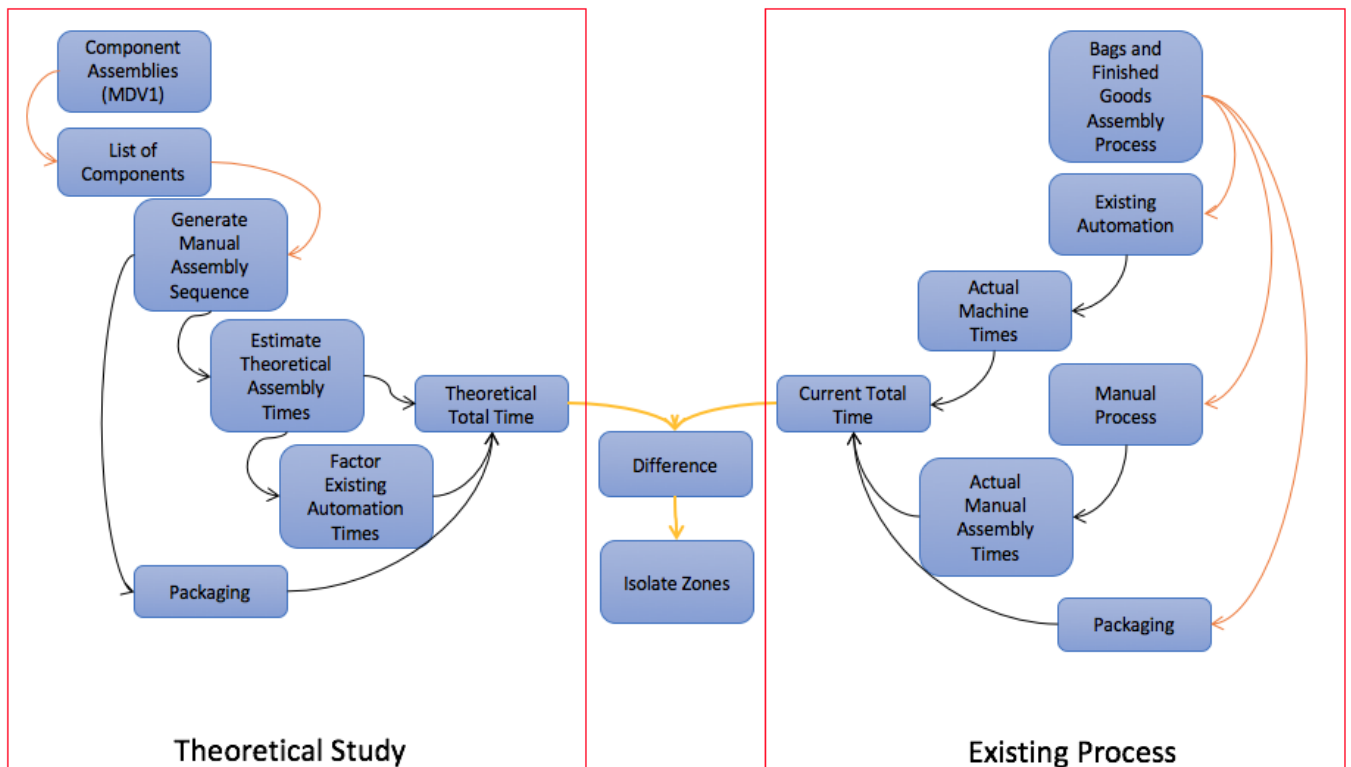


Figure 6: Flow Chart Describing Timing Data

B. Methods Understanding

To best suit the needs of building a project around the automation of a manual assembly, our team researched the general topic of automation and the key concepts in realizing a functional design. This research was based on readings from Manufacturing Engineering and Technology and separate sources on process capability, silicone rubber material properties, fastener research, grasping devices and failure mode and effects analysis[1]–[6].

C. Ergonomics

One of the main concerns voiced by the MilliporeSigma team is related to the operator ergonomics, as that has the most considerable impact on the assembly process. Due to the highly repetitive nature of the assembly process, operators have to constantly exert a force onto joints. This process carried out repeatedly over a 10-hour shift causes strain and an increasing process delay over time, decreasing the quality of operator production rates on the factory floor. According to the United States Department of Labor, Occupational Safety & Health Administration (O.S.H.A), there are specific musculoskeletal disorders (MSD's) that can affect operators exposed to highly repetitive tasks [7]. The MSD's, according to O.S.H.A, that can affect operators in tasks such as these include,

- Carpal tunnel Syndrome
- Tendinitis
- Rotator Cuff injuries
- Epicondylitis of the elbow
- Trigger Finger
- Muscle Strains

These effects of these tasks can accumulate over time and in the U.S account for 33% of operator injuries [7]. According to law, employers are responsible for the operator's wellbeing in and caused by the working environment. To combat the issues caused by these highly repetitive process, the operators at the Danvers facility are mandated to do wrist exercises to prevent such issues. Due to this process being part of the operator's normal shift, the company loses additional production time from an operator's normal shift.

D. Timing

In any assembly, process time can be equated to money value of each assembly, and the amount of time spent on each assembly translates both into the actual value of the assembly, operator ergonomics and operator fatigue. For this project, the theoretical time for producing different assemblies were computed using techniques presented in the book titled Assembly Automation and Product Design by Boothroyd and Dewhurst [8]. In the book, Boothroyd and Dewhurst present theoretical time estimation techniques based on part size, geometry, gripping method, alignments, plastic deformations, and mechanical fastening processes. The timing data can be used to compare actual process and obtain conclusions as was done in this project and explained in the previous sub-section on process understanding. Detailed timing data is presented in Appendix A.

E. Safety and Clean Room Constraints

In any production environment where there are operators involved, the safety of the operators is of the highest concern. Operator injury is considered the most extreme case in factory floor safety and this realization has also permeated the design aspect of our project. Postulated methods for machine safety include the use of light curtains, bellows, preventative

shells, emergency stops, and electrical shielding. Using these types of safety features would prevent operator injury to ensure smooth production.

To capture these issues, detailed Failure Mode Effects Analysis (FMEA) is carried out – both at the initial design phase and at the post design phase. The use of this failure model allows the user and production facility to predict and prevent any form of process interruption, operator injury, machine damage and final assembly damage or need for rework. The methods for FMEA were adapted from the work done by [1].

The clean room facility in MilliporeSigma’s Danvers plant had two rooms with different clean room standards. The clean room classifications at the Danvers facilities were 10k and 100k. Our team operated within the 10k clean room, where the main production of assemblies and packaging took place. Within these rooms the particle generation in any process must be kept to a minimum to provide a high quality of standards. Thus, our goals were to keep any frictional interactions to a minimum, and to a lesser degree. The methodology and material selection process for these reasons are presented in the methodology section and the results are shown in the results section of this paper. With safety and particle generation being of a large concern our team’s goals were to also introduce an overall safety mechanism that reduces the possibility of particle escape and protects the user from any form of bodily injury or from damaging the machine.

Referring back to Figure 2, the data as a result of process understanding and methods from various literature have been useful in isolating potential automation zones (as illustrated in Figure 3). It has already been mentioned that the tube insertion onto the connector is the activity that has been identified for automation. The major activities that are carried out for designing the machine are listed in Figure. As can be seen that all the processes are highly iterative in nature

with the first activity being the design concept generation process. The method that was employed was a variation of the 6-3-5 technique. The original technique involves a group of 6 students, who generate a list of 3 ideas of interest, and after 15 minutes the “round” ends and the design sheet is passed to the next person who reads it and either adds constructive criticism or another idea in the next five to 10 minutes; this process is repeated until the idea sheet returns to its original owner [1], [9]. The designs generated using this process is then vetted and then the most promising design is selected for detailing and subsequently analysis and prototyping. The detailed development process is explained in Chapter 3.

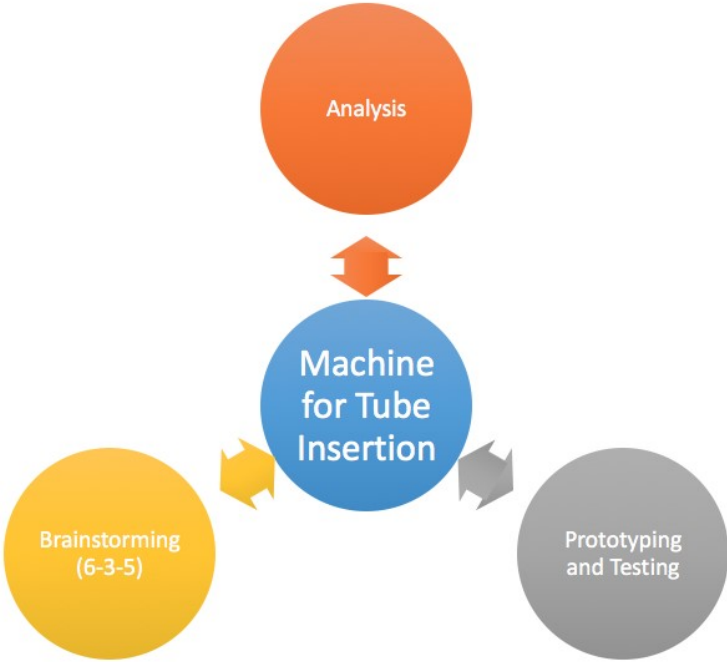


Figure 7: Diagram describing design methodology

3. Machine Design

In order to develop a machine to automate the process of tube insertion, concept generation was an important step. In order to generate machine concepts, it was important to understand the activities carried out by the operator so that we are able to replicate the operation sequence. The activity diagrams helped in identifying individual automation possibilities that could be amalgamated in a unified machine. One of the list of activities carried out by the operator, tube insertion, is presented below in Figure 8.

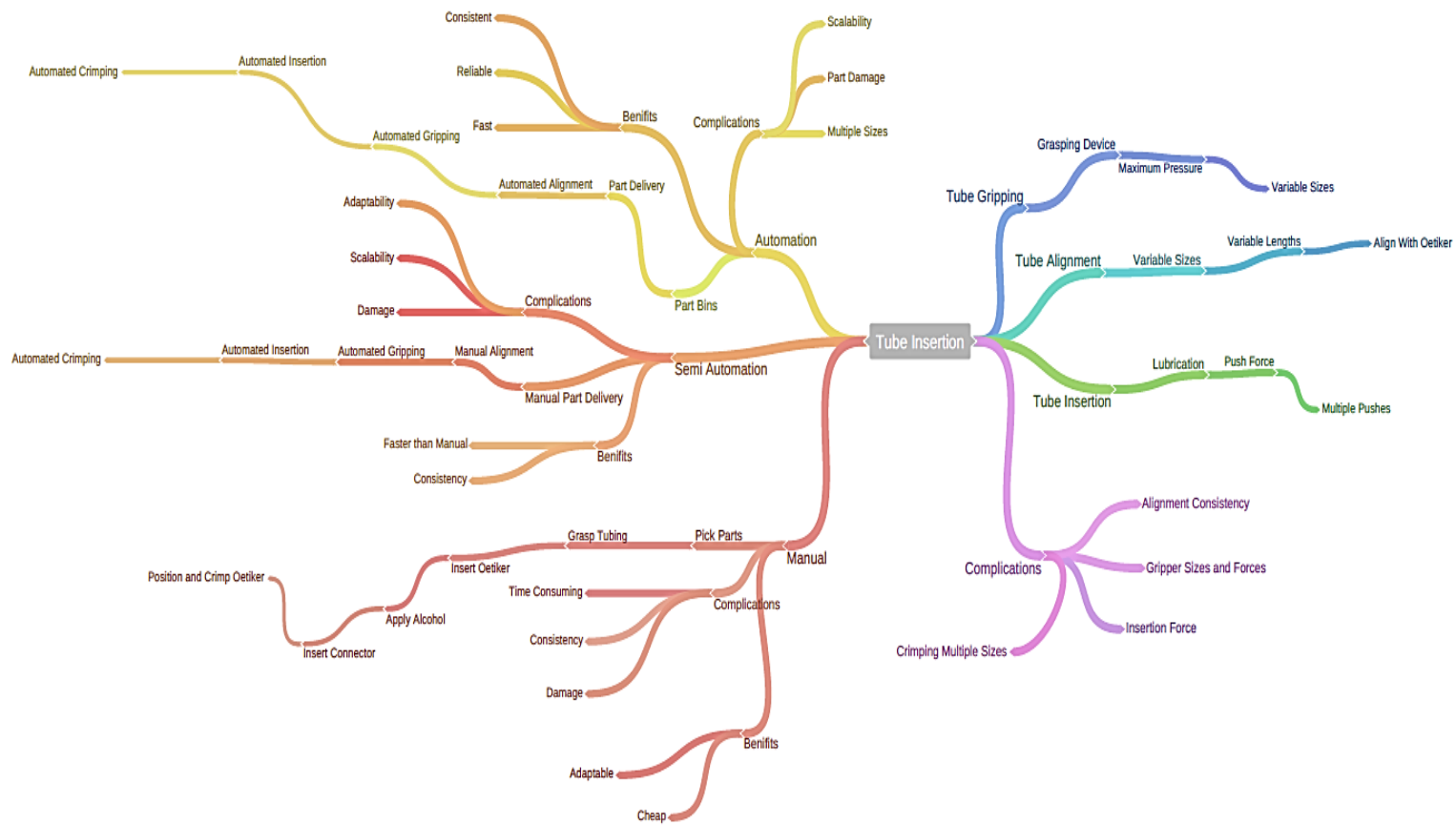


Figure 8: Process Mind Mapping Diagram

The activity diagram shows that the operator grips the tube and the connector and is forces the tube on to the connector, thus gripping is an important aspect in the project. Refer to Appendix D for all mind maps created.

A. Gripping

Our team used methods described in [6] to facilitate the generation of component grasping to aid in the individual processes, some of which are shown in Figure 10 (reproduced from *Grasping Devices and Methods in Automated Production Processes by Fantoni et al*). Using these methods, our team decided to conceptualize the potential use of friction gripping, jaw gripping, suction gripping, and Bernoulli gripping techniques to enhance gripping. Prior concepts for mechanism control, support and force exertion were also used in the conceptual process. Besides, our team looked into the use of jamming grippers, Figure 9, to provide a scalable gripping mechanism. These types of grippers allow for unique geometries to be held in place, while offering a degree of force control [6]. This approach led to several design concepts, see Appendix C, which utilized this technology to grip the highly custom geometries used in the manufacturing process at MilliporeSigma's Danvers facility.

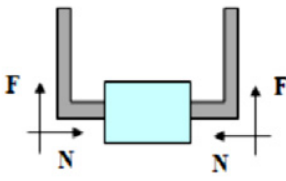
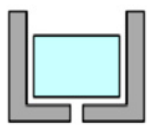
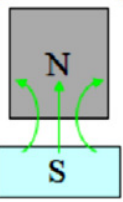
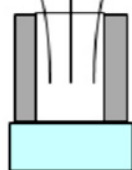
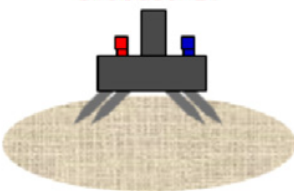
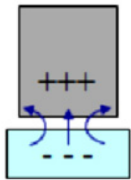
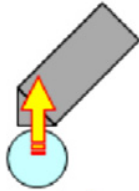
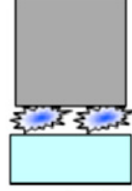
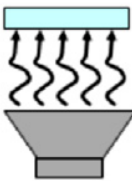
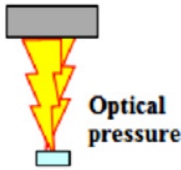
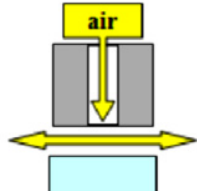
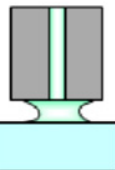
<p>Friction Gripper</p>  <p>Macro/Meso/Micro</p>	<p>Jaw Gripper</p>  <p>Macro/Meso/Micro</p>	<p>Magnetic Gripper</p>  <p>Macro/Meso/Micro</p>	<p>Suction G.</p>  <p>Macro/Meso/Micro</p>
<p>Needle G.</p>  <p>Macro</p>	<p>Electrostatic G.</p>  <p>Meso/Micro</p>	<p>Van der Waals</p>  <p>Meso/Micro</p>	<p>Ice Gripper</p>  <p>Meso/Micro</p>
<p>Acoustic G.</p>  <p>Macro/Meso/Micro</p>	<p>Laser</p>  <p>Micro</p>	<p>Bernoulli</p>  <p>Meso/Micro</p>	<p>Adhesive G.</p>  <p>Micro</p>

Figure 9: Grasping Figures Techniques from [6]

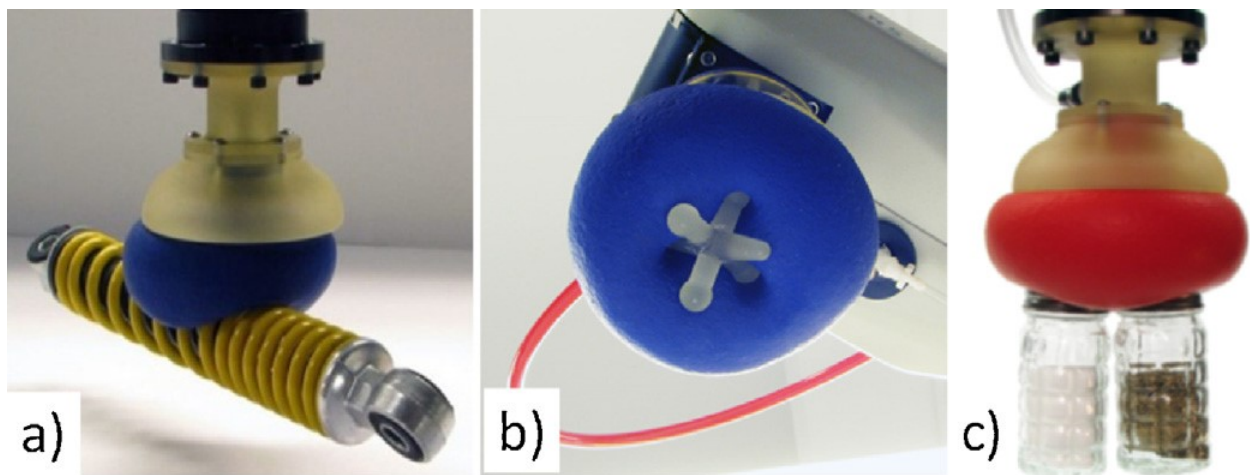


Figure 10: Jamming Grippers [6]

One of outcomes of the review on grippers is the design shown in Figure 11 , which is uses the concept of rolling rubber tubes, connected to spring loaded members to mimic basic mechanical ‘hands’. The mechanism would contact any rubber tubing parallel to three points on the tubes surface causing a high degree of friction between the gripper and the tubing. The intended action would then be performed through the mechanical translation of the ‘hand’ and thus the tube. This design concept was designed further to utilize less material while keeping the same degree of control, and in Figure 9 below this design was modeled in SolidWorks. This gripper was used in initial designs to exert the forces onto the tubing to couple them with the connectors.

This gripper design was unused in our final concept design in favor of using a single tool post to exert the required forces from the ball screw onto the tube-connector couple. It, however, was suggested in the future work section of this paper to aid in the buckling prevention of smaller tubes.

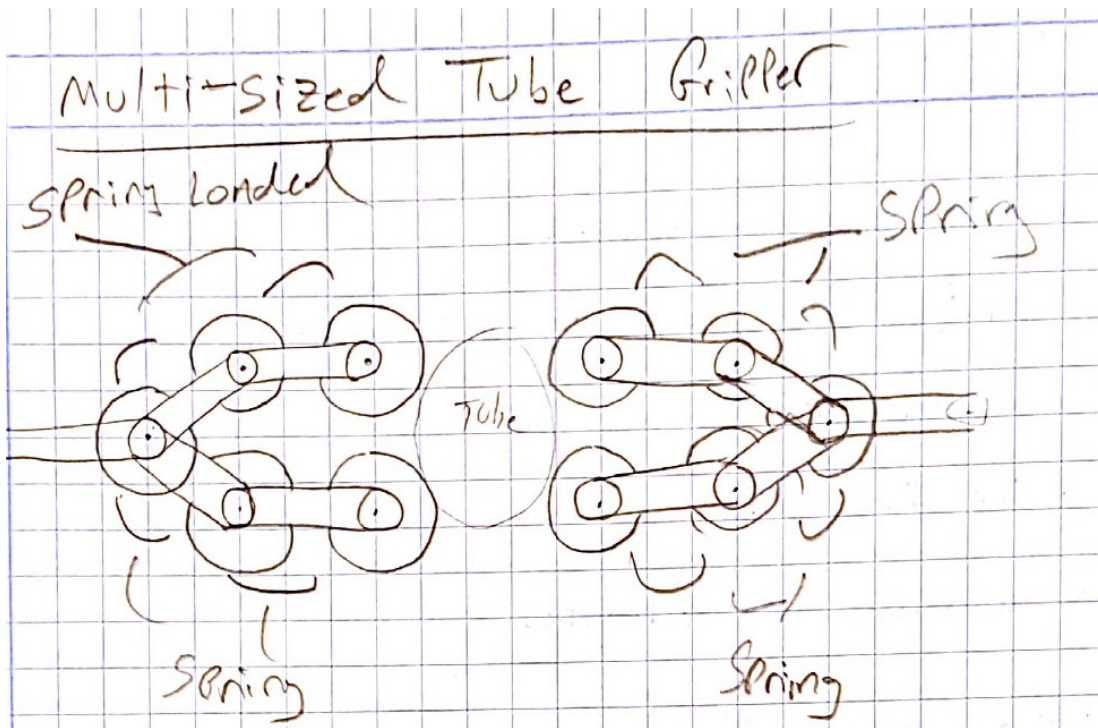


Figure 11: Component Grasping Idea 1 “Roller grip”

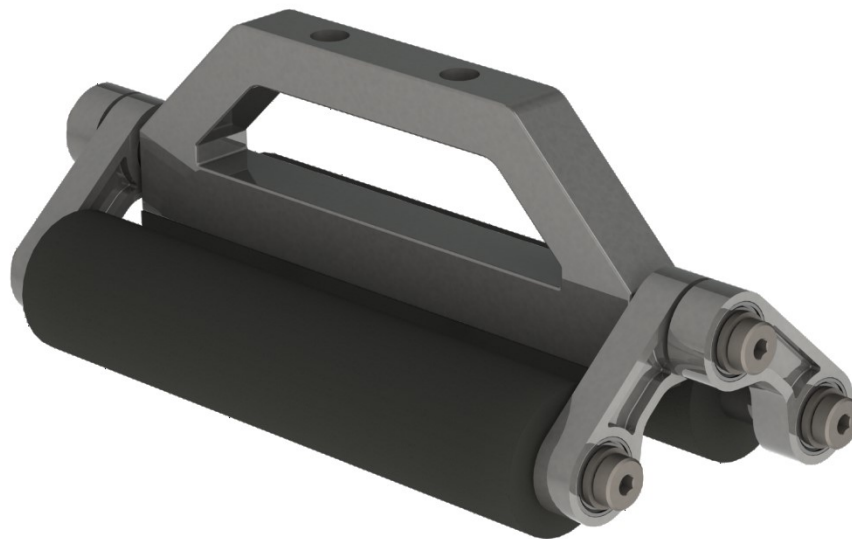


Figure 12: Friction Gripper Concept

B. 6-3-5 Designs

In order to generate concepts for this project we held a 6-3-5 design meeting. A 6-3-5 design meeting means six people generate three designs in five minutes. We adapted this for our group's needs. We set a couple of questions prompts one of which being "how to grip something". This question was broad to allow the generation of as many concepts as possible within the realm of automation. During this process our team first began with a design question and then were given time to conceptualize ideas on automation of that process. The thought process behind this method involved recalling various automation techniques studied previously to achieve the intended task. Then through concept amalgamation of like ideas, we generated basic machine design concepts. Through these initial ideas our team made design iterations by critiquing each design; this was done by adding to or taking from each idea to better suit the design to our specific needs.

Below in Figure 13 we see an example of this process. The scanned image is purely to give an example of what a result would look like. In this particular drawing the original author of this design was attempting to clamp a t-connector and in the figure each color represents each group member.

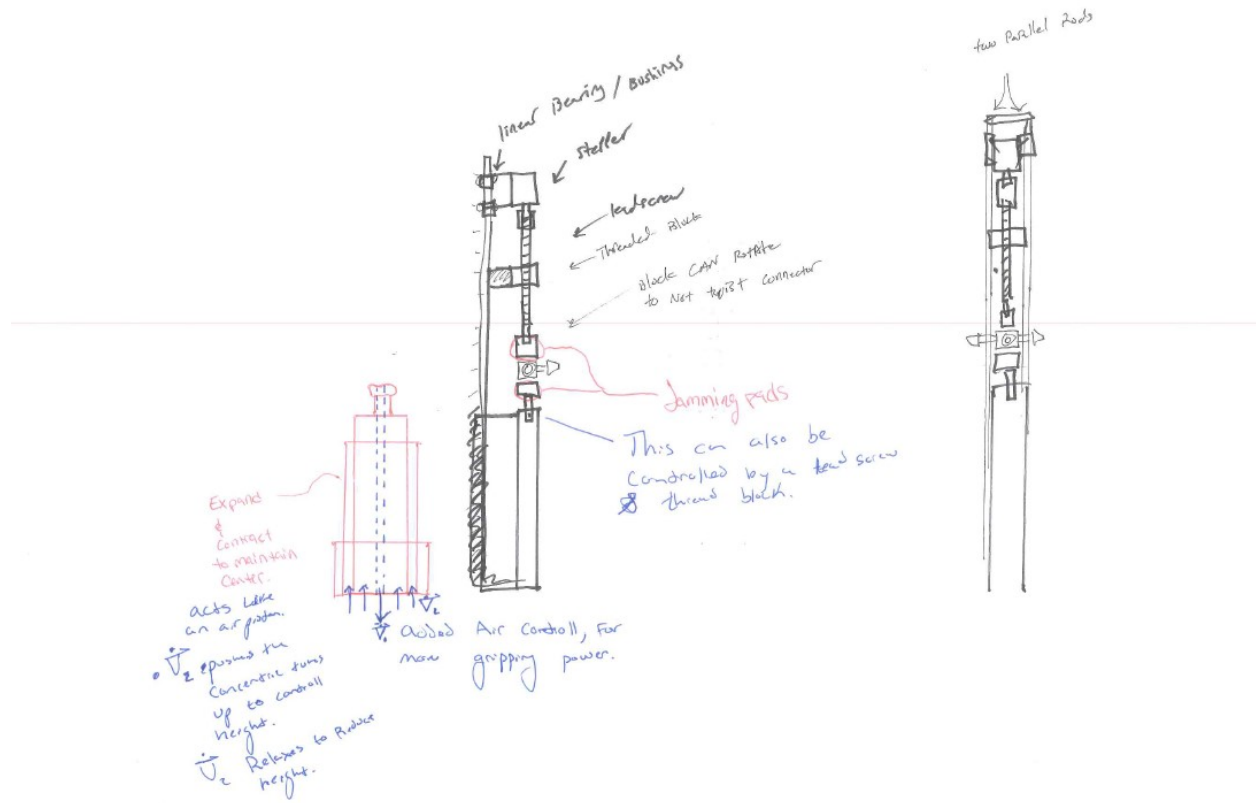


Figure 13: 6-3-5 Design Concept of General Clamping

C. Integration of Individual Automation Concepts

Following the conceptualization of several components to achieve the intended actions (or individual operator activities), our team began to hypothesize larger machine designs to perform the insertion task by integrating various designs. In Figure 14 below, we conceptualized a machine using a mandrel based support system, fed by a tube feeding chute and propelled by a tool post onto a secured connector piece to achieve the tube insertion actions needed. From this concept, the team used various ideal approaches as to how this mechanism could achieve force exertion onto the tube-connector couple. The concepts included:

- Force Application Through a Ball Screw Drive
- Pneumatic Force Plate Actuation
- Scissor Plate Force Exertion
- Gripper Based Force Methods (shown in Figure 12)

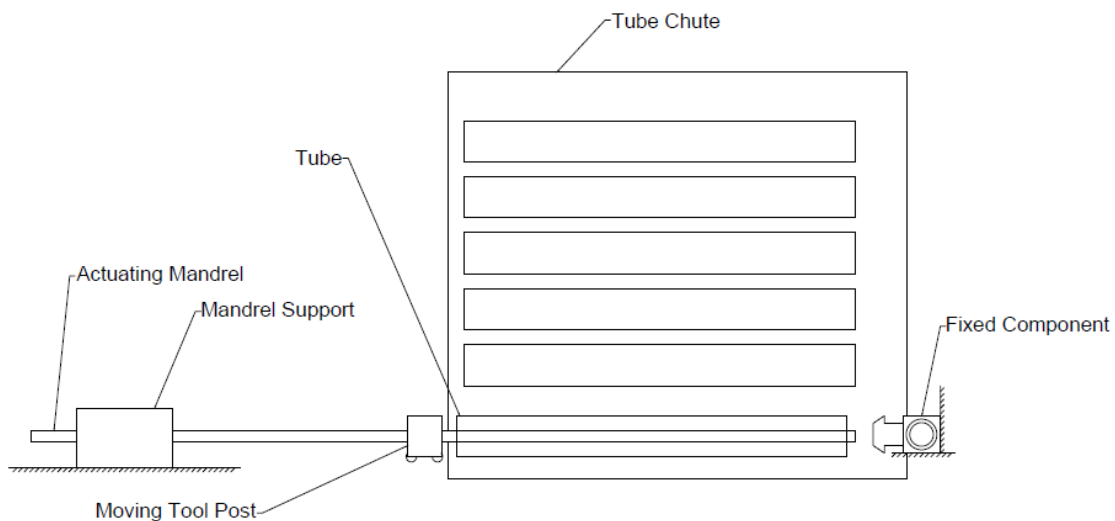


Figure 14: Re-Done Initial Mandrel Tube Support System

Figure 15 below shows one such concept, initially designed to automate the tube insertion process via a translational friction gripping action. The pivoting mandrel in Figure 15 would hypothetically allow for automatic tube feeding from an above dispensary, as well as introduce the possibility of automatic tube length cutting with diameter control. External graspers were also used to exert a force onto the tube-connector couple. Future iterations found the full automation to be undesirably restrictive to scalability. The extremely custom nature of the MilliporeSigma products lead us to the conclusion that scalability was one of the most key aspects in our machine design.

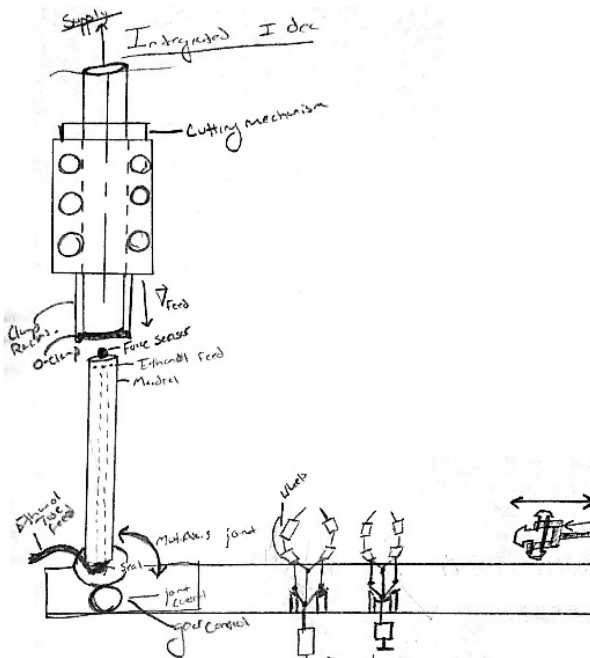


Figure 15: General Mandrel Support Tube Translational Insertion Concept

In the secondary design phase, shown in Figure 16, a pneumatic cylinder was used to exert a force onto a force plate and the tube-connector couple. This design decision was influenced by the already prevalent pneumatic systems available in the Danvers facility. The length of the machine in order to incorporate an appropriately sized pneumatic cylinder would need to be twice as long as in later designs, which changed our direction for future iterations by

excluding the use of pneumatic control force exertion. To better apply force while adhering to size constraints, our team next designed a new generation machine with the application of a ball screw.

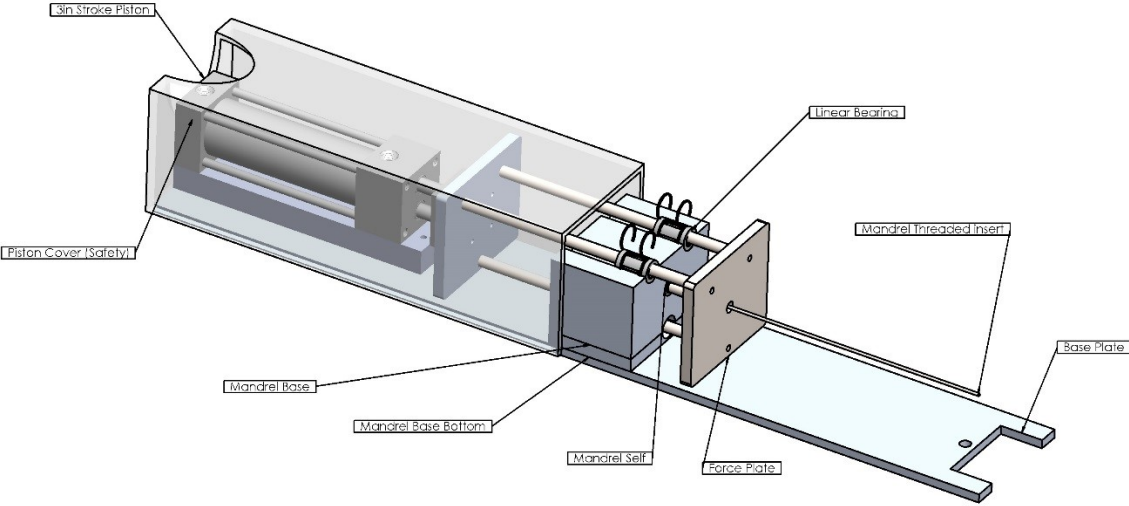


Figure 16: Mandrel Block and Force Plate Concept

Figure 17 below represents a revised design that uses a ball screw to propel the tool post forward onto a tube supported by a mandrel. Like in the previous design, Figure 16, our team again used a mandrel to support the tube’s buckling forces and vertical position restriction. In this design, however, our team sought to use an adjustable component platform and pneumatic clamp to allow the operator to adjust the padded platform to best suit the needs of the assembly.

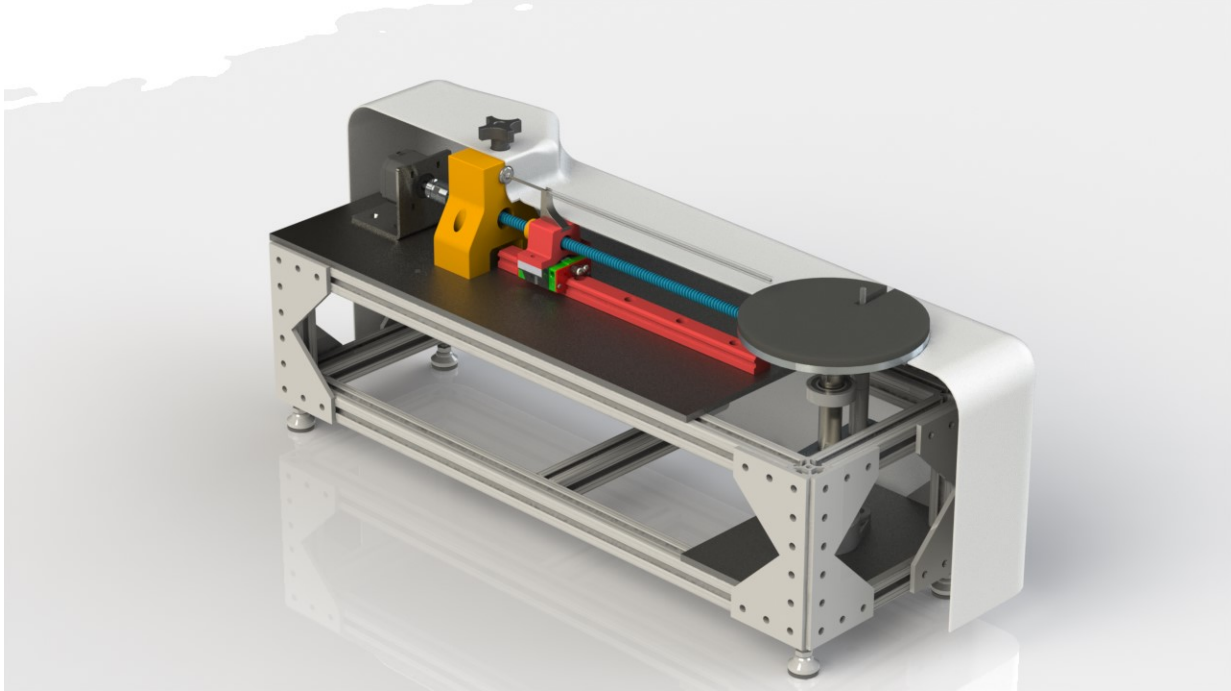


Figure 17: Design Iteration with ball screw, padded platform

From this design concept our team realized that the platform supporting the connector piece would present issues in proper component securing though its ability to rotate. This ability was intended to offer the operator greater scalability in sub-assembly securing, but the platform's ability to rotate could cause component misalignment during the insertion process; causing potential machine or product damage. Our next iteration was to introduce a raised bed, at a static height, to secure the component; as well as using an adjustable toggle clamp rather than a pneumatic clamp. This adjustable toggle clamp allows for variable force exertion onto the component to achieve a secure connection but to also prevent damage to the component. Figure 18 below highlights this current design, along with safety features such as the safety shell and the bellows. Both safety features are to prevent both operator injury and potential machine damage.

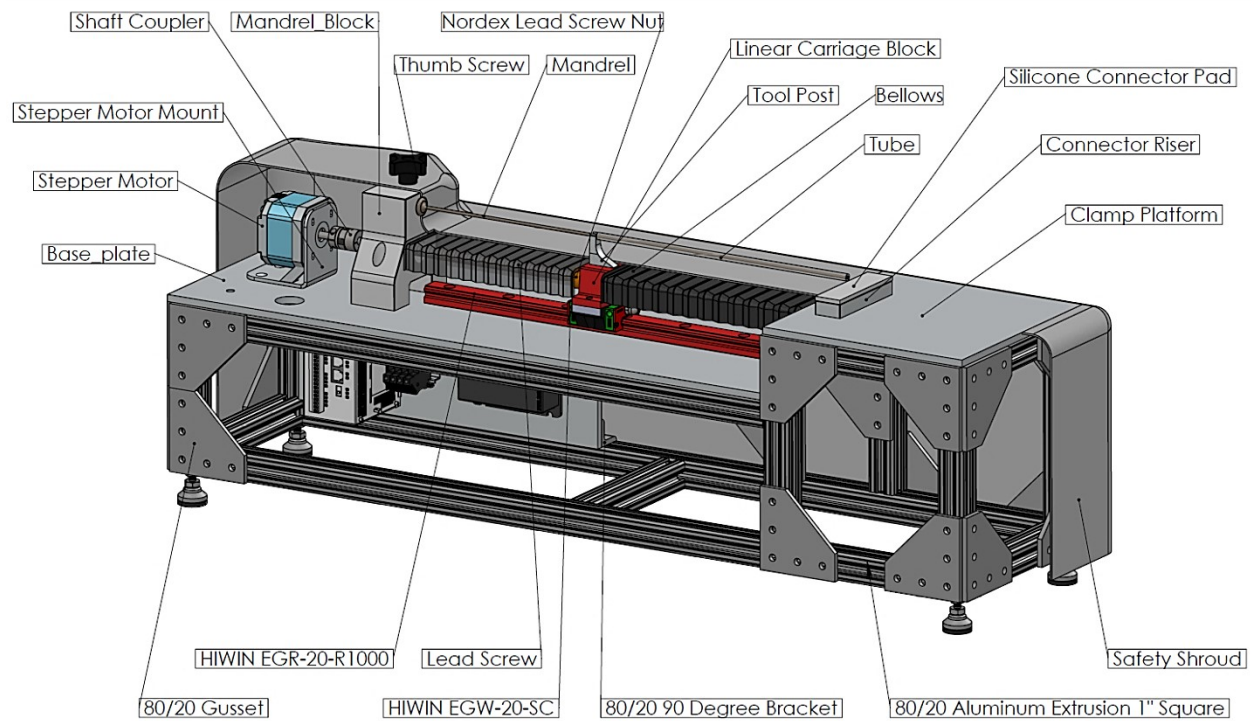


Figure 18: Current Design Concept Render

D. Material Selection

Once the design for the machine was finalized, it became necessary to select appropriate materials for the different components of the machine. Any material or component used must be of pharmaceutical grade especially if there is a contact between the component and the tubes or connectors. Therefore, the machine's mandrel and force exertion tool would need to be a clean and a non-reactive material capable of lasting under the operational loadings. Our team used the program *CESedupak* as well as *MatWeb*, both material databases, to run such an inquiry [10], [11]. During this process only pharmaceutical grade metals were considered. Each material was judged based on the material's modulus of elasticity, density, yield strength, ultimate tensile strength, indicated material reactivity and fracture toughness. These material qualities were chosen to be studied to suitably design our critical components to uphold needs for particle

generation reduction, static and fatigue strengths as well as has low reactivity with the surrounding environment.

We employed several material property graphs including a logarithmic graph comparing material strength to density to determine the material that had the highest strength to weight ratio. Fracture toughness of each material was also analyzed as a measure of particle generation. For materials where particle generation is a priority the higher the fracture toughness the less prone to chip formation a material is, therefore a material with a high fracture toughness that is under frictional forces will have a better resistance to chip formation.

E. Proof of Concept

Since the machine concept involves use of a mandrel to support a tube during insertion, our team used different methods to simulate the effectiveness. At first, basic tests were performed using tubing samples sourced from the Danvers plant. These tests were performed by inserting small tubing samples onto a smooth steel rod and using a tool and clamp system to exert a force onto the tool causing the forward motion of the tube onto the clamped connector piece. Once these ad-hoc tests were satisfactory, the team decided to develop a proof of concept mechanism to further test our design hypothesis. For this proof of concept our team used the core design of the mechanism to test the hypothetical responses of the system, but were unable to implement two of the safety systems; the safety shell and the bellows.

For this proof of concept our team chose to work with one of the smallest diameters commonly used, as found in our data, see Figure 21 below. The diameter of the used mandrel was 0.1 inches to allow for one-eighth inch inner diameter tubing to be used. This diameter was chosen to represent one of the most difficult geometries present in the data study, but can be expanded to accommodate for larger tubing.

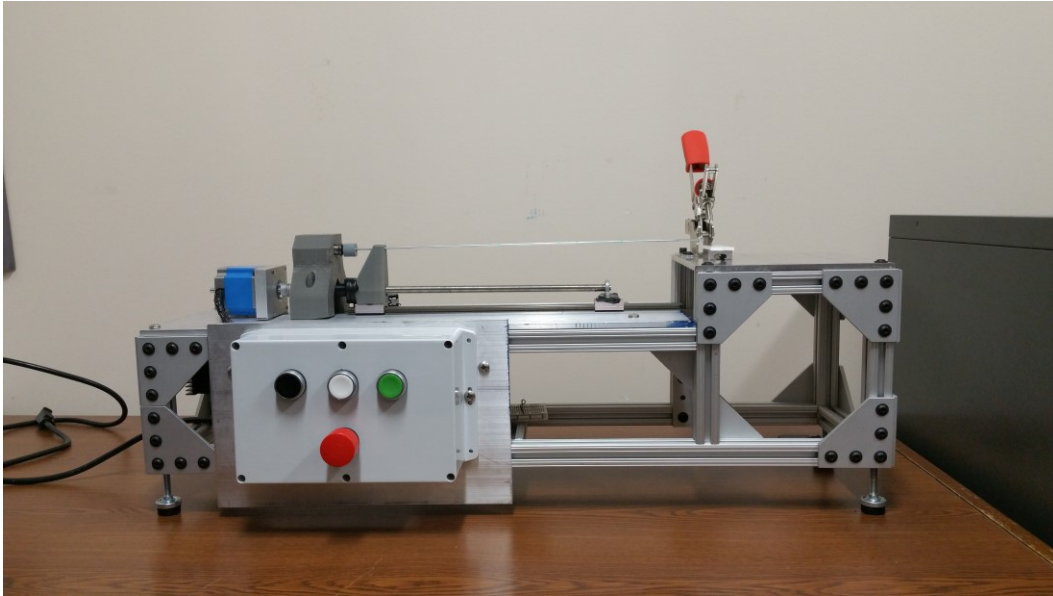


Figure 19: Proof of Concept Mechanism

In our mechanism one issue is present for tubes that have inner diameters close to that of the mandrels diameter; friction. While operating with tubes in the aforementioned situation, there are more points of contact between the tube and mandrel which causes a higher frictional interference. This interference leads to less energy being imparted into the coupling of the tube and connector and the need for a higher torque to achieve the coupling.

One issue also present in smaller, longer tubes, is the buckling of the tube itself. While operating on tubes with inner diameters close to that of the mandrel that are long, excessive buckling occurs; which causes the energy being used to perform the couple to convert into a buckling energy. To solve this issue, our team postulated the use of our friction gripper, Figure 12, to gently grasp the outer diameter of the tube to further prevent such buckling. This mechanism would be attached to the ball screw, so that as the force exertion tool is propelled the gripper also follows the motion. This would exert an additional portion of the torque being exerted by the motor onto a midsection of the tube, both preventing buckling and exerting a force onto the tube-connector couple.

Now that the automation concept has been finalized, the next step in the process is to finalize the design by assigning appropriate dimensions, selecting materials and carrying out various analyses (static, dynamic and failure mode effects). This is explained in Chapter 4.

F. Design Finalization and Analysis

i. Machine Sizing

Millipore Sigma indicated that the smaller tubes are much less ergonomically designed for the employees to work with. With this added knowledge, they also had provided a list of approximately 200 final fill assemblies that contain smaller tubing out of which bill of materials was extracted for a random sample of 96 assemblies. The histogram shown in Figure 14 shows the most common tube lengths and that approximately 82% of the tubes used are less than 16 inches in length.

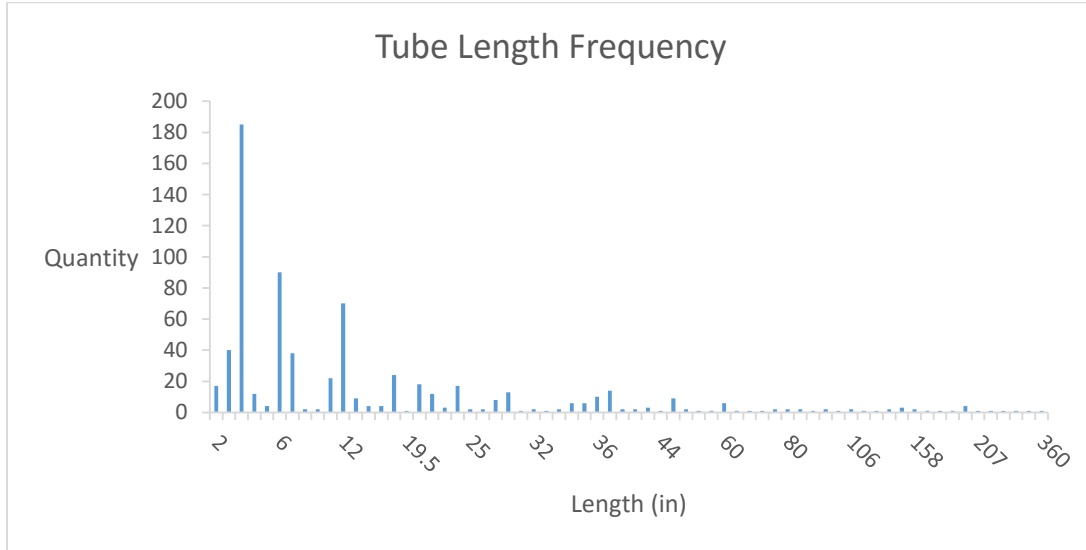


Figure 20: This chart is sample data generated by analysis of 96 assemblies from a list provided by *MilliporeSigma*

Knowing the highest occurring tube length is less than 16 inches, we are able to set our mandrel length to be approximately 16 inches or slightly longer. The next parameter we wanted

to gain with through this study is the diameter of the mandrel. To do this we had to analyze the highest occurring tube inner diameter, while also considering the request to focus on smaller diameters for ergonomic purposes. The histogram seen in Figure 21 shows that most of the tube diameters are of 1/4" inner diameter (ID) or greater. Although we are aiming to focus on 1/8" ID tubing, the design is meant to be scalable. This could be done through having replacement mandrels to satisfy the need for the higher volume ID tubing such as 1/4", 3/8" and 1/2". This allows us to say our proof of concept will represent a version that would fit approximately 8% of the IDs represented from our analysis, at 0.125inch inner diameter.

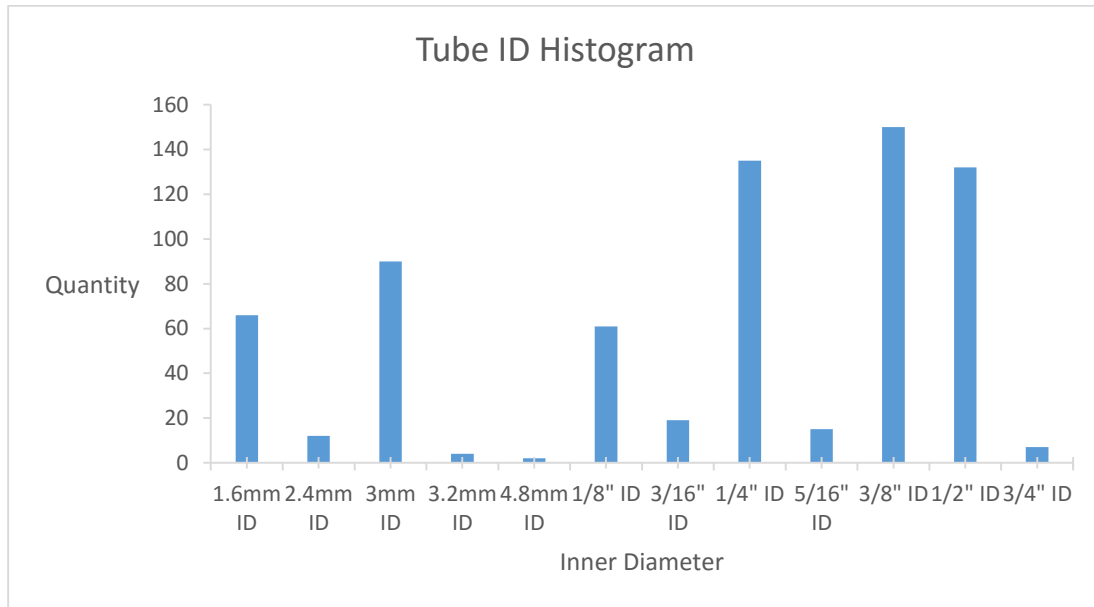


Figure 21: This chart shows the quantity of tube Inner Diameters found in our data acquisition

ii. Materials Selection

In our materials research, the team utilized several sources to find data on material strengths, weights, fracture toughness and reactivity. Our goals for the material used in the mandrel support rod included an infinite fatigue life cycle, low reactivity to the environment, fracture toughness, and a high yield strength. The Table 1 below highlight our findings on the material properties for specific metals of interest.

Table 1: Properties of Proposed Materials[10], [11]

Material	Density (lb/in³)	Modulus of Elasticity (ksi)	YS (ksi)	UTS (ksi)	Fracture-Toughness (ksi*in^{0.5})
AL 1060	0.09772	10000	24.7	8.4-13.8	
ASTM			29.2-	72.8-	
CF-12M	0.278-0.282	27.4-28.6	45	87.3	107-150
ASTM			34.8-	69.6-	
CF-20	0.278-0.282	27.7-28.9	37.7	84.1	107-150
ASTM			34.1-	69.6-	
CF-8	0.278-0.282	27.4-28.6	39.9	84.1	116-168
ASTM			42.1-	76.3-	
CF-8A	0.278-0.282	27.4-28.7	47.9	93.7	105-149
ASTM			39.2-	72.8-	
CF-8M	0.278-0.283	27.4-28.8	45	87.3	107-150
ASTM			30-	62.4-	
CN-7M	0.287-0.291	23.2-24.7	32.9	75.4	128-173

In the above table, several stainless steel alloy properties were compared, as well as a pure aluminum alloy, to gauge their material strengths and fracture toughness. Two of the constraints for this project were to use materials applicable for pharmaceutical assembly needs which for our purposes must resist particle generation. Figure 22, Figure 23 and Figure 24 below highlight our findings as material strength comparisons, fracture toughness and strength to weight ratios.

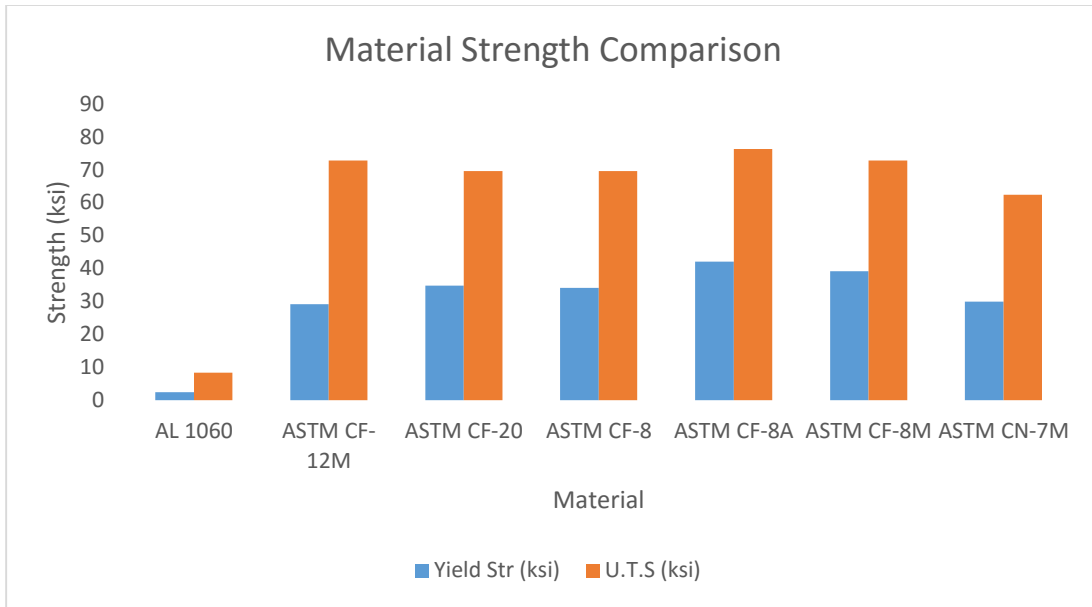


Figure 22: Material Strength Comparisons [10], [11]

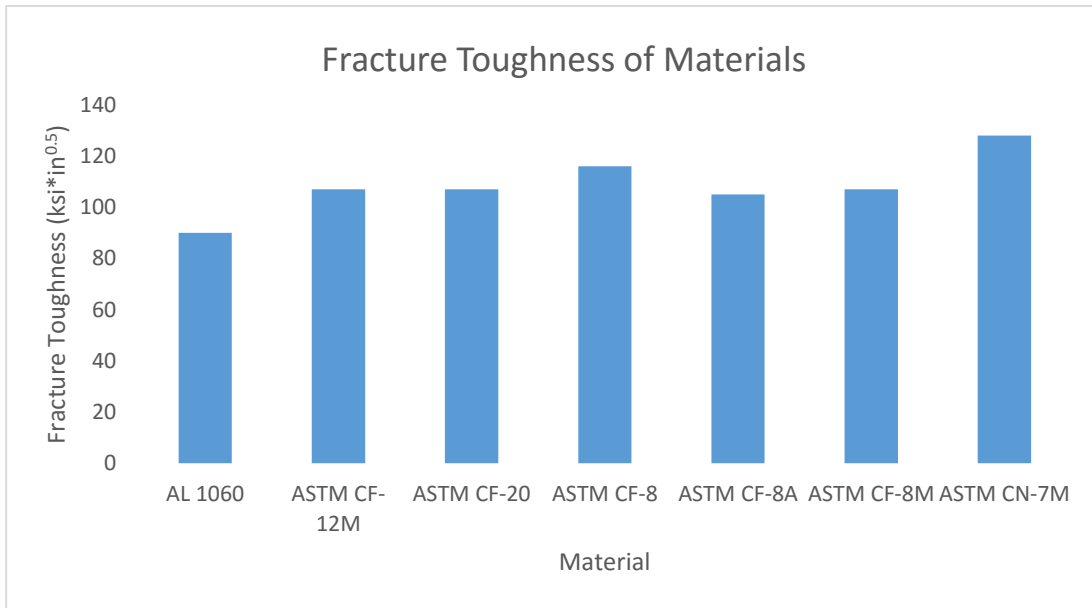


Figure 23: Fracture Toughness of Materials

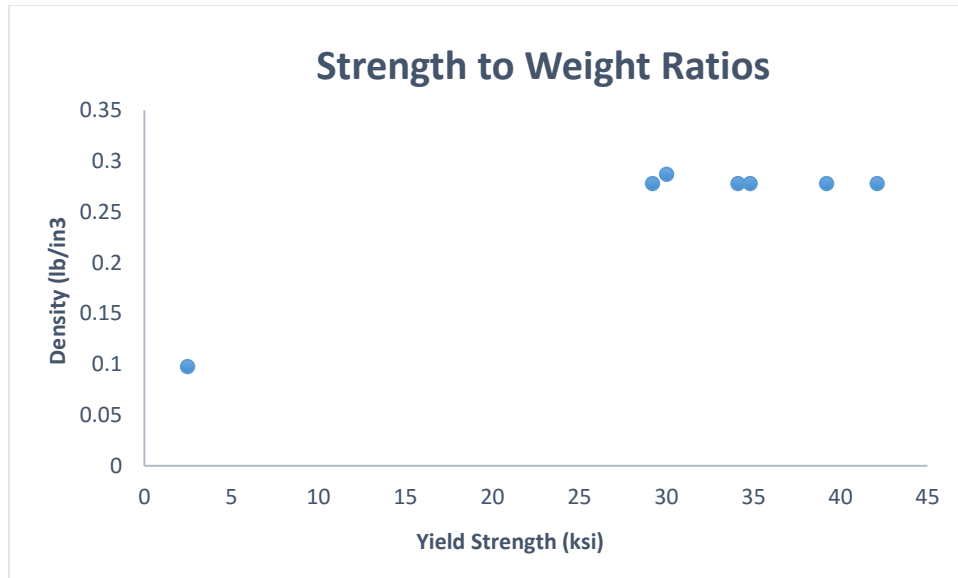


Figure 24: Strength to Weight Ratios

From this data our team chose to work with stainless steel ATSM CF 8M to build the mandrel for optimal strength and fracture toughness. This material offered a superior strength and fracture toughness, although at a higher weight comparatively to the aluminum alloy.

iii. Static and Fatigue Stress Analysis

In our final design, Figure 1, the mandrel is the machine’s main device for tube support, both in placement and excessive buckling; therefore, it is a key component in the machine’s operation. Techniques covered in *Machine Design: An Integrated Approach* by Robert L. Norton [12] were used to analyze the mandrel for critical section position, principal stresses at the critical section, shear forces, moment diagrams, slope, deflection, factors of safety and fatigue life.

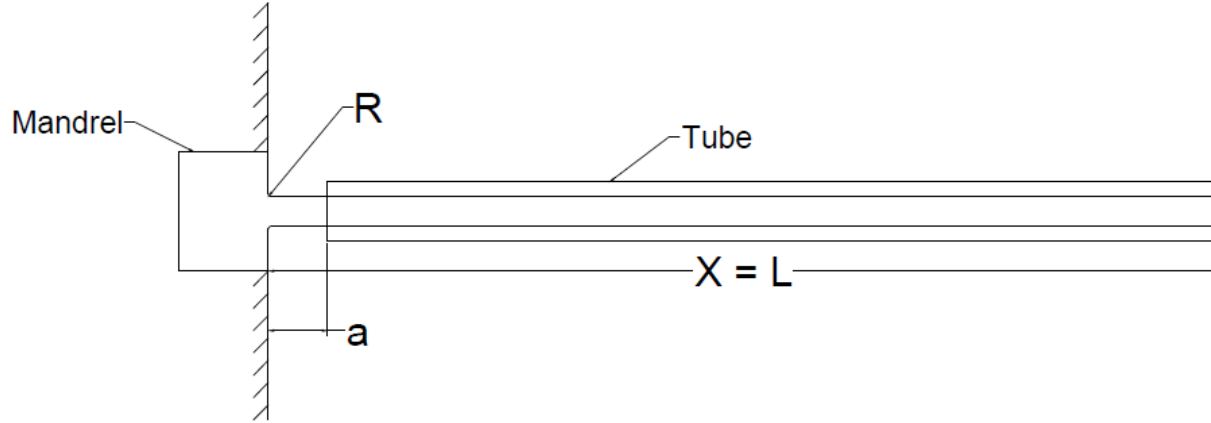


Figure 25: Mandrel Reference Diagram

This technique starts with taking a systems representation and solving for reaction forces and moments caused by active forces on the system. For our mandrel we considered the weight of the mandrel and the tube, cantilevered by the mandrel support block. Then the system is then modeled by generating singularity functions based on the loading conditions of the mandrel. The different equations that represent the loading, shear forces, moments, slopes and deflections of the system are listed below in equations 1-5.

$$q(x) = -W_m \langle x - 0 \rangle^0 - W_t \langle x - 0 \rangle^0 + V_r \langle x - 0 \rangle^{-1} + M_1 \langle x - 0 \rangle^{-2} \quad \text{Eq. 1.}$$

$$V(x) = -W_m \langle x - 0 \rangle^1 - W_t \langle x - 0 \rangle^1 + V_r \langle x - 0 \rangle^0 + M_1 \langle x - 0 \rangle^{-1} \quad \text{Eq. 2.}$$

$$M(x) = -\frac{W_m}{2} \langle x - 0 \rangle^2 - \frac{W_t}{2} \langle x - 0 \rangle^2 + V_r \langle x - 0 \rangle^1 + M_1 \langle x - 0 \rangle^0 \quad \text{Eq. 3.}$$

$$\theta(x) = \left(\frac{1}{E * I_{mandrel}} \right) \left(-\frac{W_m}{6} \langle x - 0 \rangle^3 - \frac{W_t}{6} \langle x - 0 \rangle^3 + \frac{V_r}{2} \langle x - 0 \rangle^2 + M_1 \langle x - 0 \rangle^1 \right) \quad \text{Eq. 4.}$$

$$\delta(x) = \left(\frac{1}{E * I_{mandrel}} \right) \left(-\frac{W_m}{24} \langle x - 0 \rangle^4 - \frac{W_t}{24} \langle x - 0 \rangle^4 + \frac{V_r}{6} \langle x - 0 \rangle^3 + \frac{M_1}{2} \langle x - 0 \rangle^2 \right) \quad \text{Eq. 5.}$$

These functions were graphed to indicate the critical section of the member. In this design, our mandrel includes a stress concentration at the base of the mandrel and the corresponding stress concentration factor is calculated using equation 6. [12].

$$K_t = A \left(\frac{r}{d} \right)^b \quad \text{Eq. 6.}$$

From this equation we can solve for the concentration factor for this geometry, where A and b are numerical values found from the table in *Machine Design*, by Robert Norton [12], r is the fillet radius at the critical section of the mandrel and d is the stepped diameter of the mandrel. Following the concentration factor calculation, the two dimensional principal stress were also calculated using equations 6 and 7.

$$\sigma_1, \sigma_3 = \frac{\sigma_x + \sigma_y}{2} \pm \sqrt{\left(\frac{\sigma_x - \sigma_y}{2} \right)^2 + \tau_b^2} \quad \text{Eq. 7.}$$

$$\sigma_2 = 0 \text{ psi} \quad \text{Eq. 8.}$$

From these values the Von Mises stress was calculated,

$$\sigma_{von} = \sqrt{\sigma_1^2 - \sigma_1 * \sigma_3 + \sigma_3^2} \quad \text{Eq. 9.}$$

Static elastic safety factor calculations can then be applied to find the factor of safety for the geometry and material selection.

$$N = \frac{S_y}{\sigma_{von}} \quad \text{Eq. 10.}$$

In efforts to provide a highly conservative set of calculations with our work, Modified Mohr theory was also applied to the material. Using this theory, the safety factor of material failure was calculated.

$$C_1 = \frac{1}{2} \left[|\sigma_1 - \sigma_2| + \frac{2S_{ut} - |S_{uc}|}{-|S_{uc}|} * (\sigma_1 + \sigma_2) \right] \quad \text{Eq. 11.}$$

$$C_2 = \frac{1}{2} \left[|\sigma_2 - \sigma_3| + \frac{2S_{ut} - |S_{uc}|}{-|S_{uc}|} * (\sigma_2 + \sigma_3) \right] \quad \text{Eq. 12.}$$

$$C_3 = \frac{1}{2} \left[|\sigma_3 - \sigma_1| + \frac{2S_{ut} - |S_{uc}|}{-|S_{uc}|} * (\sigma_3 + \sigma_1) \right] \quad \text{Eq. 13.}$$

$$\sigma_m = \max(C_1, C_2, C_3, \sigma_1, \sigma_2, \sigma_3) \quad \text{Eq. 14.}$$

$$N_{uts} = \frac{S_{ut}}{\sigma_m} \quad \text{Eq. 15.}$$

Our system was then analyzed for infinite fatigue life. The alternating and mean loadings of the mandrel during the loading and operating stage were calculated and the uncorrected endurance limit solved for. For this calculation, we assumed the use of a stainless steel alloy which has an uncorrected endurance limit of, $S'_e = 0.5S_{ut}$ [12]. The following assumptions were also made:

1. Room Temperature Operation
2. Machined Material
3. 99.999% Reliability
4. Axial Loading
5. Small Diameters ($d < 0,3\text{in}$)

From these assumptions, the correction factors for the endurance limit were calculated [12]. Following the corrected endurance limit calculations, the notch sensitivity correction factor was also found using equation 16.

$$k_f = 1 + q(k_t - 1) \quad \text{Eq. 16.}$$

The principal stress calculations were repeated for mean and alternating forces. To solve for the fatigue safety factors related to our system design the case 3 fluctuating stress equation was employed [12].

Using equations 1-17,

$$N_f = \frac{S_e S_{ut}}{\sigma'_a * S_{ut} + \sigma'_m * S_e} \quad \text{Eq. 17.}$$

By using the stress analysis techniques described in the previous section, we were able to locate the critical section of the mandrel and that location at the point of connection to the mandrel support block; otherwise denoted $x = 0$, see Figure 25. The analysis in the analysis appendix, and resulting diagrams of the 16 in mandrel show that the highest support forces and moments occur at this point, while the highest deflections and slope occur at the end of the member. These findings were conclusive with both our proof of concept and SolidWorks analysis, shown in Figure 26 and Figure 27. Our team also found that the mandrel had, under the indicated loading conditions, an elastic safety factor of 7.6 indicating that the calculations reveal a significant allowance for additional forces.

Our team also used SolidWorks to check our findings and gauge the amount of deflection under normal operation, Figure 26 and Figure 27 below are finite element analysis run on the member. In this analysis our team used the loading conditions resulting from the mandrel's weight and the distributed weight of the tube. Under these conditions, our member is at its highest loading due to its temporary fixed-free configuration. The two predominant analyses used was the von Mises stresses and the deflection of the mandrel; each of which were performed by the same loading conditions within the program.

The mesh type used was a SolidWorks standard high quality mesh, with 9201 elements sized at 0.0797 inches.

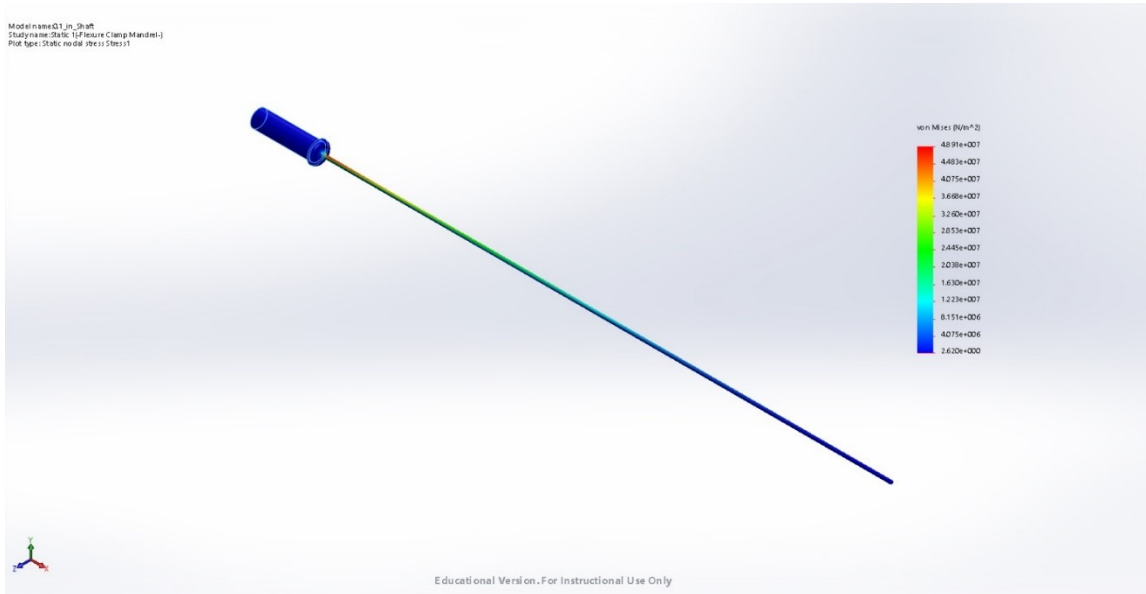


Figure 26: Mandrel Finite Element Analysis: Von Mises Stresses



Figure 27: Mandrel Finite Element Analysis: Deflection

These, computer generated, analyses show that the maximum deflection will occur at the end of the mandrel where the coupling action takes place, Figure 27 but the highest stress levels occur at the connection between the mandrel and its support in Figure 26. These analyses show

similar results as found from the loading graphs generated by the singularity function analysis and the proof of concept build. The SolidWorks analysis shows the displacement of the tip of the mandrel to be approximately 9.5mm during open loading at a 0.1 in diameter, while the analytical analysis shows a slightly higher deflection at approximately 12mm. Potential sources of this difference include slight differences in material properties from SolidWorks and analysis methodology variances.

The calculations also show that the member exhibits a fatigue safety factor of 6.3. Using this data, along with other calculations available in the stress analysis appendix, our team constructed an infinite life diagram showing the materials corrected endurance over a period of one billion cycles.

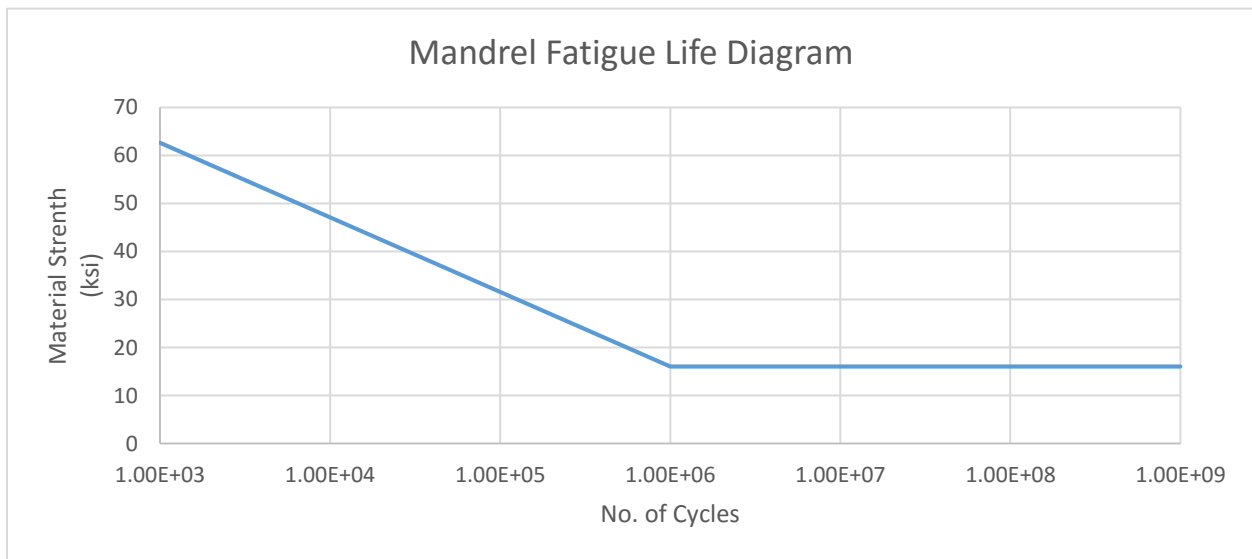


Figure 28: Stainless Steel Mandrel Fatigue Life Diagram

iv. Dynamic Modeling of the system

Our team also modeled the dynamics of the system using the bond graph analysis technique illustrated in *System Dynamics: Modeling, Simulation, and Control of Mechatronic*

Systems by Karnopp et al., [13]. Using this technique, differential equations representing the energy storage components of the system are generated, which can then be used to predict the dynamic responses of the system; this is an energy based method. The table below highlights both mechanical translation and rotational quantities used in the analysis and understanding of a dynamic system in this approach.

Table 2: Mechanical Translation and Rotation Quantities [13]

Quantity	Mechanical Translation	SI Units
Effort, e	Force, F	N
Flow, f	Velocity, V	m/s
Momentum, p	Momentum, P	N-S
displacement, q	Displacement, X	M
Power, P	F(t)V(t)	Watt
Energy, E	Integral(F*dx), Integral(V*dp)	Joules

Quantity	Mechanical Rotation	SI Units
Effort, e	Torque, t	N*m
Flow, f	Angular Velocity, ω	rad/s
Momentum, p	Momentum, P_t	N-S
displacement, q	Displacement, θ	m
Power, P	t(t), $\omega(t)$	Watt
Energy, E	Integral(t*d θ), Integral(ω *d P_t)	Joules

Using this process, our team categorized the different sub-systems into electrical, mechanical translation and mechanical rotation. Then using appropriate notations and procedures, bond graph was constructed and the associated equations were generated. Our team also used a mixture of empirical testing hypotheses and approximation equations to solve for the bond element values.

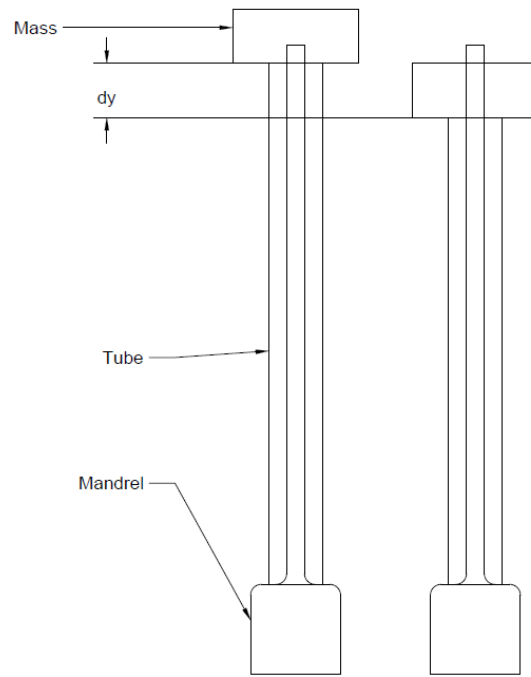


Figure 29: Empirical Test Configuration for K Coefficient

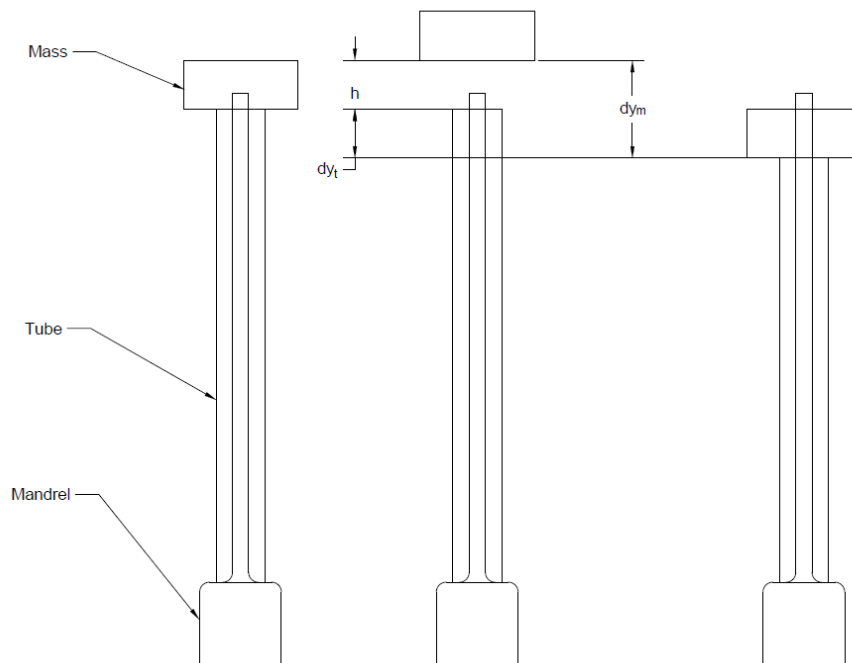


Figure 30: Empirical Test Method for Damping Coefficient

Using the two different test methods shown in Figure 29 and Figure 30 above, the two very important C and R values can be calculated. By placing the static mass onto the tube the spring coefficient K can be calculated using the following equation.

$$K = \frac{Mg}{x} \quad \text{Eq. 18.}$$

Using the previously determined K coefficient, the test setup for the damping coefficient the following equation can be used to find D.

$$D = \frac{Mg(dy_m) - \frac{1}{2}K(dy_t)^2}{dy_t\sqrt{2gh}} \quad \text{Eq. 19.}$$

The equation for calculating the K coefficient is derived from the basic force equation for a spring compressed from neutral length x amount. The equation for the damping coefficient was derived using conservation of energy. The energy being input into the system from the dropped mass's change in height d_{ym} , the spring energy from compressing length d_{yt} , and the remaining energy being dissipated by the drag based on the impact speed $\sqrt{2gh}$.

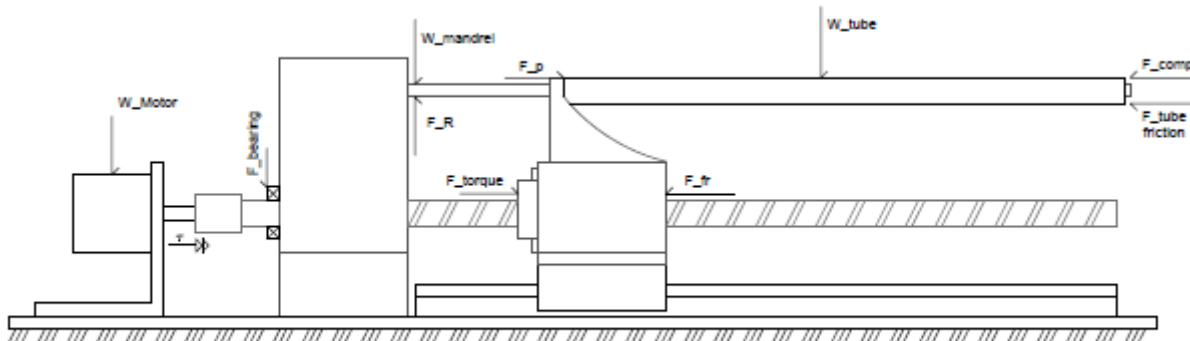


Figure 31: Cross Sectional View of the Core Mechanism

Using bond graphs analysis technique our team was able to generate a causal bond graph representing our system, Figure 32. The state variables were then used to find the state equations, below.

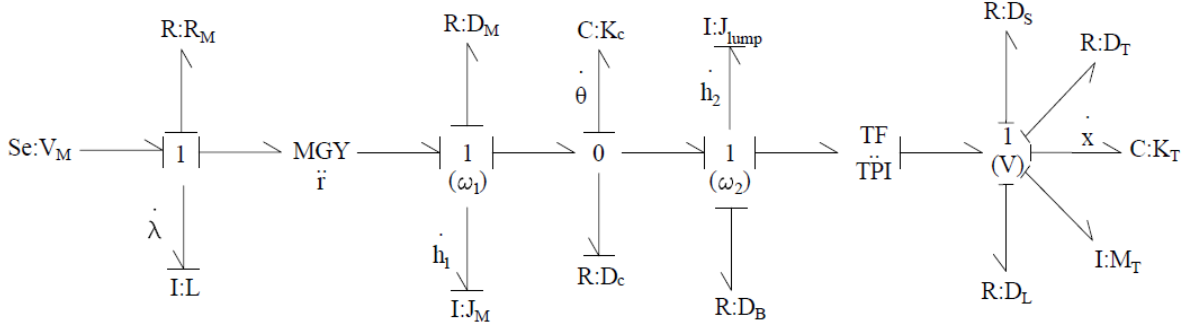


Figure 32: Casual Bond Graph of our System

Using the state variables from the figure above our team derived the state equations for the system.

$$\dot{\lambda}, \dot{h}_1, \dot{h}_2, \dot{\theta}, \dot{x} = f(\lambda, h_1, h_2, \theta, x, Se: V_m) \quad \text{Eq. 20.}$$

$$\dot{\lambda} = E(t) - R \frac{\lambda}{L} - \ddot{r} \frac{h_1}{J_m} \quad \text{Eq. 21.}$$

$$\dot{h}_1 = \ddot{r} \frac{\lambda}{L} - D_m \frac{h_1}{J_m} - k_c \theta \quad \text{Eq. 22.}$$

$$\dot{\theta} = \frac{h_1}{J_m} - \frac{h_2}{J_{lump}} \quad \text{Eq. 23.}$$

$$\dot{h}_2 = \frac{k_c \theta - \frac{D_B h_2}{J_{lump}} - T\ddot{P}I k_T x}{1 + \frac{T\ddot{P}I^2}{J_{lump}} (D_S + D_T + D_L + M_T)} \quad \text{Eq. 24.}$$

$$\dot{x} = T\ddot{P}I \frac{h_2}{J_{lump}} \quad \text{Eq. 25.}$$

The next steps of this analysis method was to assign causality, based on the system's bond graph diagram. With the assigned causality our team generated state variables and equations. These equations represented the differential form of the system's dynamics, Laplace transforms were then applied to find a system of equations representing the quantities of interest, denoted by the differential state variables. MATLAB was used in conjuncture with the matrix form of these equations to plot these equations over time.

$$\begin{bmatrix} \dot{\lambda} \\ \dot{h}_1 \\ \dot{\theta} \\ \dot{h}_2 \\ \dot{x} \end{bmatrix} = \begin{bmatrix} -\frac{R}{L} & -\frac{r}{J_M} & 0 & 0 & 0 \\ \frac{\dot{r}}{L} & -\frac{D_M}{J_M} & -k_c & 0 & 0 \\ 0 & \frac{1}{J_M} & 0 & -\frac{h_2}{J_{lump}} & 0 \\ 0 & 0 & k_c & -\frac{D_B h_2}{J_{lump}} & -T\dot{P}I k_T \\ 0 & 0 & \frac{T\dot{P}I^2}{1 + \frac{T\dot{P}I^2}{J_{lump}}(D_s + D_M + D_L + M_T)} & \frac{T\dot{P}I^2}{1 + \frac{T\dot{P}I^2}{J_{lump}}(D_s + D_M + D_L + M_T)} & \frac{T\dot{P}I^2}{1 + \frac{T\dot{P}I^2}{J_{lump}}(D_s + D_M + D_L + M_T)} \\ 0 & 0 & 0 & \frac{T\dot{P}I}{J_{lump}} & 0 \end{bmatrix} \begin{bmatrix} \lambda \\ h_1 \\ \theta \\ h_2 \\ x \end{bmatrix}$$

$$+ \begin{bmatrix} V_m(t) & 0 & 0 & 0 & 0 \\ 0 & 0 & 0 & 0 & 0 \\ 0 & 0 & 0 & 0 & 0 \\ 0 & 0 & 0 & 0 & 0 \\ 0 & 0 & 0 & 0 & 0 \end{bmatrix} \begin{bmatrix} V_m(t) \\ \tau_1(t) \\ \omega(t) \\ \tau_2(t) \\ x(t) \end{bmatrix}$$

In this system our expected dynamic response includes the responses caused by the damping and stiffness of the tube as well as the damping of friction on each component. What our model predicts is that as the tubing is being compressed onto the connector the tubing will exert a force backwards onto the tool post as well as having a damping effect on this process; this reaction will cause the motor to exert a higher amount of torque until the tube-connector couple is made. When performing this task on longer tubes, as we compress the tube over the barb of the connector we expect a coefficient that will continue to increase as the buckling within the tube increases. This increase in friction is the most critical variable within this process as it could potentially stall the tube on the mandrel.

After deriving the state equations for the most difficult case, we found the system to be too complex to solve. In order to get the dynamic response, the model had to be simplified. Using lumped parameter analysis, the system was reduced to a simple Mass, Spring, and Damper system. Figure 33 below shows a diagram of the simplified model.

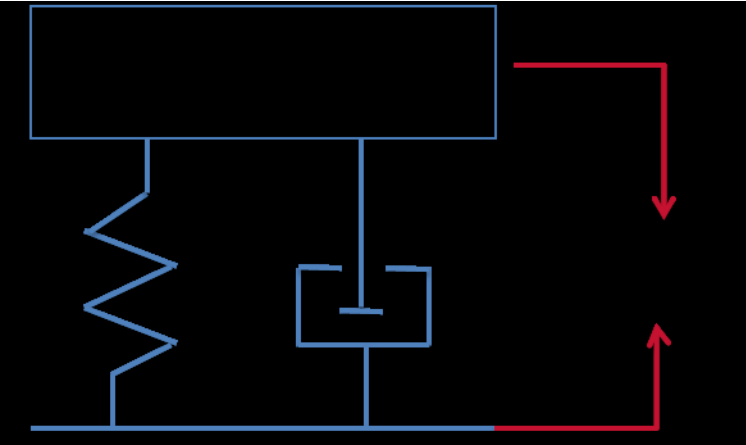


Figure 33: Lumped Parameter Simplified Model

Using this new system, the basic equations of motion were then derived and solve using Matlab. Figure 34 below shows the normalized amplitude of oscillation at the tool post during insertion.

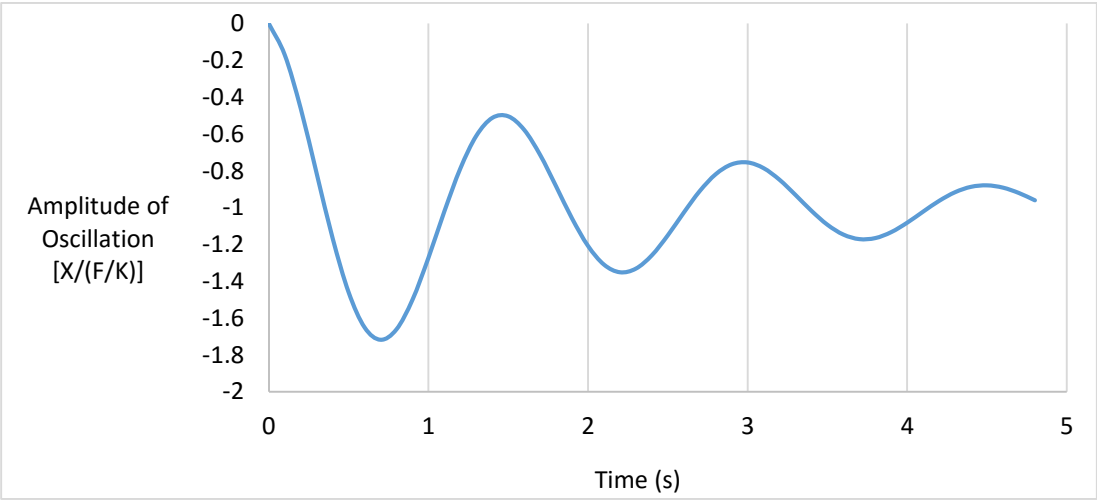


Figure 34: Normalized Amplitude of Oscillation at Tool Post During Insertion

This result shows the system to be underdamped. This is due to the simplified approach on solving the system with a lumped parameter model. With further empirical testing, more

damping effects can be added to better model the real system. This would bring the theoretical analysis closer to the actual overdamped system.

v. Failure Mode Effects Analysis (FMEA)

To best suit the needs of this project both a process failure mode and effects analysis and a design failure mode and effects analysis were completed for the proposed mechanism. These analysis techniques were used to find any potential mechanism or operational failures. For these studies the company's standards of safety and RPN's were used to fit our machines design and process. This process was repeated until the mechanism had no RPN's over 300.

In Table 3 we have performed a design failure mode effects analysis (DFMEA). This chart details areas we see to be of most concern and potential recommended actions to fix the listed potential failure modes. Of our most prevalent problems that we will face would be the failure within the mandrel and within the stepper motor. The mandrel risk priority number (RPN) may appear too large but this function is also being assisted when the coupler is fixed within place. Since the mandrel uses the coupler as a sort of simple support, it lowers the risk of deformation due to bending. The next area of worry is the stepper motor's ability to generate torque. As we are using a stepper motor as a price reduction to create a proof of concept model it would not be ideal in an actual setting. For a completed model we would suggest a DC motor, potentially a small servo motor.

Table 3: Design failure mode effects analysis (DFMEA)

Project Number		WPI MQP 2.2.3				Project Name	Automation of a Manual Process				
Assumptions		Machine is in use									
Risk ID	Function	Review System/Design/Process/Service Function	Potential Failure Mode	Potential Effect(s) of Failure	Current Controls	SEV	FRE	DET	RPN	Recommended Action / Target Date	
1	Stepper Motor Coupler	Motor Output	Torsional Deformation of the coupler	Machine damage	Visual Inspection	7	3	3	63	Replace stepper motor coupler	May 16'
2	Stepper Motor Coupler	Motor Output	Component loosens on lead screw and stepper motor shaft	Machine Damage, Connection not performed	Visual Inspection	7	3	3	63	Replace Stepper motor Coupler	May 16'
3	Mandrel	Tubing carriage	Deformation due to bending		Visual Inspection	7	4	5	140	Replace mandrel	May 16'
4	Tube Pushing Device	Tubing connecting mechanism	Deformation of the post	Machine damage	Load Cell Implementation	7	2	4	56	Replace tool pushing device	May 16'
5	Stepper Motor	Motor operation	Failure to produce necessary torque	Connection not performed, machine damage	No current control	5	4	6	120	Switch to DC Motor	May 16'
6	Stepper Motor	Motor Fixture	Stepper motor loosens from fixture	Machine Damage	Visual Inspection	7	2	4	56	Tighten loose components, Replace worn parts	May 16'
7	Lead Screw	Tool pushing device translation	Excessive wear due to excess force	Connection not performed, machine damage	Visual Inspection	7	2	3	42	Replace lead screw	May 16'
8	Mandrel Block	Clamping mandrel into fixed position	Wear to threads in flexure clamp	Machine damage, loose mandrel	Visual Inspection	7	3	5	105	Replace mandrel block	May 16'
9	Linear Rail	Tool pushing device translation	Corrosion of the surface of the linear rail.	Machine damage, Particle generation	Visual Inspection	7	3	2	42	Replace linear rail	May 16'
10	Connector Clamp	Connector fixturing	Excess force applied	Product Waste	Visual Inspection	7	6	5	210	Redesign of connector clamp	May 16'
11	Connector Clamp	Connector fixturing	Auto adjusting feature failure	Connector not fixed in place	Visual Inspection	6	3	5	90	Clean Connector Clamp/ Replace Connector Clamp	May 16'

Project Number			WPI MQP 2.2.3 (Continued)			Project Name		Automation of a Manual Process			
Assumptions			Machine is in use								
Risk ID	Function	Review System/Design/Process/Service Function	Potential Failure Mode	Potential Cause(s) of Failure	Current Controls	SEV	FRE	DET	RPN	Recommended Action / Target Date	
12	Technician	Tool Output	Finger cut on sharp edge	Personal Injury, Machine down	Safety Shell	10	3	3	90	-	May 16'
13	Technician	Tool Output	Bodily member caught in machine input	Personal Injury, Machine down	Safety Shell	10	4	2	80	Caution Label, S.O.P, Rubber Guard	May 16'
14	Machine	Exposed power wire	Movement of device causes wear on power cord	Personal Injury	Safety Shell, Electrical Component Shielding	10	3	3	90	Regular Visual Inspection	May 16'
15	Machine	Mandrel Damage	Damaged Part	Improper Use/Loading	S.O.P, U.S.R	7	3	5	105	Training	May 16'
16	Technician	Component Clamp	Finger compressed	Personal Injury	S.O.P, Warning Label	10	7	2	140	Training	May 16'
17	Assembly	Tubing	Minor Damage	Improper Use	S.O.P, Warning Label	6	5	5	150	Training	May 16'

Through our analyses we found that this machine would achieve the intended motion with a considerable life cycle. Our static and fatigue stress analyses show that the key component, the mandrel, shows a significant elastic safety factor and fatigue safety factor of 7.6 and 6.3, respectively, under normal operation. This design also utilizes several methods of machine safety features to anticipate any failure modes involving the operations and design.

4. Conclusions

In this project, our main goal was to identify potential automation possibilities among various manual operations and develop concepts that can be used to automate the process as well as improve workplace ergonomics while maintaining a high degree of safety and low degree of particle generation. After using an iterative design process, our team synthesized a machine capable to automating the tube insertion actions integral to the processes at MilliporeSigma's Danvers facility. This device utilizes several safety measures, including stop switches and a safety shell, to prevent machine damage, operator injury and assembly damage. Along with initial observations, our team used assembly component data to optimize the design length of the machine's mandrel. This data yielded that a 16-inch mandrel will allow for 82% of assembly tube length needs to be met. The team also found that our design, a 0.1in diameter mandrel, will cover 8% of the total assemblies, but that the majority of the assemblies produced are 0.25in inner diameter and below.

Our design, through integrating a force exertion mechanism between the tube and connector component, reduces the amount of time spent exerting un-needed forces onto a worker's hands, wrists, forearms and shoulders through the tube-connector assembly process. With less strain being exerted onto workers on the factory floor an improvement in the workplace ergonomics is achieved by reducing the risks of MSD's due to these straining and repetitive procedures. In future work the savings due to ergonomic improvements can be studied.

During the design phase of this project, our team compared several materials of interest for various properties. Our team found that the material *ASTM CF8*, stainless steel, was not only applicable in pharmaceutical processes but theoretically offered a high yield strength and fracture toughness. During the analysis phase of this project our team also found this material choice to

be suitable for a high reliability and an infinite fatigue life under normal operation, theoretically lasting over one-billion cycles.

One specific goal of this project was to offer a design that allowed for scalability of assembly potential. For this reason, our team chose to employ use of a toggle clamp fixture, specifically located, to secure the coupler component being clamped. In our design by using the toggle clamp allows for a variable force output, clamping force, which can be adjusted based on the size and force requirements of the current assembly. The use of the toggle clamp also allows the operator of this machine to clamp various types of connectors, granting a higher degree of application across sub-assembly production. These methods also allow the present assembly's connector to be inserted into a tube on each of its nozzles; an action allows this machine to be used for various configurations.

Our designs also take into weighted consideration the safety of the operations involving this system. The team factored in a design failure mode and effects analysis (F.M.E.A) as well as a process F.M.E.A to predict any potential safety concerns. The team discovered throughout this process that implementation of a safety shell, surrounding the mechanism, would help prevent any operators from injuring themselves on the machines internal mechanisms. To add to this idea our team also implemented a bellows to prevent access, through the safety-shell's opening, to a revolving lead screw, or a translating linear plate.

5. Recommendations and Future Work

In this project our team explored the use of an auto-adjusting toggle clamp to uniquely cater to the needs of each component. Through use of a specific toggle clamp, fine control of the force exerted on the assembly components can be realized. In the process of designing this machine our team discovered that the toggle clamps commercially available, which would allow the operator to exert a smaller force, do not apply a small enough to prevent component damage across all components. Toggle clamps that do produce a small enough force over a large enough area are small and difficult to operate and would cause unnecessary strain on the operator to compress. To realize a solution to this issue, it is recommended to employ design methods to design and build an auto-adjusting toggle clamp capable of lower force exertion, with larger gripping area.

With the exertion force onto the components of a sub-assembly needing to be regulated, the use of several force and position sensors would need to be integrated into the design to achieve a higher degree of force control. To monitor the amount of exerted force between the tube, connector and tool post the use of a compression load cell, with a center hole, is recommended. These devices, in use with the proper program, will allow the user to operate the mechanism and have a translation program relate the cell's output voltage to a quantified force.

While the mechanism designed in this paper utilizes a toggle clamp to secure the connection piece in place, a PLC controlled pneumatic gripping system could be designed for use with this mechanism. Such a system would also provide the operator with superior force control to meet any user specified requirements, as well as offer a wide range in gripping scalability based on the exertion member. In early concepts the use of pneumatic systems were present, due

to the pre-existing clean air supply system in the Danvers facility, therefore such a system would be a possible solution in the tube-connector coupling process.

Another recommendation for future work on this machine would be the implementation of an outer diameter gripping mechanism, such as the one in Figure 12, to prevent excessive buckling in longer tubes. In our current design the largest issue present is that in smaller tubes, inner diameter with longer lengths, is excessive buckling and energy loss due to this buckling. To prevent this level of buckling the previously designed outer diameter grip could be used as an additional adjustable attachment to the current tool post, or as an additional member on the Linear-Rail-Ball-Screw system. By integrating outer diameter gripping the force exerted around the outer diameter of the tube wouldn't allow for further buckling, thus having this energy being used to achieve the tube-connector couple.

This outer diameter gripper concept could also be extended to insertions which cannot utilize the mandrel, allowing tubes of any length to be inserted. The proposed machine alteration would have the operator remove the mandrel from the support block and lay the tube into the gripping mechanism, then proceed to activate the grip and mechanism. This method of insertion may not be as robust as the mandrel method due to the time required to perform the task and lesser force already required to couple the components. This method would, however, allow for greater flexibility to the machine in irregular length tubing.

Our team also postulated the implementation of a fully automatic tube insertion onto the mandrel. This would further benefit workplace ergonomics by removing the operator's involvement in tube control and loading. This mechanism would work by having a mandrel which is adjustable, increase in angle, relative to the x-axis, to allow another mechanism to load a tube onto it; it would then return to a zero-degree angle parallel to the x-axis thus being in-line

with the connector component platform. By the automation of tube loading, the process would be designed so that the tube would be inserted onto the mandrel without varying forces caused by operator variances.

6. References

- [1] K. N. Otto and K. L. Wood, *Product design: techniques in reverse engineering and new product development*. Upper Saddle River, NJ: Prentice Hall, 2001.
- [2] S. Kalpakjian, *Manufacturing engineering and technology*, 6th ed. New York: Prentice Hall, 2010.
- [3] W. L. Pearn, C. C. Wu, and C. H. Wu, “Estimating process capability index C_{pk} : classical approach versus Bayesian approach,” *J. Stat. Comput. Simul.*, vol. 85, no. 10, pp. 2007–2021, Jul. 2015.
- [4] G. Bessieris, “Robust process capability performance: An interpretation of key indices from a nonparametric viewpoint,” *TQM J.*, vol. 26, no. 5, pp. 445–462, Aug. 2014.
- [5] A. Colas, R. Malczewski, and K. Ulman, “Silicone Tubing for Pharmaceutical Processing.” Dow Corning Corporation, 2004.
- [6] G. Fantoni, M. Santochi, G. Dini, K. Tracht, B. Scholz-Reiter, J. Fleischer, T. Kristoffer Lien, G. Seliger, G. Reinhart, J. Franke, H. Nørgaard Hansen, and A. Verl, “Grasping devices and methods in automated production processes,” *CIRP Ann. - Manuf. Technol.*, vol. 63, no. 2, pp. 679–701, 2014.
- [7] “Safety and Health Topics | Ergonomics.” [Online]. Available: <https://www.osha.gov/SLTC/ergonomics/>. [Accessed: 15-Mar-2016].
- [8] G. Boothroyd, *Assembly automation and product design*, 2nd ed. Boca Raton, FL: Taylor & Francis, 2005.
- [9] D. Silverstein, P. Samuel, and N. DeCarlo, *The innovator’s toolkit: 50+ techniques for predictable and sustainable organic growth*, Second edition. Hoboken, N.J. : Chichester: Wiley ; John Wiley [distributor], 2012.
- [10] M. F. Ashby and D. Cebon, *CES EduPack 2015*. Granta Design Limited.
- [11] “Aluminum 1060-H112,” *MatWeb Material Property Data*. [Online]. Available: <http://www.matweb.com/search/DataSheet.aspx?MatGUID=2a4da324f182413597fcfc4374d22e06&&ckck=1>. [Accessed: 15-Mar-2016].
- [12] R. L. Norton, *Machine design: an integrated approach*, Fifth edition. Boston: Prentice Hall, 2014.
- [13] D. Karnopp, D. L. Margolis, and R. C. Rosenberg, *System dynamics: modeling and simulation of mechatronic systems*, 5th ed. Hoboken, NJ: Wiley, 2012.

7. Appendix A: Theoretical Timing Data

Various assemblies from the MilliporeSigma EPDM file server were collected for analysis. Using theoretical timing data provided by Boothroyd [8], estimations for different assembly times were created. The different actions required for assembly were separated and various handling timing penalties were assigned. The hard to reach penalty was used as a general case when a component was difficult to manipulate or to put into position. The timing data for two assemblies are presented in Table 5 and Table 6 below. The timing data from many different assemblies allowed the creation of a generalized timing data set shown in Table 4 below.

Table 4: Generalized Timing Data for Assemblies

Part	Time Breakdown (s)				Hard to Reach Penalty (s)	Total No Penalty (s)	Total with Penalty (s)
	Handling	Insertion	Crimping				
Oetiker > 15mm	Handling	Insertion	Crimping		0.71	9.63	10.34
	1.13	1.5	7				
6mm <= Oetiker <= 15mm	Handling	Insertion	Crimping		0.74	9.93	10.67
	1.43	1.5	7				
Oetiker < 6mm	Handling	Insertion	Crimping	Tool Handling	0.77	11.51	12.28
	1.88	1.5	7	1.13			
Filter	Handling	Insertion					
	4.1	6.5					
AMESIL CLAMP	Handling	Insertion			0.75	7.1	7.85
	5.6	1.5					
Dust Cover	Handling	Insertion			0	9	9
	5	4					
Connector	Handling	Insertion			0	7.5	7.5
	1	6.5					
Tubing	Handling				0.9	4.1	5
	4.1						
Plug	Handling	Insertion			0	7.5	7.5
	1	6.5					
Bag Two Handed	Handling				0	5	5
	5						
Bag One Hand	Handling				0	1.84	1.84
	1.84						
Pinch Clamp	Handling	Insertion			0.71	2.63	3.34
	1.13	1.5					
Plate One Hand	Handling				0.71	1.5	2.21
	1.5						
Plate Two Handed	Handling				0.9		
	4.1						

Table 5: Theoretical Timing for Assembly X.1

Category	Part	Manual Assembly Time Breakdown				Count	Sub-Totals (s)
		Assembly X.1					
Cover	Dust cover	Handling	Insert			5	45
		5	4				
Connector	End Connector w/ Gasket	Handling	Insert			5	37.5
		1	6.5				
Oetiker	Oetiker Clamps	Handling	Insert	Crimping		28	280
		1	1.5	7.5			
Tubing	Pharma Tubing	Handling				8	32.8
		4.1					
Tubing	Braided Silicone Tubing	Handling				7	28.7
		4.1					
Bag	Nova Septum bag	Handling				2	3.38
		1.69					
Filter	Opticap XL4 Filter	Insert	Insert	Insert	Handling	2	47.2
		6.5	6.5	6.5	4.1		
Filter	Millibarrier	Insert	Insert	Handling		1	14.13
		6.5	6.5	1.13			
Clamp	Amesil Clamp	Insert	Handling			4	28.4
		1.5	5.6				
Filter	Opticap XL50 Filter	Handling	Insert	Insert		1	14.13
		1.13	6.5	6.5			
Connector	Tee Connector	Handling	Insert	Insert	Insert	3	61.5
		1	6.5	6.5	6.5		
Plug	End Plug	Handling	Insert			2	15
		1	6.5				
Clamp	Zip Tie	Handling	Insert			2	22.7
		4.35	7				
Clamp	Nova Seal	Insert	Handling			2	10
		4	1				
Total							640.44

Table 6: Theoretical Timing Data for Assembly X.2

Category	Part	Manual Assembly Time Breakdown Assembly X.2				Sub-Totals (s)
Bag	Bag					0
Clamp	Right Pinch Clamp	Insert				1.5
		1.5				
Clamp	Center Pinch Clamp	Insert				1.5
		1.5				
Clamp	Left Pinch Clamp	Insert				1.5
		1.5				
Oetiker	Bag Port Right Oetiker	Insert	Crimping	Handling	Handling	11
		1.5	7.5	1	1	
Oetiker	Bag Port Middle Oetiker	Insert	Crimping	Handling	Handling	11
		1.5	7.5	1	1	
Oetiker	Bag Port Left Oetiker	Insert	Crimping	Handling	Handling	11
		1.5	7.5	1	1	
Tubing	Right Tubing	Insert	Handling			11.6
		7.5	4.1			
Tubing	Center Tubing	Insert	Handling			11.6
		7.5	4.1			
Tubing	Left Top Tubing	Insert	Handling			11.6
		7.5	4.1			
Tubing	Left Bottom Tubing	Handling				4.1
		4.1				
Connector	Large to Small Connector	Handling	Insert	Insert		14
		1	6.5	6.5		
Oetiker	Large Connector Side Oetiker	Insert	Crimping	Handling	Handling	11
		1.5	7.5	1	1	
Oetiker	Small Connector Side Oetiker	Insert	Crimping	Handling	Handling	13.5
		4	7.5	1	1	
	Leur Fem	Handling	Insert			7.5
		1	6.5			
Oetiker	Leur Fem Oetiker	Insert	Crimping	Handling	Handling	11
		1.5	7.5	1	1	
Plug	Plug	Handling	Insert			7.5
		1	6.5			
Cover	Dust Cover	Handling	Insert			9
		5	4			
	Middle MPC Fem	Handling	Insert	Insert		14
		1	6.5	6.5		
	Middle MPC Fem Oetiker	Insert	Crimping	Handling	Handling	11
		1.5	7.5	1	1	
Plug	Middle MPC Fem Plug	Handling	Insert			7.5
		1	6.5			
	Right MPC Fem	Handling	Insert	Insert		14
		1	6.5	6.5		
Oetiker	Right MPC Fem Oetiker	Insert	Crimping	Handling	Handling	11
		1.5	7.5	1	1	
Plug	Middle MPC Fem Plug	Handling	Insert			7.5
		1	6.5			
Total						214.9

8. Appendix B: Mandrel Stress Analysis

A. Mandrel Static Stress Analysis

i. Material Properties

Material: Stainless Steel

$$E := 27.4 \cdot 10^6 \text{ psi} \quad S_{ut} := 69.6 \text{ ksi}$$

$$S_y := 24.7 \text{ ksi} \quad S_{uc} := 34.8 \text{ ksi}$$

$$S_{\text{compression}} := 24.7 \text{ ksi} \quad \rho := 474 \frac{\text{lb}}{\text{ft}^3} \quad \rho_t := 81.2 \frac{\text{lb}}{\text{ft}^3}$$

$$S_{ft} := 56.4 \text{ ksi} \cdot \text{in}^{0.5}$$

$$S_m := 0.9 \cdot S_{ut} = 62.64 \text{ ksi}$$

ii. Piece Dimensions

Mandrel

$$D := 0.3 \text{ in} \quad d_{\text{out}} := 0.25 \text{ in}$$

$$d := 0.1 \text{ in} \quad d_{\text{in}} := 0.125 \text{ in}$$

$$r := 0.15 \text{ in}$$

$$l_{\text{mandrel}} := 16 \text{ in} \quad I_{\text{mandrel}} := \left[\frac{(\pi \cdot d^4)}{64} \right]$$

$$J_{\text{mandrel}} := 2 \cdot I_{\text{mandrel}}$$

$$A_{cs} := \left(\frac{\pi}{4} \right) \cdot d^2 = 7.854 \times 10^{-3} \cdot \text{in}^2$$

$$c_{\text{rod}} := \frac{d}{2} = 0.05 \text{ in}$$

iii. Silicone Tubing

$$l_{\text{tube}} := 12 \text{ in}$$

$$A_{\text{cst}} := \left(\frac{\pi}{4} \right) \cdot (d_{\text{out}}^2 - d_{\text{in}}^2)$$

$$I_{\text{tube}} := \left[\frac{\pi \cdot (d_{\text{out}}^4 - d_{\text{in}}^4)}{64} \right]$$

$$J_{\text{tube}} := 2 \cdot I_{\text{tube}}$$

iv. Stress Concentration Factors

$$\frac{D}{d} = 3$$

$$\frac{r}{d} = 1.5$$

$$A_{\text{sc}} := 0.89334$$

$$b := -0.30860$$

$$k_t := A_{\text{sc}} \cdot \left(\frac{r}{d} \right)^b = 0.788 \text{ (Calculated Stress Concentration Factor)}$$

$$k_t := \begin{cases} A_{\text{sc}} \cdot \left(\frac{r}{d} \right)^b & \text{if } k_t \geq 1 \\ 1 & \text{otherwise} \end{cases} \quad k_t = 1$$

B. Force Analysis and Singularity Functions

i. Step Function

$$x := 0, 0.01 \cdot l_{\text{mandrel}} \cdot l_{\text{mandrel}}$$

$$S_{xx}(x, z) := \text{if}(x \geq z, 1, 0)$$

ii. Weight Functions of the Mandrel

$$V_{\text{mpi}} := A_{\text{cs}} \cdot l_{\text{in}} = 7.854 \times 10^{-3} \cdot \text{in}^3$$

$$m_{\text{I}} := V_{\text{mpi}} \cdot \rho = 2.154 \times 10^{-3} \cdot \text{lb}$$

$$w_{\text{m}} := \frac{(m_{\text{I}} \cdot g)}{\text{in}} = 2.154 \times 10^{-3} \cdot \frac{\text{lbf}}{\text{in}}$$

iii. Weight Functions of the Tube

$$V_{\text{tpi}} := A_{\text{cst}} \cdot l_{\text{in}} = 0.037 \cdot \text{in}^3$$

$$w_{\text{t}} := \frac{(m_{\text{It}} \cdot g)}{\text{in}} = 1.73 \times 10^{-3} \cdot \frac{\text{lbf}}{\text{in}}$$

$$m_{\text{It}} := V_{\text{tpi}} \cdot \rho_{\text{t}} = 1.73 \times 10^{-3} \cdot \text{lb}$$

iv. Static Stress Analysis for a Cantilevered Configuration

- Tube on Mandrel, Not inserted into coupler
- Using Centroidal location for distributed mass

v. Reactionary Components

$$V_{\text{r}} := w_{\text{t}} \cdot l_{\text{tube}} + w_{\text{m}} \cdot l_{\text{mandrel}} = 0.055 \cdot \text{lbf}$$

$$M_{\text{I}} := w_{\text{m}} \cdot l_{\text{mandrel}} \cdot \left(\frac{l_{\text{mandrel}}}{2} \right) + w_{\text{t}} \cdot l_{\text{tube}} \cdot \left[\frac{(l_{\text{mandrel}} - l_{\text{tube}})}{2} \right] = 0.317 \cdot \text{lbf} \cdot \text{in}$$

$$q(x) := -w_m \cdot S(x, 0) \cdot (x - 0)^0 - w_t \cdot S(x, 0) \cdot (x - 0)^0 + V_r \cdot S(x, 0) \cdot (x - 0)^{-1} + M_1 \cdot S(x, 0) \cdot (x - 0)^{-2}$$

vi. Shear Function

$$v(x) := -w_m \cdot S(x, 0) \cdot (x - 0)^1 - w_t \cdot S(x, 0) \cdot (x - 0)^1 + V_r \cdot S(x, 0) \cdot (x - 0)^0$$

vii. Moment Function

$$M(x) := \left(\frac{-w_m}{2} \right) \cdot S(x, 0) \cdot (x - 0)^2 - \left(\frac{w_t}{2} \right) \cdot S(x, 0) \cdot (x - 0)^2 + V_r \cdot S(x, 0) \cdot (x - 0)^1 + M_1 \cdot S(x, 0) \cdot (x - 0)^0$$

viii. Slope Function

$$\theta(x) := \left(\frac{1}{E \cdot I_{\text{mandrel}}} \right) \cdot \left[\left(\frac{-w_m}{6} \right) \cdot S(x, 0) \cdot (x - 0)^3 - \left(\frac{w_t}{6} \right) \cdot S(x, 0) \cdot (x - 0)^3 + \left(\frac{V_r}{2} \right) \cdot S(x, 0) \cdot (x - 0)^2 \dots \right. \\ \left. + M_1 \cdot S(x, 0) \cdot (x - 0)^1 \right]$$

ix. Deflection Function

$$\delta(x) := \left(\frac{1}{E \cdot I_{\text{mandrel}}} \right) \cdot \left[\left(\frac{-w_m}{24} \right) \cdot S(x, 0) \cdot (x - 0)^4 - \left(\frac{w_t}{24} \right) \cdot S(x, 0) \cdot (x - 0)^4 + \left(\frac{V_r}{6} \right) \cdot S(x, 0) \cdot (x - 0)^3 \dots \right. \\ \left. + \left(\frac{M_1}{2} \right) \cdot S(x, 0) \cdot (x - 0)^2 \right]$$

x. Static Stress Analysis Under Mandrel and Tube Weight

$$\sigma_y := k_t \cdot \left[\frac{(M(0) \cdot c_{\text{rod}})}{I_{\text{mandrel}}} \right] = 3.232 \times 10^3 \cdot \text{psi} \quad \sigma_x := 0 \quad \tau_b := \left[\frac{(4 \cdot V_r)}{3 \cdot A_{\text{cs}}} \right] = 9.376 \cdot \text{psi}$$

xi. Principal Stresses

$$\sigma_1 := \frac{(\sigma_x + \sigma_y)}{2} + \sqrt{\left[\frac{(\sigma_x - \sigma_y)}{2} \right]^2} + \tau_b^2 = 3.232 \times 10^3 \cdot \text{psi}$$

$$\sigma_2 := 0 \text{psi}$$

$$\sigma_3 := \frac{(\sigma_x + \sigma_y)}{2} - \sqrt{\left[\frac{(\sigma_x - \sigma_y)}{2} \right]^2} + \tau_b^2 = -0.027 \cdot \text{psi}$$

xii. Von-Mises Stress

$$\sigma_{\text{von}} := \sqrt{\sigma_1^2 - \sigma_1 \cdot \sigma_3 + \sigma_3^2} = 3.232 \times 10^3 \cdot \text{psi}$$

xiii. Static Elastic Safety Factor

$$N_{\text{elasticSF}} := \frac{S_y}{\sigma_{\text{von}}} = 7.643$$

xiv. Modified Mohr Theory

$$C_1 := \left(\frac{1}{2}\right) \cdot \left[(\sigma_1 - \sigma_2) + \left[\frac{(2 \cdot S_{\text{ut}} - S_{\text{uc}})}{-S_{\text{uc}}} \right] \cdot (\sigma_1 + \sigma_2) \right] = -3.232 \text{ ksi}$$

$$C_2 := \left(\frac{1}{2}\right) \cdot \left[(\sigma_2 - \sigma_3) + \left[\frac{(2 \cdot S_{\text{ut}} - S_{\text{uc}})}{-S_{\text{uc}}} \right] \cdot (\sigma_2 + \sigma_3) \right] = 5.44 \times 10^{-5} \cdot \text{ksi}$$

$$C_3 := \left| \left(\frac{1}{2}\right) \cdot \left[(\sigma_3 - \sigma_1) + \left[\frac{(2 \cdot S_{\text{ut}} - S_{\text{uc}})}{-S_{\text{uc}}} \right] \cdot (\sigma_3 + \sigma_1) \right] \right| = 6.464 \text{ ksi}$$

$$\sigma_m := \max(C_1, C_2, C_3, \sigma_1, \sigma_2, \sigma_3) = 6.464 \text{ ksi}$$

$$N_{\text{utssf}} := \frac{S_{\text{ut}}}{\sigma_m} = 10.768$$

xv. Buckling Analysis of the Mandrel

*During Tube Insertion

xvi. Assumptions

- Fixed-Pinned Geometry
- Eccentrically loaded member
- Fixture at $x = l$. mandrel acts as a simple support

$$F_{\text{friction}} := 1 \text{ lbf}$$

$$K_{\text{mandrel}} := \sqrt{\left(\frac{I_{\text{mandrel}}}{A_{\text{cs}}}\right)} = 0.025 \text{ in}$$

$$l_{\text{eff}} := 0.8 \cdot l_{\text{mandrel}} \quad (\text{AISC Recommended Value for fixed-pinned})$$

$$l_{\text{eff}} = 12.8 \text{ in}$$

$$S_r := \left(\frac{l_{\text{eff}}}{K_{\text{mandrel}}}\right)$$

$$S_r = 512$$

$$S_{\text{rd}} := \pi \cdot \sqrt{\frac{(2 \cdot E)}{S_y}}$$

$$S_{\text{rd}} = 147.976$$

$$\text{type} := \begin{cases} \text{"Euler"} & \text{if } S_r > S_{\text{rd}} \\ \text{"Johnson"} & \text{otherwise} \end{cases}$$

$$\text{type} = \text{"Euler"}$$

$$P_{\text{cr}}(S_r) := \begin{cases} \left[A_{\text{cs}} \cdot \left[\frac{(\pi^2 \cdot E)}{(S_r)^2} \right] \right] & \text{if type} = \text{"Euler"} \\ \left[A_{\text{cs}} \cdot \left[S_y - \left[\left(\frac{1}{E} \right) \cdot \left(\frac{S_y \cdot S_r}{2 \cdot \pi} \right)^2 \right] \right] \right] & \text{otherwise} \end{cases}$$

$$SF_b := \frac{\sqrt{(P_{\text{cr}}(S_r))^2}}{F_{\text{friction}}} = 8.102$$

C. Fatigue Analysis

i. Assumptions

- Room Temperature
- Machined Material
- 99.999% reliability
- Modified-Mohr Theory
- Slight Axial Loading
- $d < 0.3\text{in}$, $C_{\text{size}}=1$
- Ultimate Tensile Strength Less than 200ksi, $S_e=0.5S_{\text{ut}}$ (Steel)

$$S_{\text{ep}} := 0.5 \cdot S_{\text{ut}} = 3.48 \times 10^4 \text{ psi}$$

$$S_{\text{utn}} := 69.6$$

$$C_{\text{load}} := 0.7 \quad C_{\text{size}} := 1 \quad C_{\text{surfrac}} := 4.51 \cdot S_{\text{utn}}^{-0.265} = 1.465$$

$$C_{\text{surf}} := \begin{cases} 4.51 \cdot S_{\text{utn}}^{-0.265} & \text{if } C_{\text{surfrac}} \leq 1 \\ 1 & \text{otherwise} \end{cases}$$

$$C_{\text{surf}} = 1$$

$$C_{\text{temp}} := 1$$

$$C_{\text{rely}} := 0.65 \quad (\text{For } 99.999\% \text{ reliability})$$

$$\text{Corrected Endurance Strength:} \quad S_e := C_{\text{load}} \cdot C_{\text{size}} \cdot C_{\text{surf}} \cdot C_{\text{temp}} \cdot C_{\text{rely}} \cdot S_{\text{ep}} = 16.053 \text{ ksi}$$

Fatigue Strength percentage to Original Strength: $\left(\frac{S_e}{S_{ut}}\right) \cdot 100 = 23.065$

ii. Notch Sensitivity Factor

$k_t = 1$ $a := 0.093$ (Machine Design: Norton,2014) $r_{nsf} := \frac{r}{in}$

$$q_{nsf} := \frac{1}{\left(1 + \frac{a}{r_{nsf}^{0.5}}\right)} = 0.806$$

$$k_f := 1 + q_{nsf} \cdot (k_t - 1) = 1$$

iii. Alternating and Mean Components of Stress

$$F_{max} := w_t \cdot l_{tube} + w_m \cdot l_{mandrel}$$

$$F_{min} := w_m \cdot l_{mandrel}$$

$$F_a := \frac{(F_{max} - F_{min})}{2} = 0.01 \cdot \text{lbf}$$

$$F_m := \frac{(F_{max} + F_{min})}{2} = 0.045 \cdot \text{lbf}$$

$$M_a := F_{max} \cdot \left(\frac{l_{mandrel}}{2}\right) - F_{min} \cdot \left(\frac{l_{mandrel}}{2}\right)$$

$$M_m := F_m \cdot \left(\frac{l_{mandrel}}{2}\right)$$

$$M_a = 0.166 \cdot \text{lbf} \cdot \text{in}$$

$$M_m = 0.359 \cdot \text{lbf} \cdot \text{in}$$

$$\sigma_a := k_f \cdot \frac{M_a \cdot c_{rod}}{I_{mandrel}} = 1.692 \times 10^3 \cdot \text{psi}$$

$$\sigma_m := k_f \cdot \frac{M_m \cdot c_{rod}}{I_{mandrel}} = 3.655 \times 10^3 \cdot \text{psi}$$

$$\sigma_{xa} := 0$$

$$\sigma_{xm} := 0$$

$$\tau_a := \left[\frac{(4 \cdot F_a)}{3 \cdot A_{cs}}\right] = 1.762 \cdot \text{psi}$$

$$\tau_m := \left[\frac{(4 \cdot F_m)}{3 \cdot A_{cs}}\right] = 7.614 \cdot \text{psi}$$

$$\sigma_{pa} := \sqrt{\sigma_{xa}^2 + \sigma_a^2 - \sigma_{xa} \cdot \sigma_a + 3(\tau_a^2)}$$

$$\sigma_{pm} := \sqrt{\sigma_{xm}^2 + \sigma_m^2 - \sigma_{xm} \cdot \sigma_m + 3(\tau_m^2)}$$

$$N_{\text{fatigue}} := \frac{S_e \cdot S_{ut}}{\sigma_{pa} \cdot S_{ut} + \sigma_{pm} \cdot S_e} = 6.334$$

9. Appendix C: Design Concepts

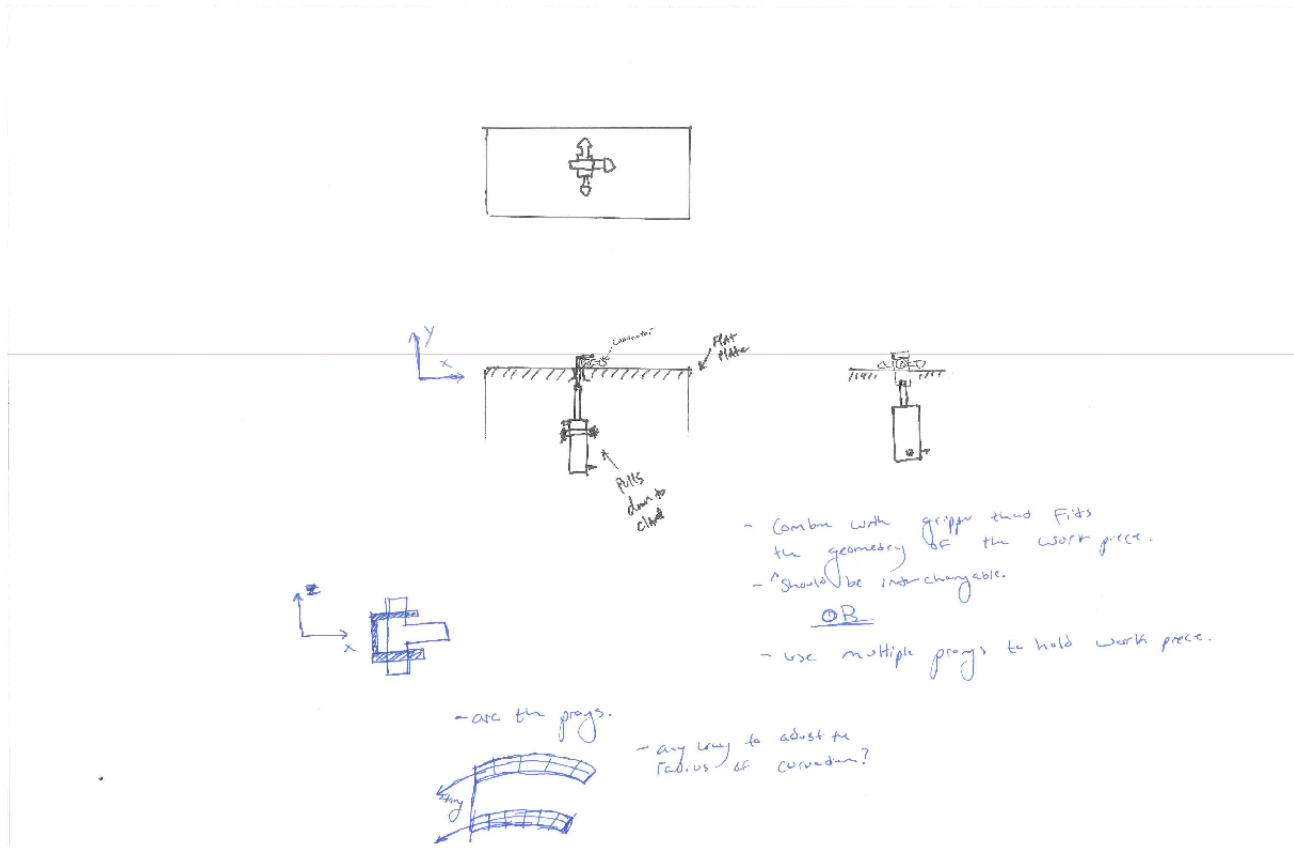


Figure 35: Pneumatic Connector Clamping Device

This 6-3-5 design concept was for the clamping of work components during the operation of any machine. In its design small grips were used, to secure two or more sections of the component, and operated by pneumatics.

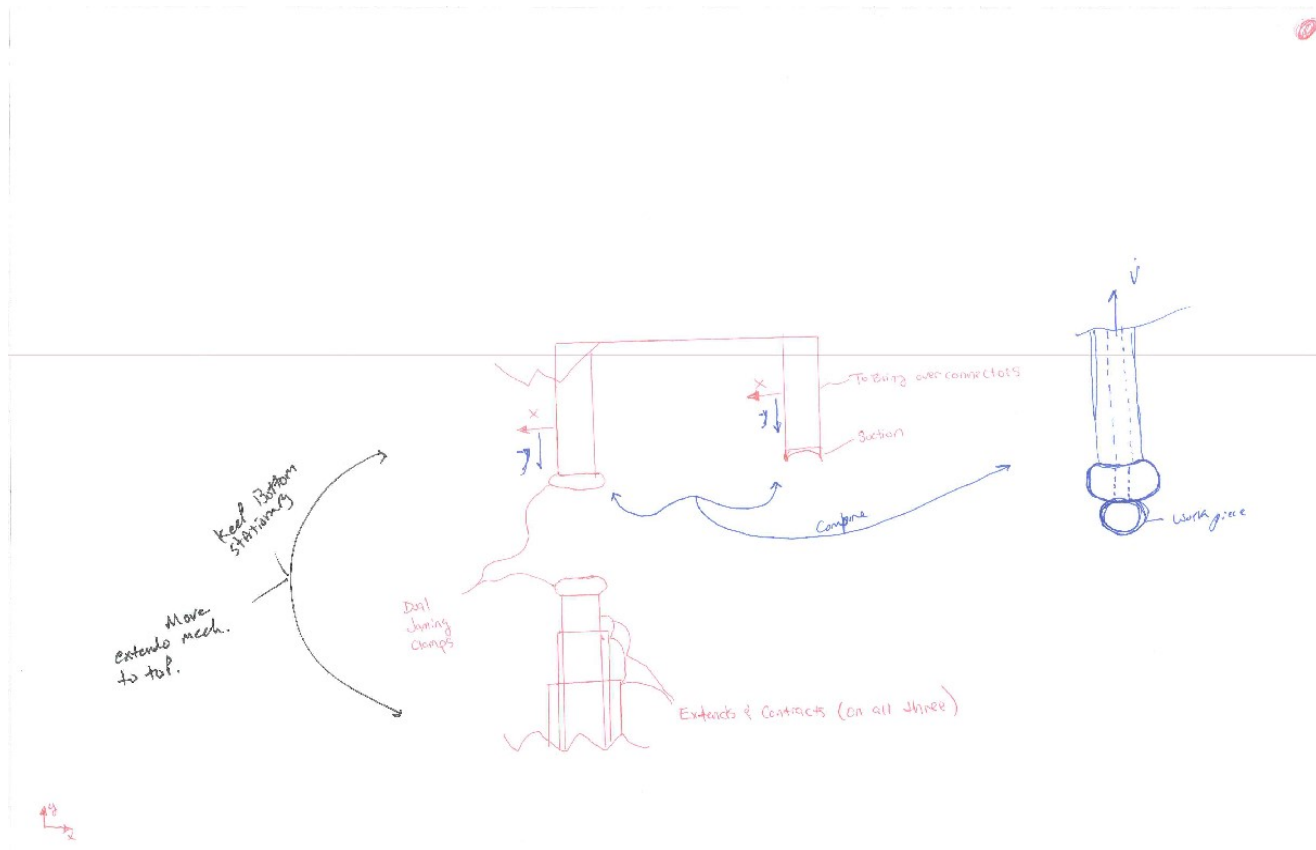


Figure 36: Pneumatic Wide Range Clamping Device

In this design concept, jamming grips were used to secure work pieces both by dual jamming grips and pneumatic suction.

This idea was excluded from our design iterations due to a high amount of process interference caused by the jamming grip.

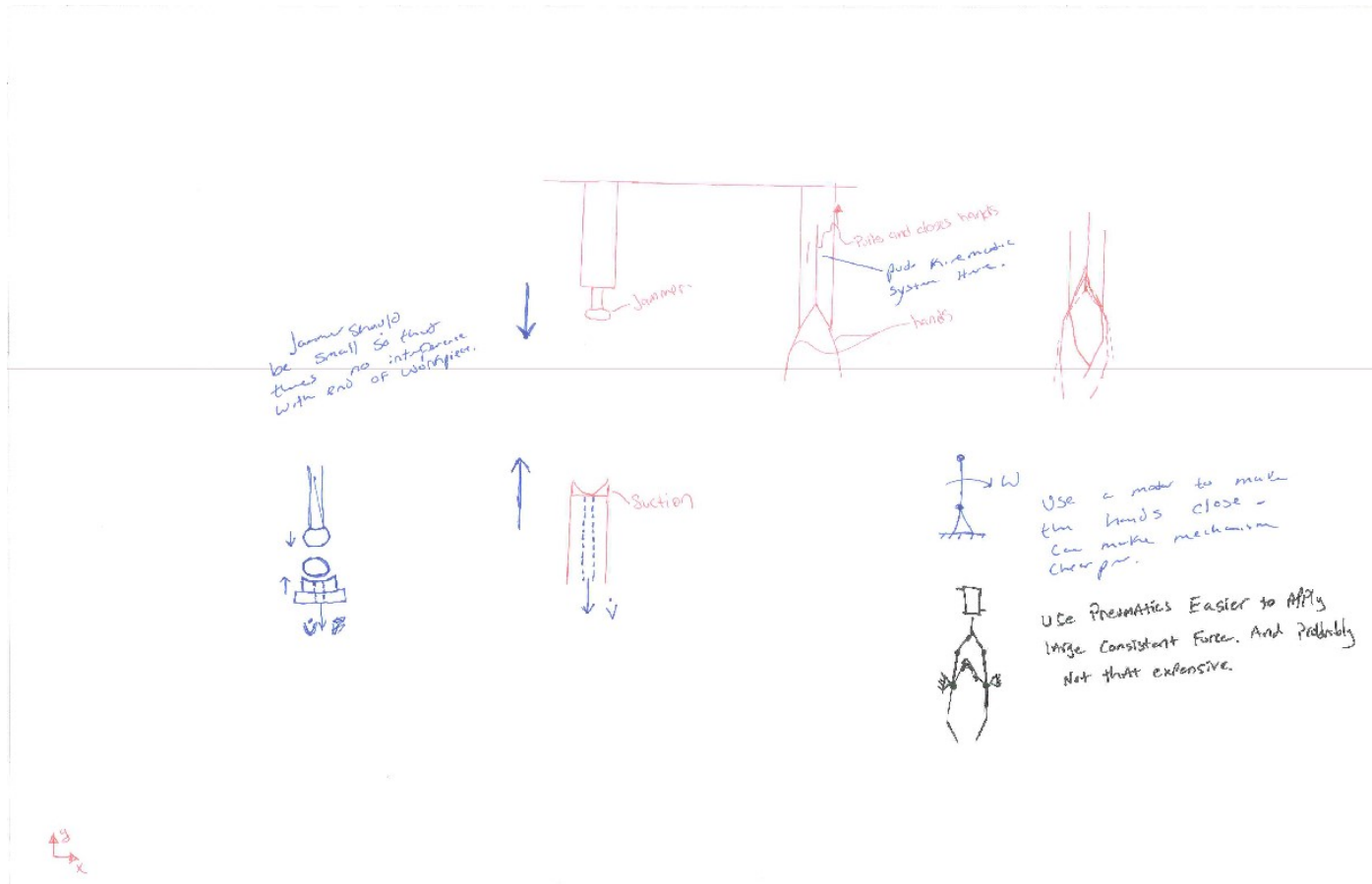


Figure 37: Retracting Connector Clamping Mechanism

This retracting clamp mechanism used both an upper jamming grip and a suction grip, respectively, to grasp the component during operation. It also used a retracting grip for component grasping.

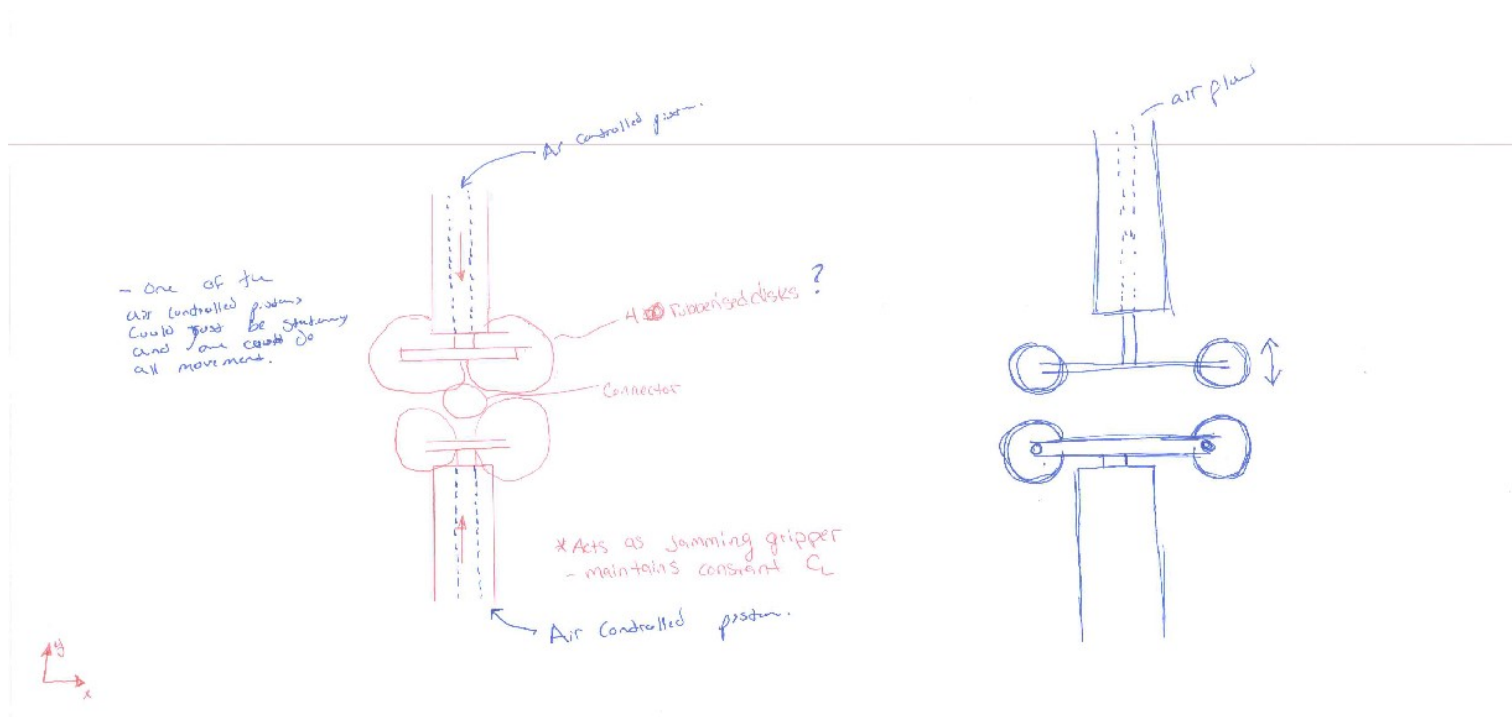


Figure 38: Pneumatic Connector Clamp

This design was again on component gripping, and it used both pneumatic suction and rubber wheels to hold the component in place.

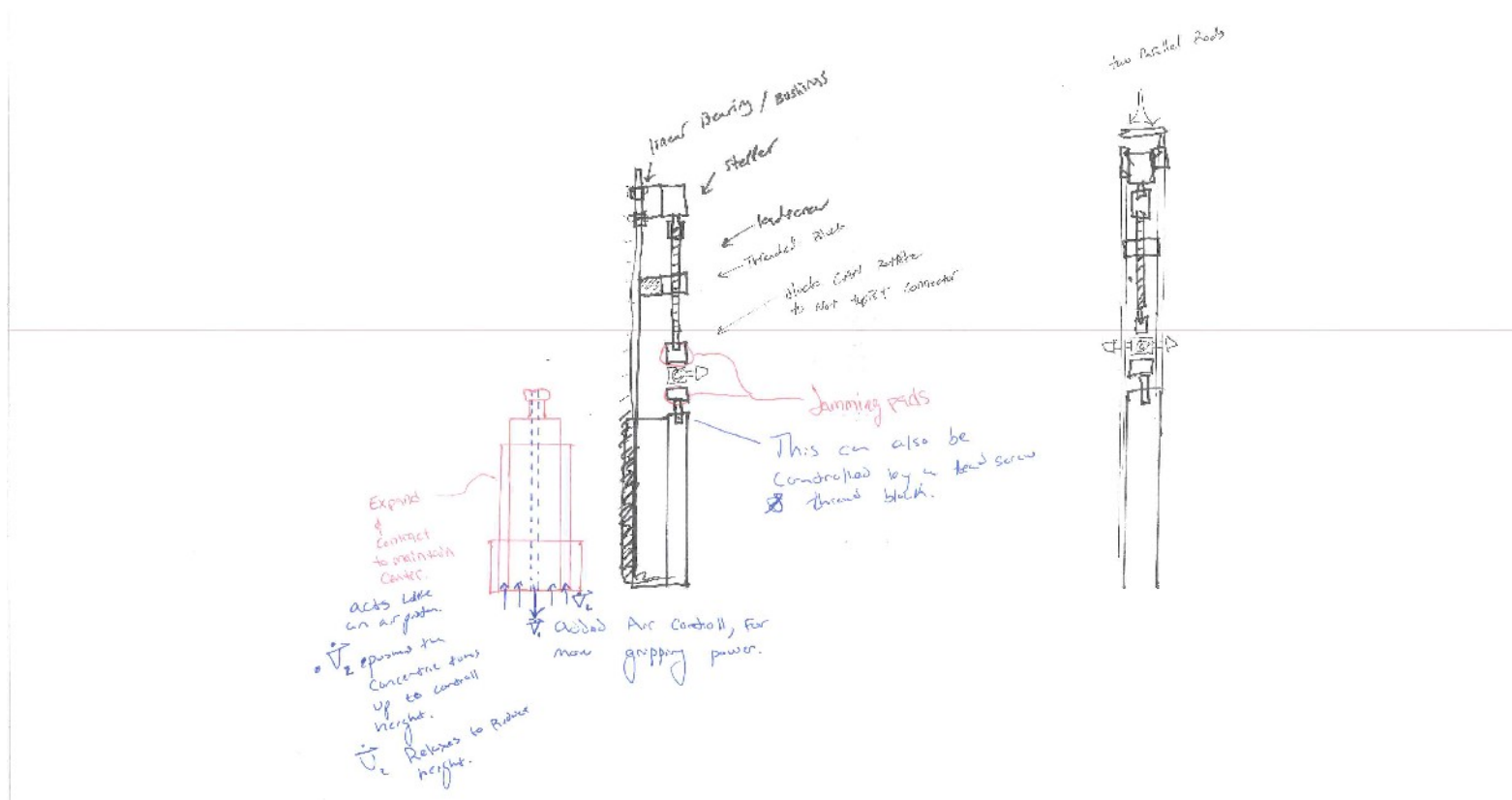


Figure 39: Pneumatic Connector Clamping Device

Figure 39, above, shows an idea for component clamping for use in operation. This machine used lead screws to compress the component during operation to prevent unwanted movement, but also offered less interference during this operation to allow a full coupling of the sub-assembly.

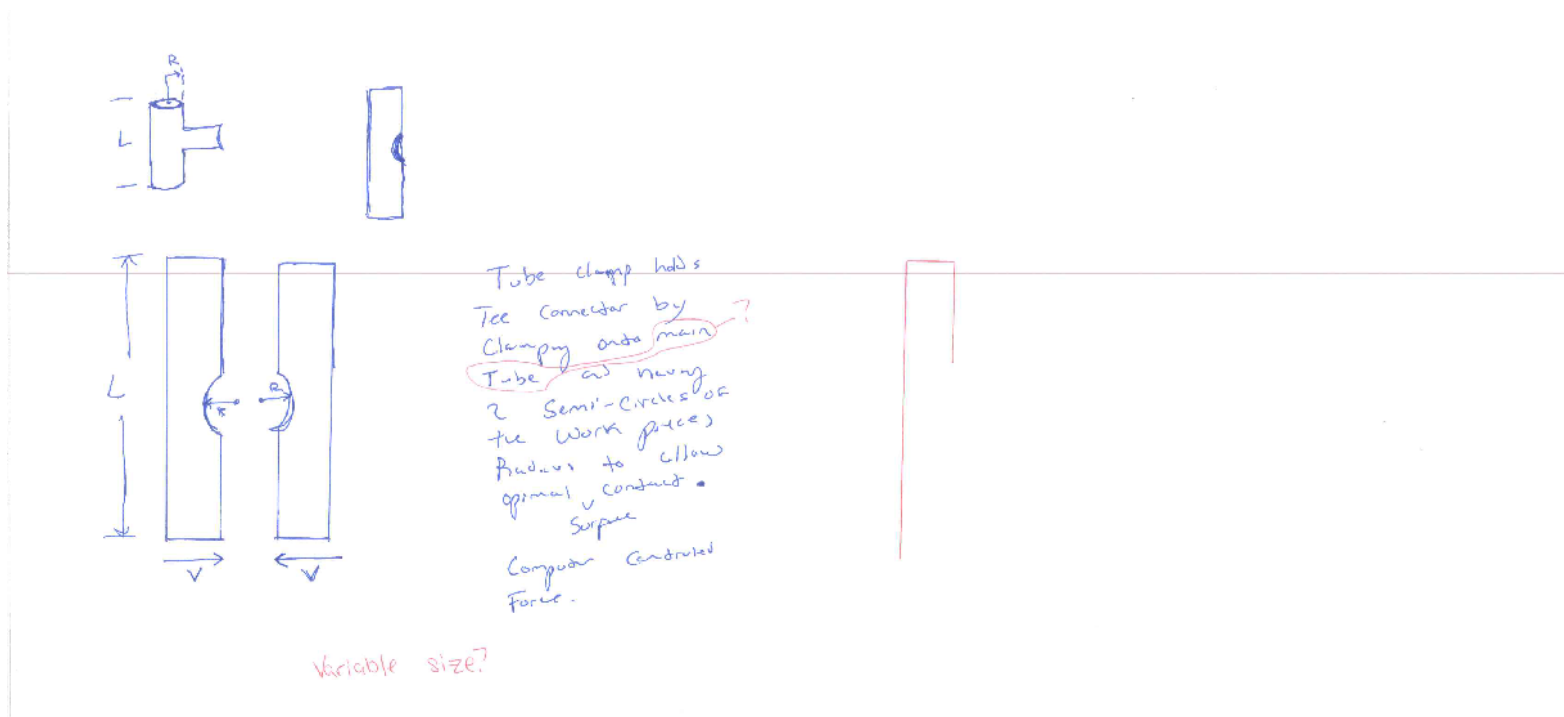


Figure 40: Connector Specific Clamp Tooling

Figure 40, above, shows an early idea for component securing. In its design a semi-cylindrical clamp is clamped around the connector piece during operation, with the nozzles free on each end to allow for tube insertion. This idea was scrapped due to the highly specific nature of the design.

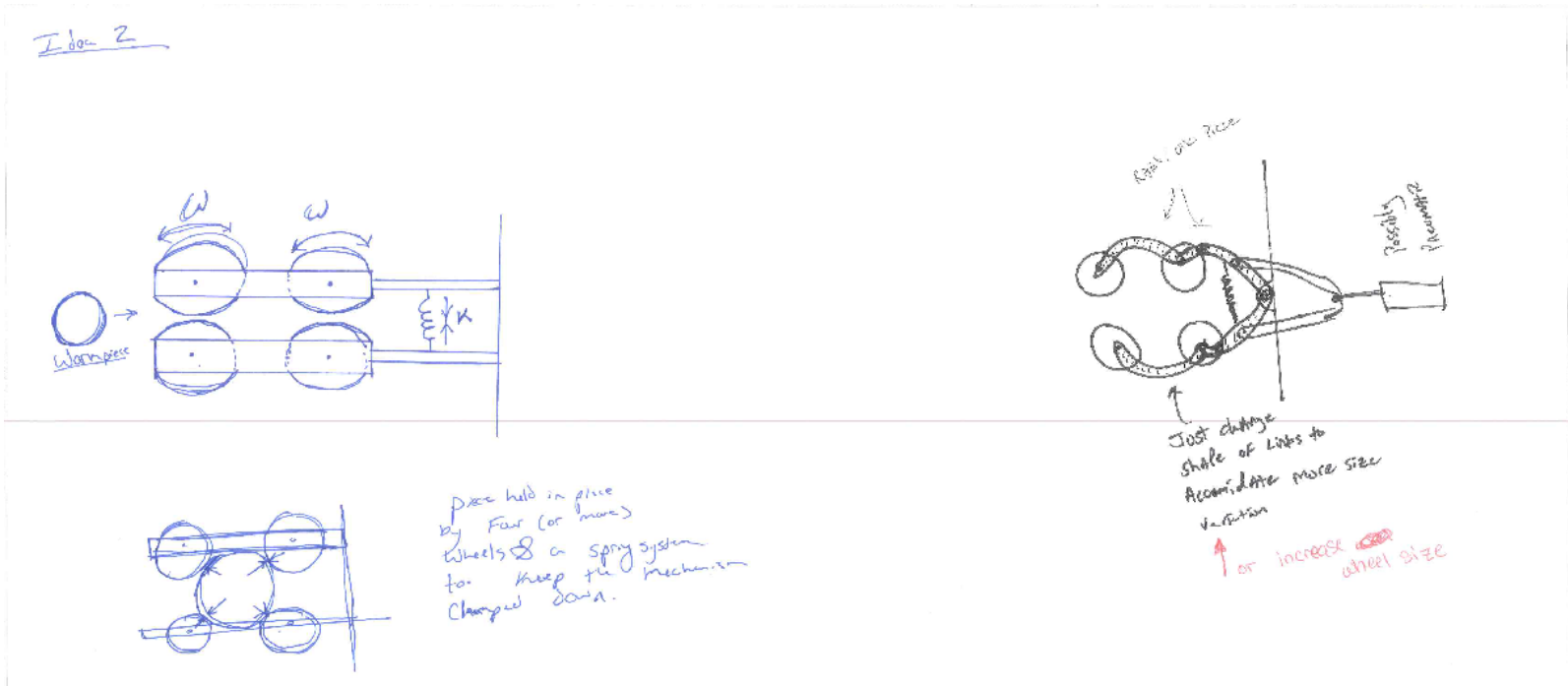


Figure 41: Tube Gripper for a Large Range of Sizes

Figure 41, above, shows an early concept for the friction gripper shown in Figure 12. This concept used cylindrical rubber members with high frictional coefficients to secure the tube in place, or to completely grip them, during tube insertion. This design also used spring actuated motion to allow the grip to open to the desired size for various diameter tubing.

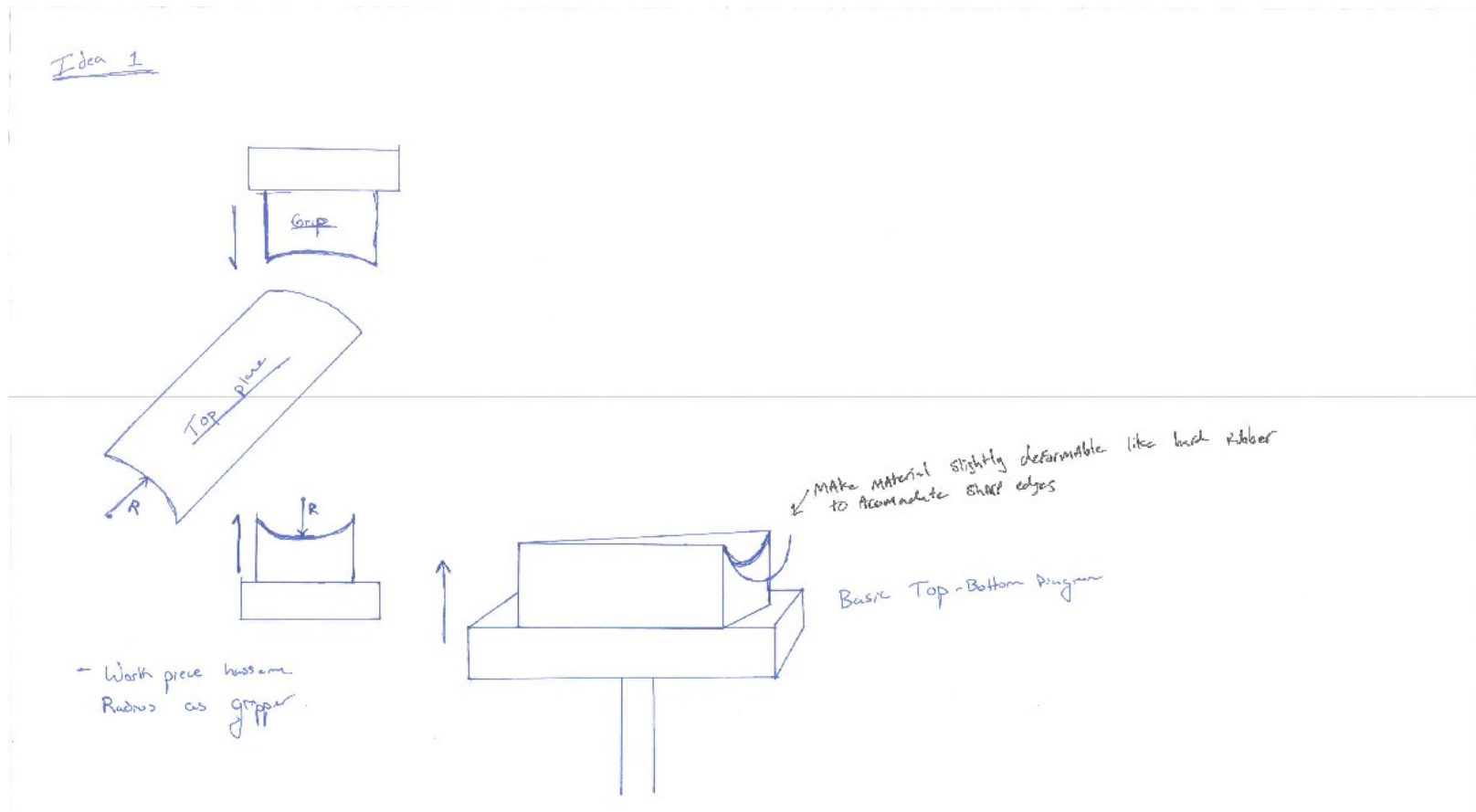


Figure 42: Soft Concave Connector Pads for Clamping

In this last component concept, Figure 42, a semi-cylindrical pad was used to grip the components during tube insertion. In this idea the component would be secured between two pads during operation to prevent moving, but would offer a cushion to the product to prevent damage.

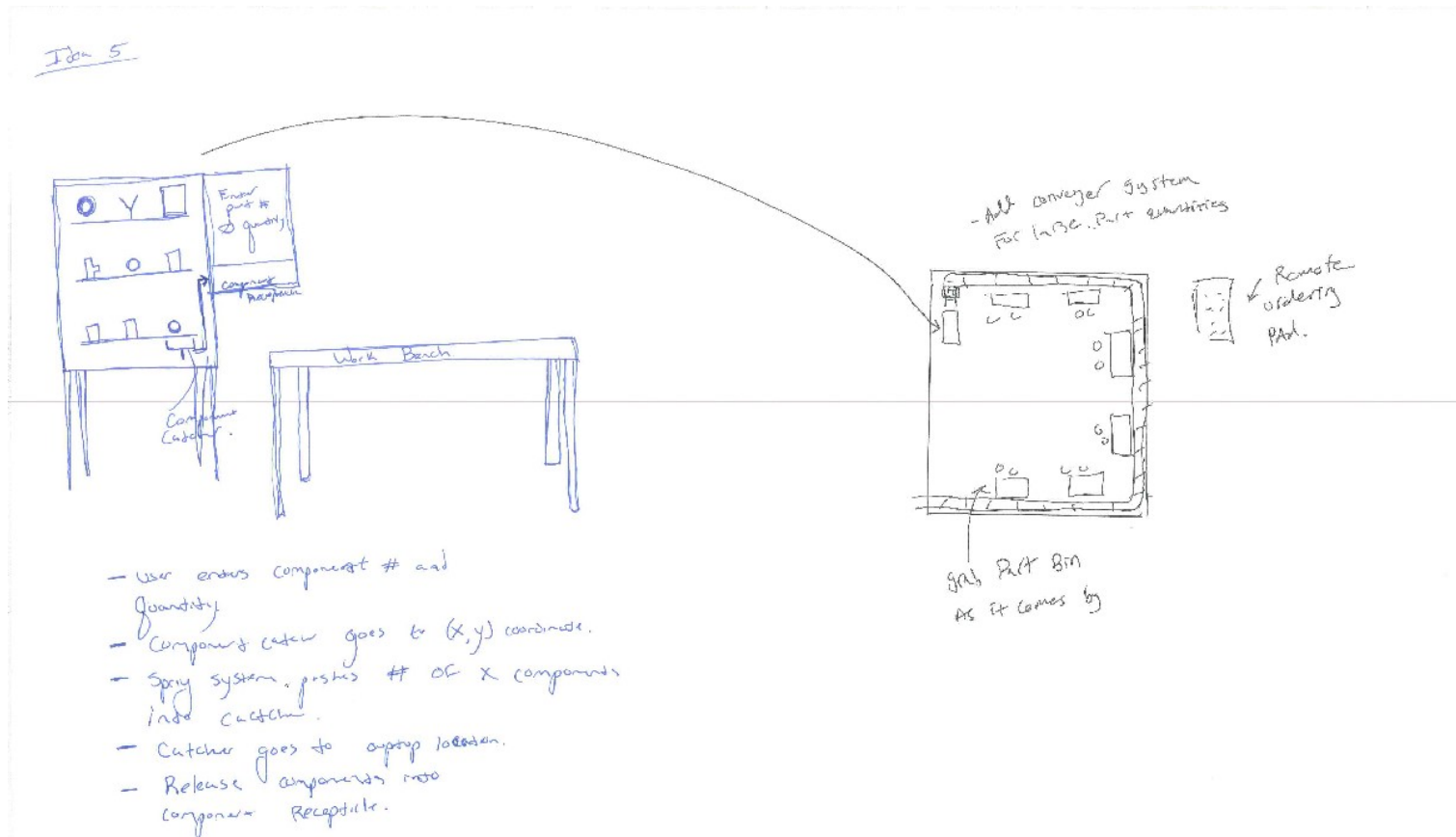


Figure 43: Part Dispensing Machine

Our team also explored the idea of material delivery systems to improve the factory floor operations. During visits it was noted that on occasion parts were dropped onto the factory floor and had to be subsequently disposed of, so our team conceptualized several methods for automated part delivery. In Figure 43, above, the idea was to have a vending machine styled queue system that dispensed

parts onto a conveyor belt, which delivered them to the desired location. A similar concept is seen in Figure 46, Figure 47, Figure 48, and Figure 49.

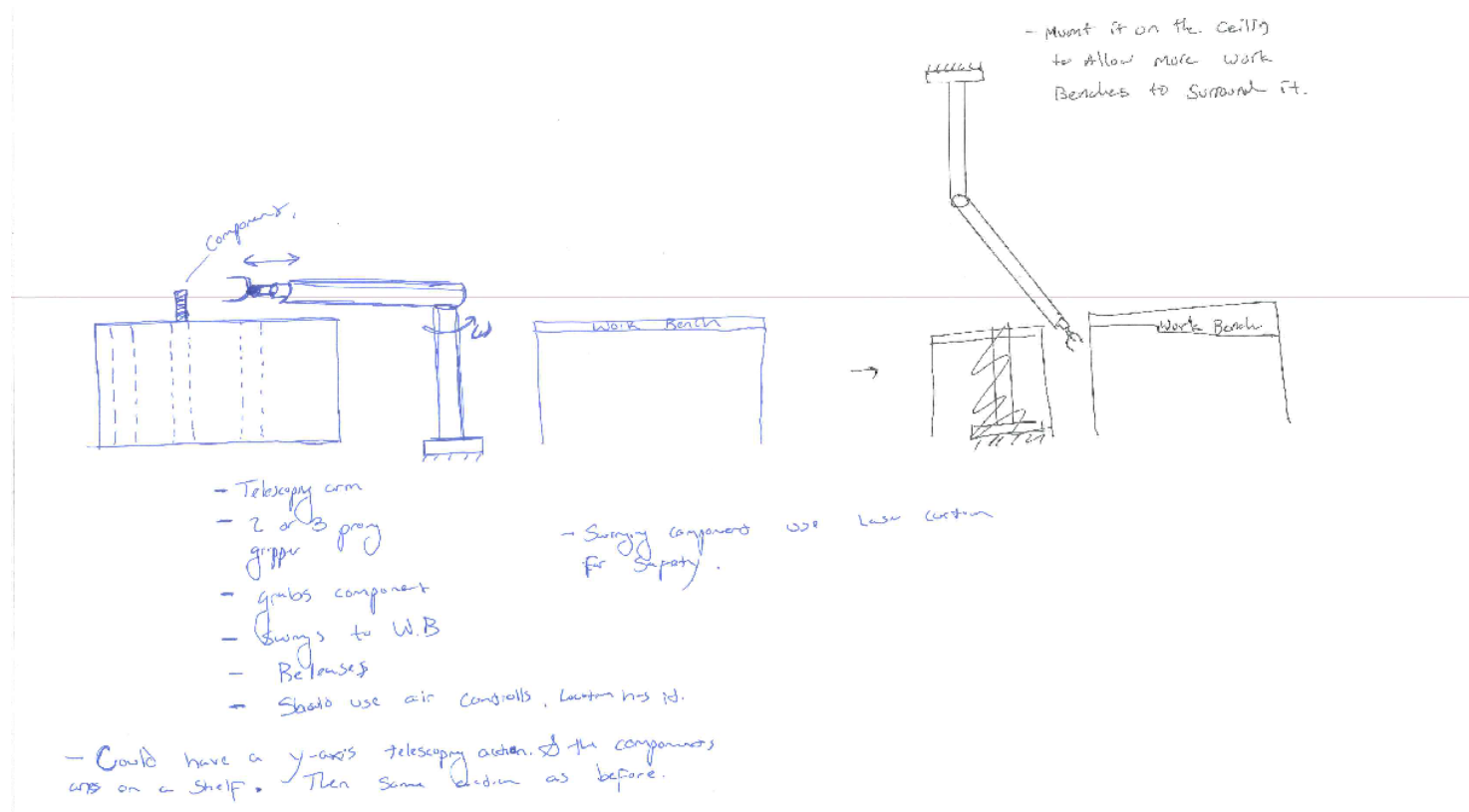


Figure 44: Part Manipulation and Delivery

Figure 44 shows a controlled robotic arm for part delivery. In this concept the computer controlled arm would deliver parts to certain work stations. This idea was scrapped due to the high initial investment, low savings and space requirements.

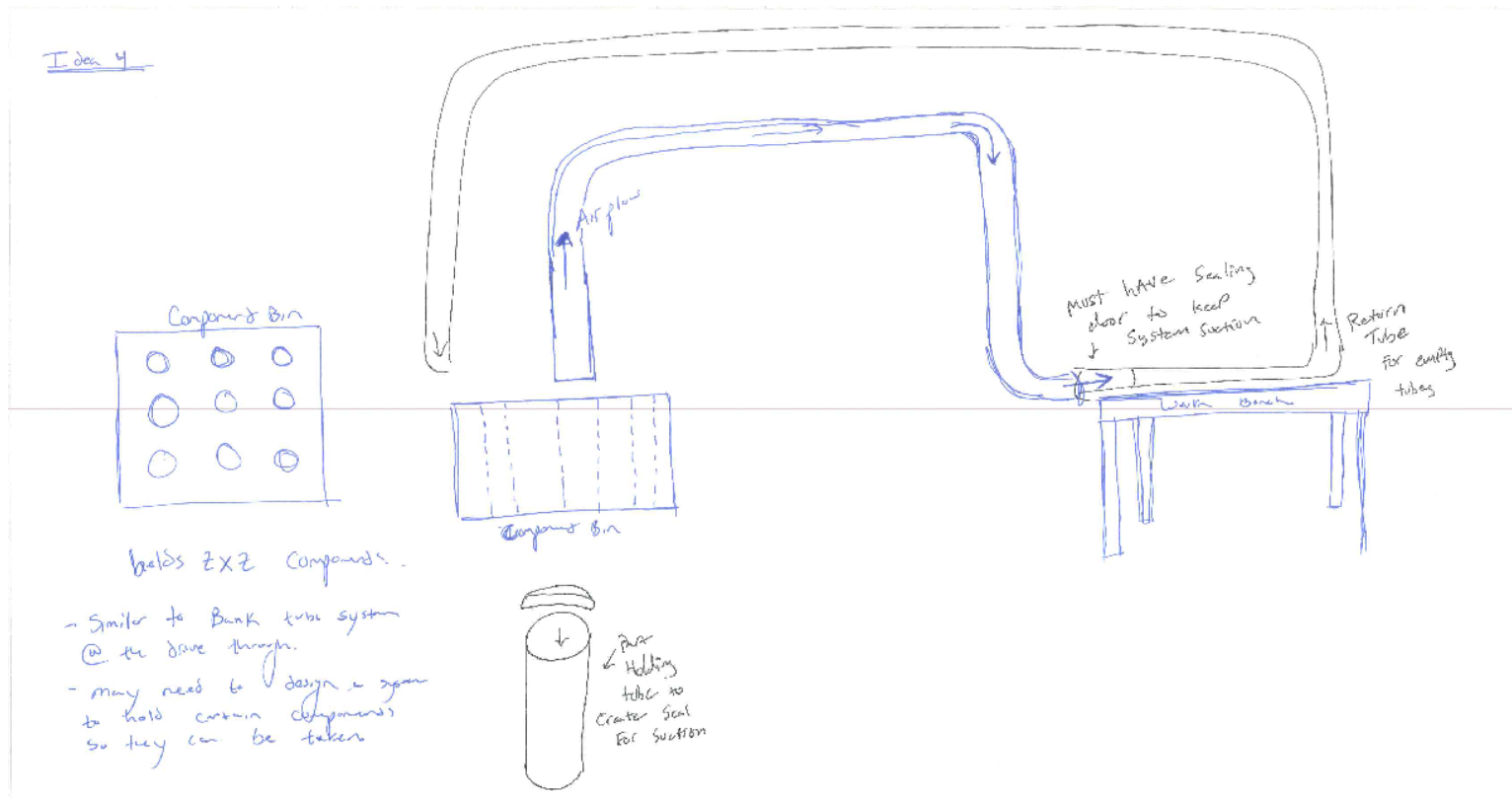


Figure 45: Pneumatic Part Delivery System

Figure 45 is a pneumatic controlled part delivery system, designed with the already present air system. In this concept a pneumatic tube would receive a package containing the desired parts and through pneumatic tubes would deliver them to the intended work station. This concept was scrapped due to the large space requirements.

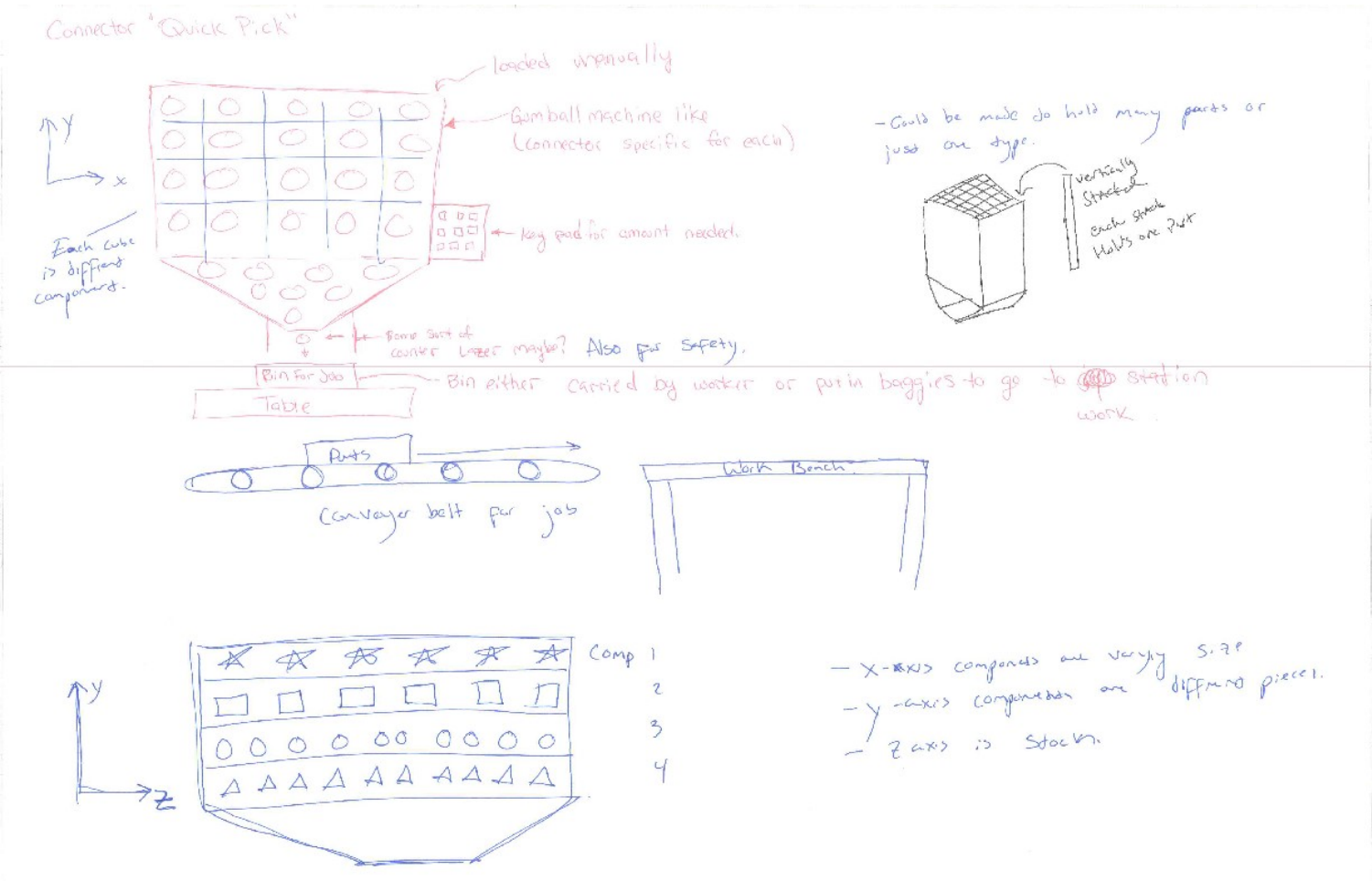


Figure 46: Part Organization as well as Part Delivery

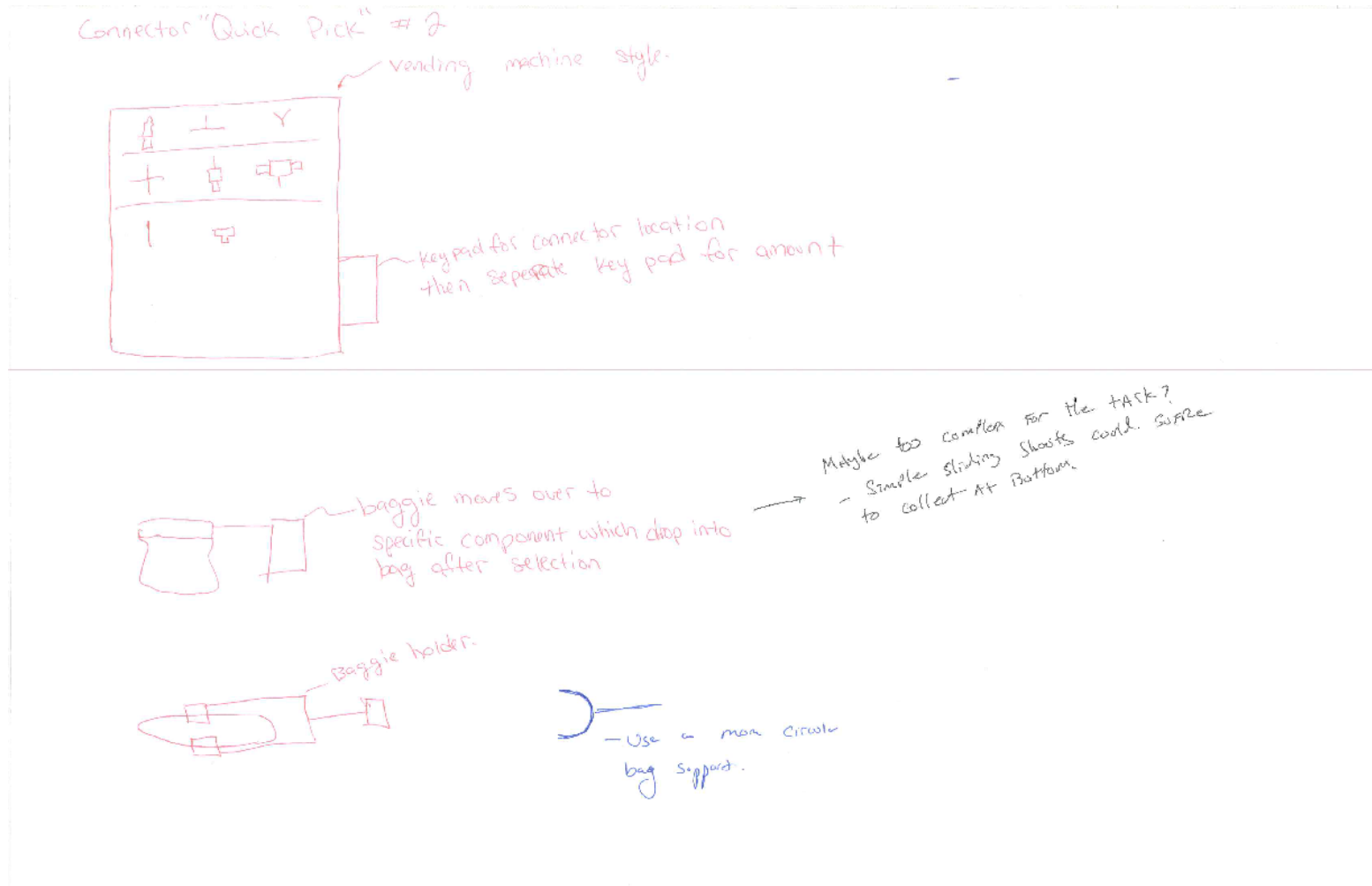


Figure 47: Connector Dispenser for Quick Part Kitting

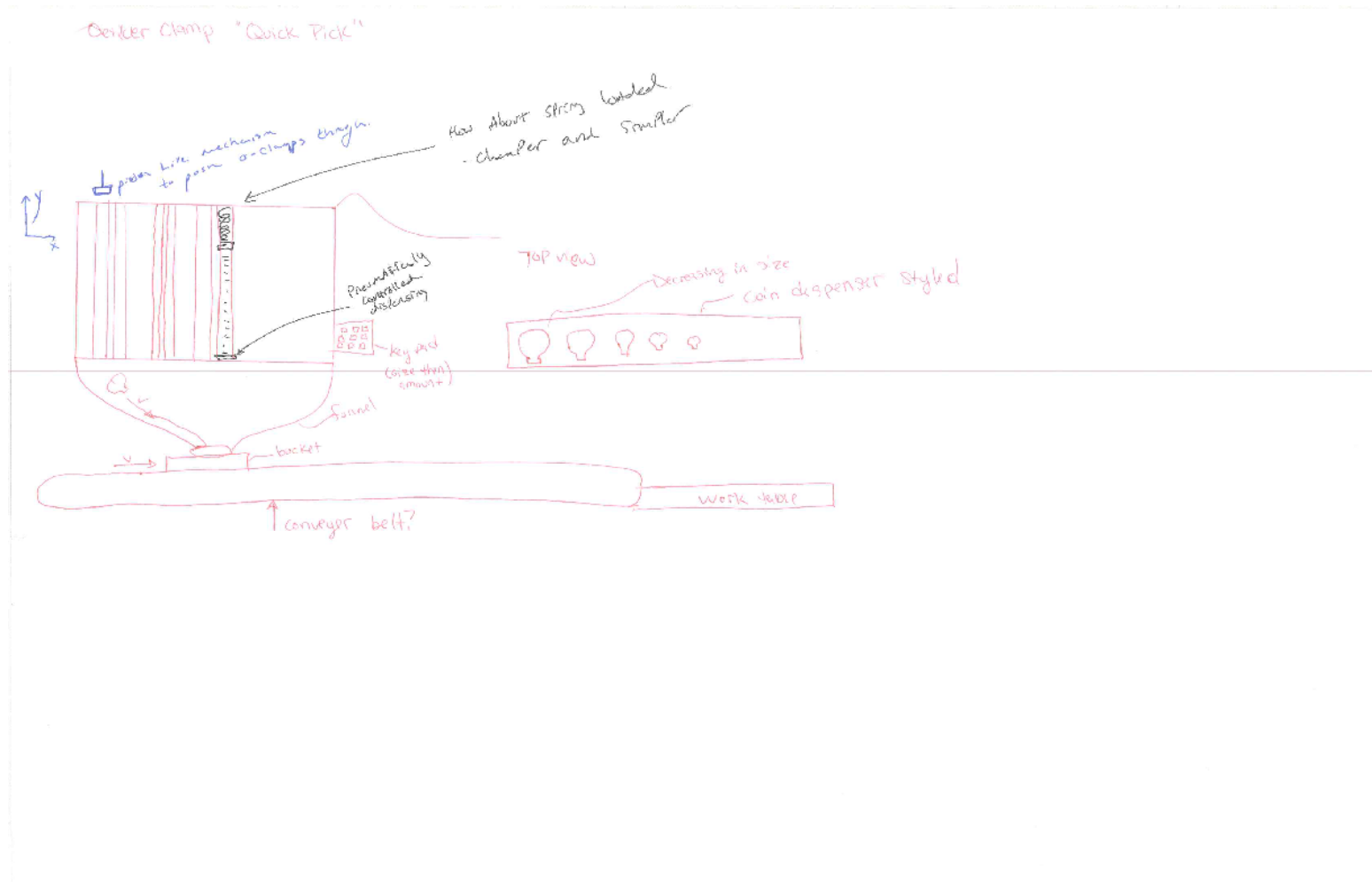


Figure 48: Part Delivery System

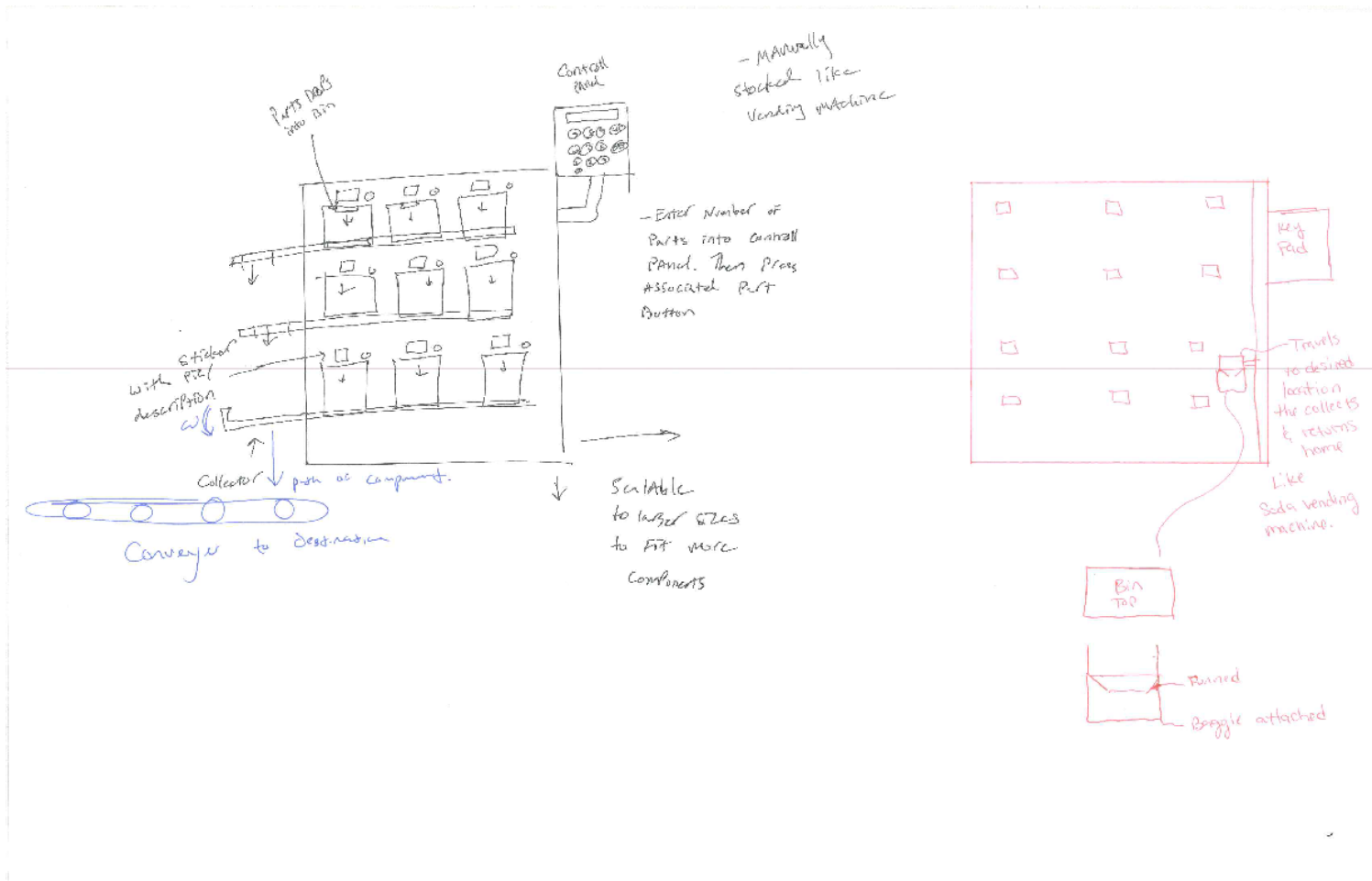


Figure 49: Automated Part Dispenser and Delivery System

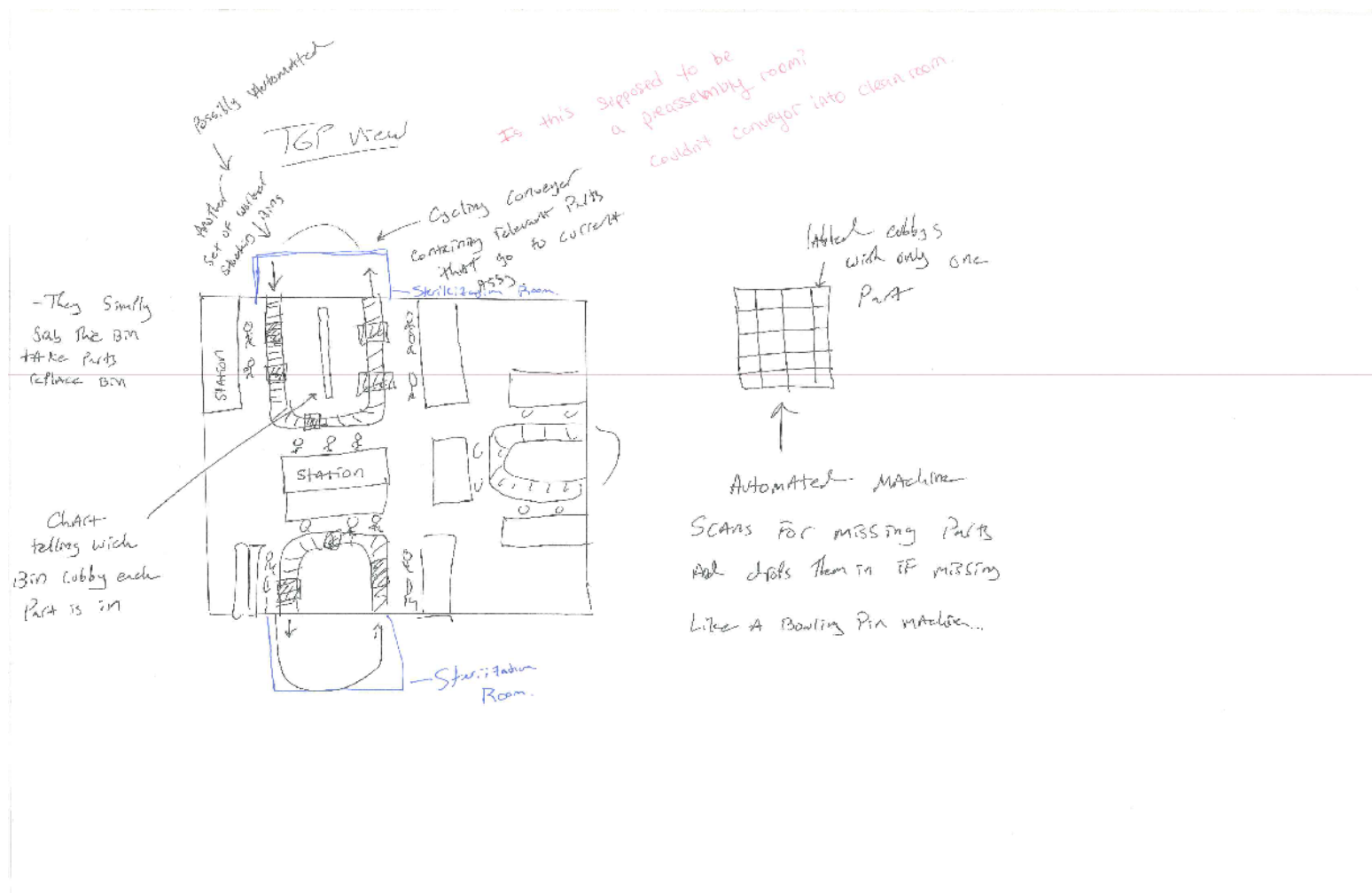


Figure 50: Room Optimization and Part Delivery System

10. Appendix D: Brain-Mapping Diagrams for Unused Projects

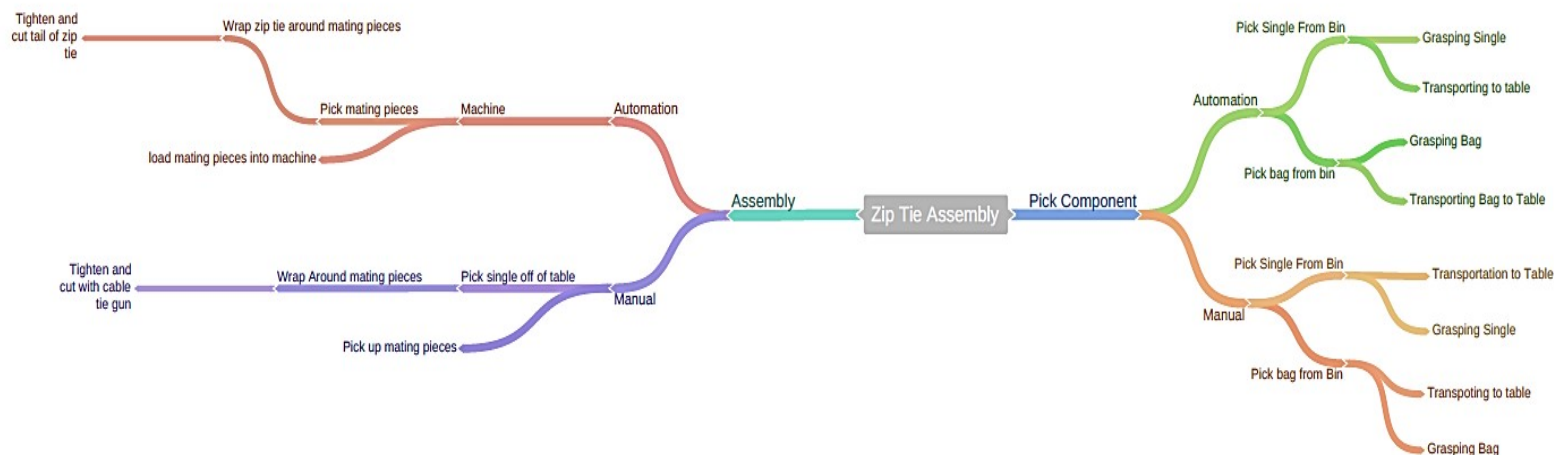


Figure 51: Zip Tie Process Diagram

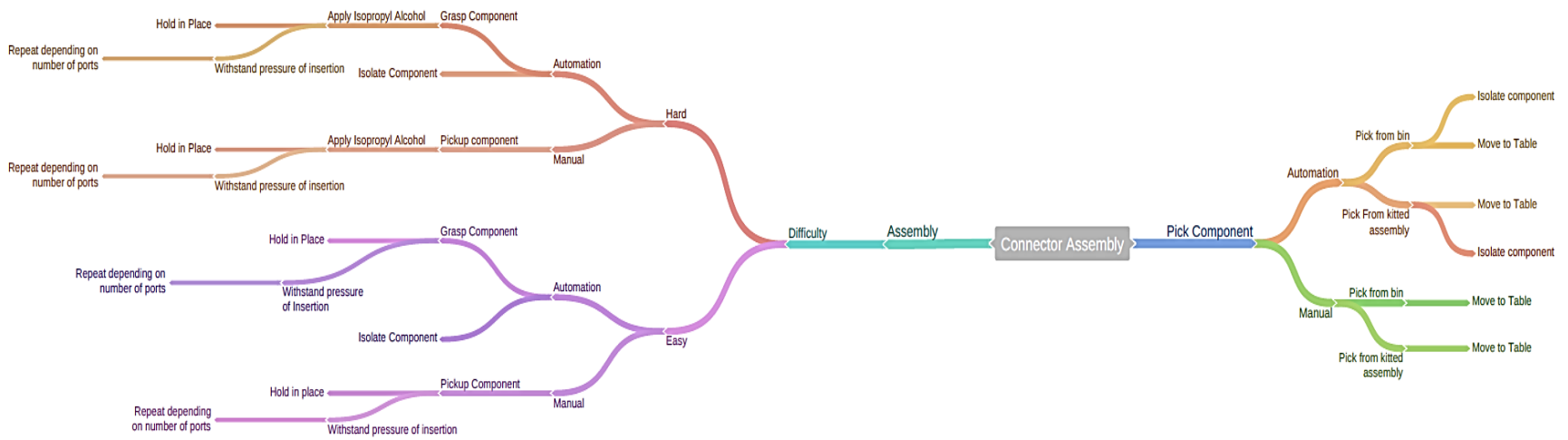


Figure 52: Connector Assembly Process

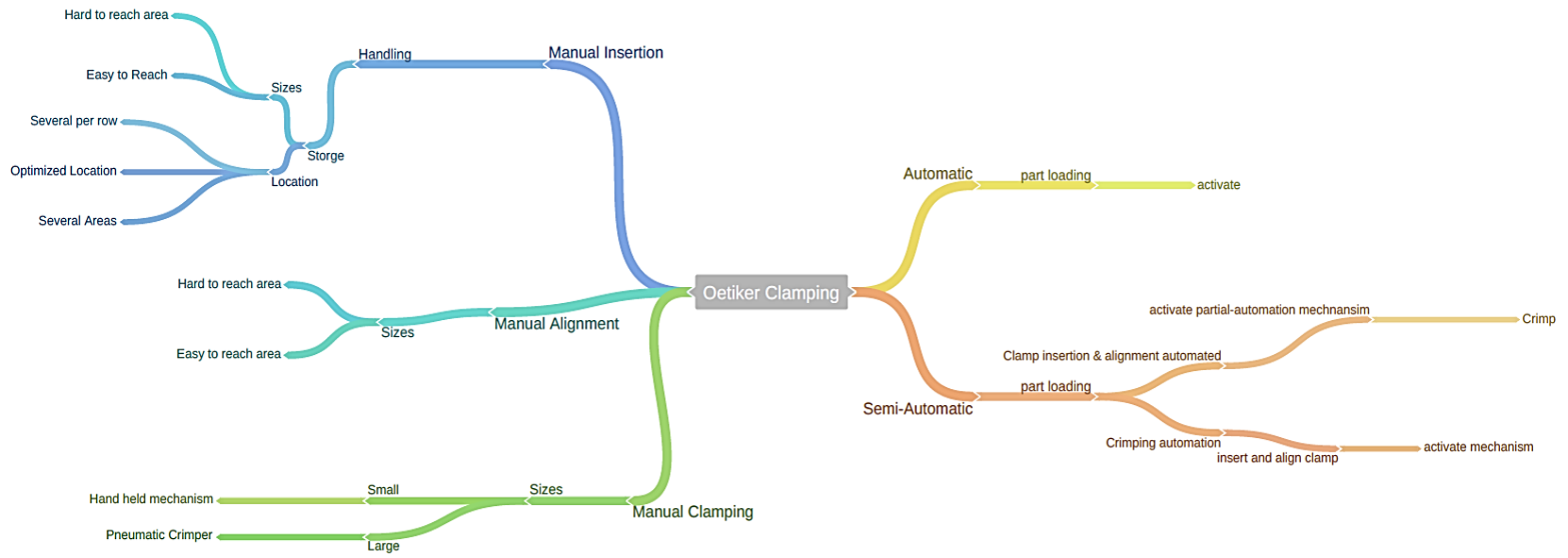


Figure 53: Oetiker Clamping Process

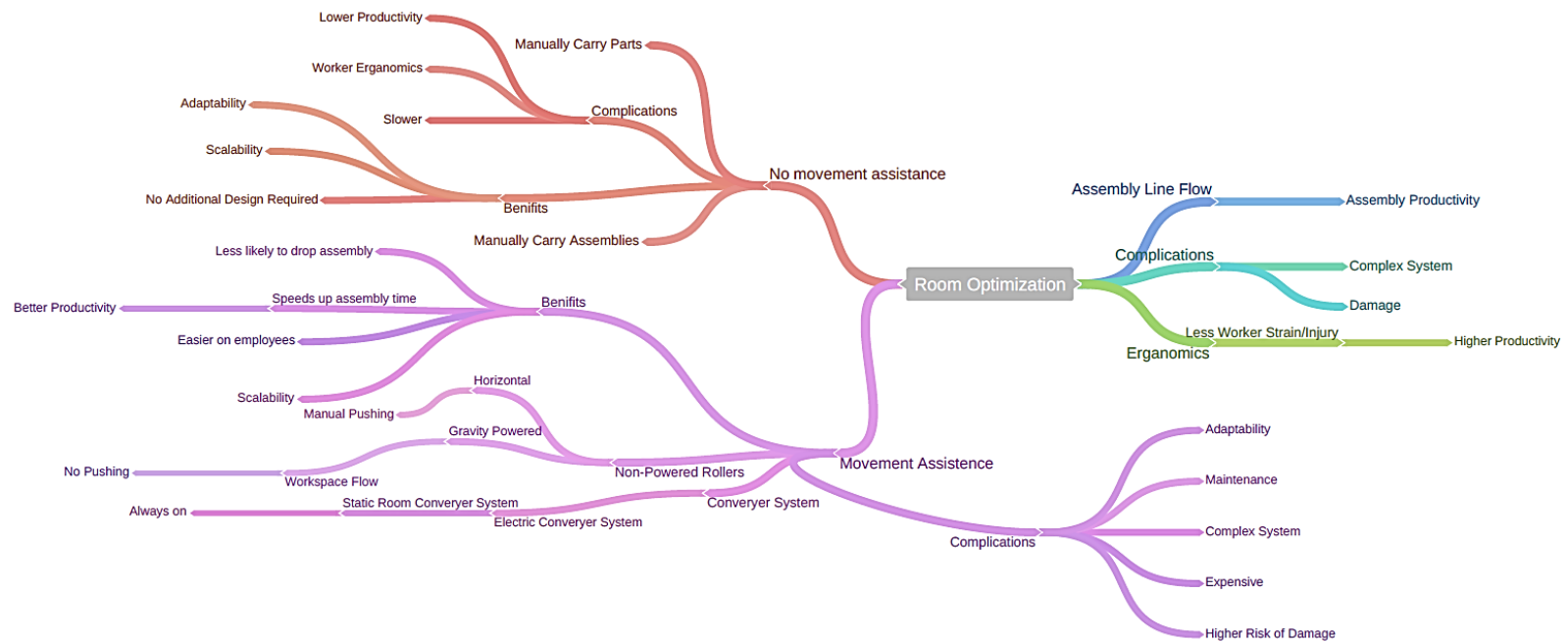


Figure 54: Room Optimization and Material Presentation Process